Obesity associated colon tumorigenesis:

An assessment of tumor phenotype

by

Swati Saxena

A thesis

presented to the University of Waterloo

in fulfillment of the

thesis requirement for the degree of

Master of Science

in

Biology

Waterloo, Ontario, Canada, 2006

I hereby declare that I am the sole author of this thesis. This is a true copy of the thesis, including any required final revisions, as accepted by my examiners.

I understand that my thesis may be made electronically available to the public.

Abstract

Colon cancer and obesity are two significant and related pathological states with multiple etiological factors. In this dissertation, it was hypothesized that tumor growth is accelerated in the altered state of obesity due to their resistance towards tumor necrosis factor-α (TNF-α) mediated cytotoxicity. Physiologically elevated TNF-α in an obese state induces increased nuclear transcription factor-κB (NF-κB) activity, known to transcribe genes crucial to cell survival. Insulin resistance, oxidative stress, and a pro-inflammatory environment are few of the biological consequences of TNF-α and NF-κB pathway activation, and further contribute to disease progression.

Three major studies were conducted to investigate phenotypical changes in obesity associated tumors. Firstly, characteristics of the TNF-α resistant phenotype were preliminarily assessed by evaluating the effects of exogenous TNF-α treatment to HT-29 cells. Elevated levels of NF-κB in response to exogenous TNF-α gave an indication that this pathway is critical for cell survival. Furthermore, upregulation of TNF-α receptor 2 (TNFR2) suggested another strategy by which the cells were utilizing exogenous TNF-α for a survival advantage. Inhibition of NF-κB via St. John's Wort treatment demonstrated that HT-29 cells may be sensitized towards TNF-α mediated cytotoxicity.

Zucker obese (Zk-Ob), Zucker lean (Zk-Ln), and Sprague Dawley (SD) animal models were used to assess tumor phenotype *in vivo*. Remarkable physiological differences between genotypes were observed. Zk-Ob rats had significantly higher body and organ weights as well as plasma TNF-α, insulin, leptin, and oxidative markers than Zk-Ln and SD animals. Tumor incidence and multiplicity were also notably higher in Zk-Ob rats. Protein analyses demonstrated increased levels of TNF-α, TNFR2, NF-κB, IκB kinase β (IKKβ), insulin receptor (IR), insulin like growth factor-I-receptor (IGF-IR), and mitogen activated protein kinase (MAPK) in Zk-Ob tumors than Zk-Ln counterparts. In all groups, tumors generally had higher protein expression than surrounding, normal appearing colonic mucosa. It is well known that these molecules are involved in signaling pathways that influence and co-operate with each other in rendering growth autonomy to tumor tissue.

A higher number of lesions in the distal than proximal colon in Zk-Ob rats was observed, supporting the emerging concept that genotype/physiological state of the host affects development and distribution of tumors. Thus, a third study was conducted to explore differences between distal and

proximal tumor phenotype. Results demonstrated that expression of TNFR2, NF-κB, IR, IGF-IR, and MAPK p44 were significantly higher in distal than proximal tumors. This observation suggested that development of tumors in different regions of the colon varied under the same physiological conditions. Moreover, phenotype of distal tumors appeared to be upregulating survival pathways in comparison to proximal lesions, possibly explaining the higher tumor incidence in the distal colon.

Research documented in this thesis supported the hypothesis that the physiological status of the host intricately affects tumor phenotype. In particular, the TNF-α resistant phenotype was most prominent in Zk-Ob tumors, and appeared to be associated with upregulation of multiple signaling pathways cooperating towards tumorigenesis.

Acknowledgements

This thesis marks the conclusion of an amazing two year experience in graduate school. Behind this endeavor stand many individuals who have helped me to grow and learn as a student, and my deepest thank you to all.

A sincere thank you to my advisor, Dr. Ranjana P. Bird, for always motivating me to be a critical thinker, and constantly question the direction of my research. Your dedication as a teacher and a scientist is truly inspiring, and I gratefully appreciate the confidence, guidance, and intellectual freedom you have supported me with throughout this journey.

I would also like to gratefully acknowledge my committee members, Dr. Niels Bols and Dr. Brian Dixon, for all their valuable suggestions, time, and efforts towards this thesis.

A special thanks to various members of the Department of Biology for all their assistance, whether by technical expertise or use of their facilities and equipments. Analyses of oxidative stress markers by Dr. Prem Kumarathasan at the Ottawa Health Research Institute has provided significant insight towards this research, and is much appreciated.

Working with all my lab members has been a truly wonderful experience, and I have learned a great deal from everyone. Thank you all for your encouragement, and for making our lab a great place to laugh and learn.

Thank you Nita, for your valuable friendship. I would have never been able to get through this without your intuition (that I still need to learn never to doubt!), and of course the spiced chais that kept us going throughout the afternoons. Your care has been instrumental towards completing this project.

Thanks Daddy, for always inspiring me to be a better person along with a better scientist, and having faith in my choices. Mom, you organize my life, and I truly appreciate how much you have supported me through your weekly care packages, and daily insistence on eating something green. Shivam, thanks for always standing by my side, and giving me strength from your smile and positive attitude.

Gaurav, I could not have done this without your love and support. Thank you for always picking me up when I fall, and encouraging me to look ahead towards possibilities I would never have considered.

For

Mummy and Daddy

Table of Contents

List of Tables

List of Figures

Introduction

Cancer and obesity are two significant causes of mortality considerably impacted by genetic and environmental etiological factors. While the epidemiological association between these two pathological states is well established, biochemical and molecular links are under review. Both are multi-factorial diseases with many contributing and interactive variables, making it difficult to isolate one particular causal mechanism. In this thesis project, TNF-α and NF-κB pathways were focused on due to their central roles in the manifestation of colon carcinogenesis and obesity.

It was hypothesized that tumors are accelerated in the altered state of obesity associated colon cancer due to their resistance towards TNF-α mediated cytotoxicity. Furthermore, physiologically elevated TNF-α induces increased expression of transcriptionally active NF-κB, known to transcribe genes crucial to cell survival. A pro-inflammatory environment, oxidative stress, and insulin resistance are few of the biological consequences of TNF-α and NF-κB pathway activation, and further contribute to disease progression. Three major studies were conducted to investigate this hypothesis, and their objectives and specific aims are described as follows.

Study 1: Effects of TNF-α and NF-κB inhibitors on HT-29 colon cancer cells

HT-29 colon adenocarcinoma cells were used as a preliminary approach to understand cellular and molecular changes associated with the TNF-α resistance phenotype. Specific aims of this study were:

- To determine changes at protein levels of TNFR1, TNFR2, NF-κB, IκBα, and IKKβ in HT-29 cells treated to exogenous TNF-α.
- To assess whether inhibition of NF-κB via St. John's Wort extracts and standards augment TNF-α mediated cytotoxicity in otherwise resistant HT-29 cells.

Study 2: Tumor incidence and phenotype in Zk-Ob, Zk-Ln, and SD rats

The second study utilized Zucker-obese (Zk-Ob) rats, an ideal model system for investigating obesity associated colon cancer, due to their inherent characteristics of elevated TNF-α levels and metabolic dysregulation. In addition, lean counterparts, Zucker-lean (Zk-Ln) rats, and Sprague dawley (SD) rats functioned as control groups.

The primary objective of this study was to determine if tumors appearing in Zk-Ob rats are biologically different from those in Zk-Ln and SD rats. It was hypothesized that the physiological state of Zk-Ob rats would affect tumor phenotype. In particular, elevated levels of TNF-α in these animals would exert a tumor promoting effect by inducing increased expression of transcriptionally active NF-κB, known to transcribe genes important for cell survival.

In order to accomplish this objective, this study was divided into three components with the following aims:

Study 2A: Assessment of physiological, hematological, and biochemical parameters in Zk-Ob, Zk-Ln, and SD rats

Specific aims of this study were to determine effects of genotypes of Zk-Ob, Zk-Ln, and SD rats on:
- Body and organ weights
- Complete blood count
- Plasma levels of TG, HDL, cholesterol, glucose, insulin, leptin, TNF-α, sTNFR1, and sTNFR2
- Plasma levels of oxidative stress markers

Study 2B: Assessment of tumor parameters in Zk-Ob, Zk-Ln, and SD rats

Specific aim of this study was to determine effects of genotypes of Zk-Ob, Zk-Ln, and SD rats on:
- tumor incidence, multiplicity, and distribution pattern along the colonic axis

Study 2C: Assessment of protein expression patterns in tumors and colonic mucosa of Zk-Ob, Zk-Ln, and SD rats

Specific aims of this study were to determine effects of genotypes of Zk-Ob, Zk-Ln, and SD animals on tumor and colonic mucosal protein expression of the following:

- TNF-α, TNFR1, and TNFR2
- NF-κB, IκBα, and IKKβ
- IRα, IRβ, and IGF-IRα
- MAPK p42/p44

Study 3: Differences in protein expression patterns in distal and proximal tumors of Zk-Ob rats

In study 2B, it was observed that the tumor distribution pattern along the colonic axis was different in Zk-Ob versus Zk-Ln and SD rats. To be specific, it was noted that the majority of tumors in Zk-Ob rats were located in the distal regions of the colon. This observation was in keeping with recent interests generated in the field of cancer biology that proximal and distal tumors represent biologically different disease states. An overall abundance of tumors in Zk-Ob rats allowed a more detailed comparison of tumor phenotype with regards to location along the colonic axis.

Specific aim of this study was:

To determine if tumors in Zk-Ob rats present in the distal colon exhibit different phenotypes from those in the proximal colon. In particular, expression of key proteins of the TNF-α, NF-κB, and insulin pathways were investigated as identified below:

- TNF-α, TNFR1, and TNFR2
- NF-κB, IκBα, and IKKβ
- IRα, IRβ, and IGF-IRα
- MAPK p42/p44

Chapter 1
Colon Cancer

1.1 Cancer

The probability of an individual developing cancer in their lifetime lies between 30-50% (Park and Pezzuto 2002). One of the leading causes of mortality today, cancer is a general descriptive term for the abnormal growth of cells. Constantly working towards maintaining a homeostatic equilibrium, the body must also regulate a balance between cell death and proliferation. Disruption of this balance due to various causative factors often results in an altered response to growth control, potentially leading to cancer development.

Numerous classes of genes such as proto-oncogenes, and mutated counterparts oncogenes, regulate cell division and apoptosis. Overexpression or dysregulation of these may initiate and promote carcinogenesis (Philip et al. 2004).

The progression of cancer, carcinogenesis, is a multi-step process involving stages of initiation, promotion, and cell proliferation (Macarthur et al. 2004). Cells first undergo transformation upon which they exhibit altered growth properties and morphology due to genetic or environmental factors such as chemical carcinogens, irradiation, and bacterial or viral infections (Goldsby et al. 2003). Animal studies have demonstrated that transformed cells in culture are capable of inducing tumor formation when transplanted *in vivo* (Reddy 2004). Transformation itself has two stages, initiation and promotion, the latter of which leads to malignancy. Initiation involves changes in the cell genome and irreversible DNA damage affecting protein expression, and a decreased responsiveness to growth control mechanisms. On the other hand, promotion involves clonal selection and propagation of initiated cells

Uncontrolled cell division often results in formation of neoplasms (new growth) which are characterized as a benign, or a non-invasive, non-indefinite type of growth. Conversely, malignant tumors are an invasive, indefinite growth that may metastasize to other regions of the body through the lymphatic or circulatory system (Goldsby et al. 2003).

4

1.2 Colon

The large intestine, the terminal part of the gastro-intestinal tract, is a muscular tube about 1.5 meters in length. Specifically, the colon consists of the caecum (with an attached appendix), ascending, transverse, descending and sigmoid components, and ends with the rectum. Primary functions of the colon involve processing of waste material, reabsorption of water and nutrients, and mucous production (Moore and Dalley 1999).

Histologically, the colon has four distinct layers of mucosa and muscle: mucosa, submucosa, muscularis externa and serosa (Figure 1-1) (Moore and Dalley 1999). The innermost mucosal layer consists of invaginations known as crypts lined with colonic epithelium. Unlike the small intestine, colonic crypts have no villi for nutrient absorption. Crypts are supported by the lamina propria consisting of connective tissue, blood vessels, and immune cells including lymphocytes and macrophages (Moore and Dalley 1999). This mucosal layer is the most common origin for colon cancers.

Colonic epithelium is a highly diverse and dynamic system involving constant cell renewal (Ding et al. 1998). Continually proliferating stem cells situated at the base are responsible for replenishing the entire epithelium every 3-8 days (Cotran et al. 1999). This cell regeneration occurs within the base two-third portion of the crypt. As the cells migrate upwards they differentiate into specialized cell types including absorptive, mucous secreting, endocrine, and anti-bacterial protein secreting Paneth cells (Figure 1-2) (Radtke and Clevers 2005).
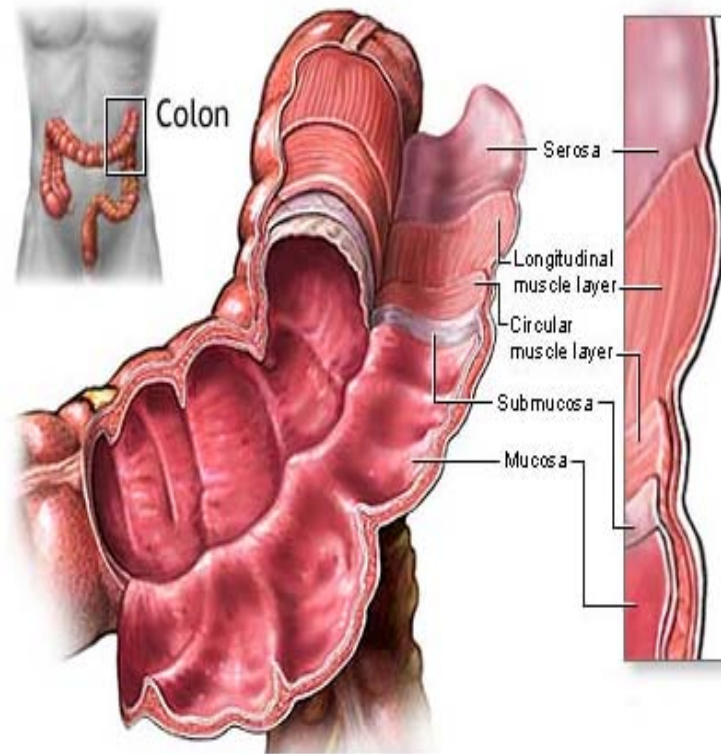
Figure 1-1: Histology of the colon.

The colon consists of layers of muscle and mucosa; mucosa, submucosa, muscularis externa and serosa. The inner most mucosal layer consists of invaginations known as crypts lined with colonic epithelium, which are the most common origin for cancer development.
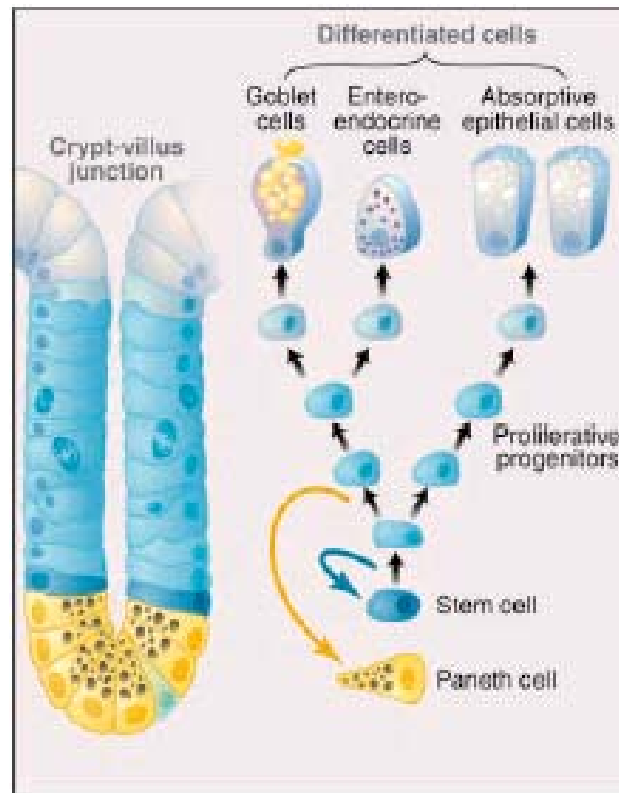
Figure 1-2: Differentiation of colonic epithelium.

Structure of a colonic crypt is displayed. Stem cells situated at the base of the crypt differentiate into specialized cell types found in mucosal layer, and regenerate the entire epithelium every 3-5 days (Radtke and Clevers 2005).

1.2.1 Colon Carcinogenesis

Colon cancer is the second leading cause of cancer-related deaths for both men and women in North America, and over 100 000 new cases are estimated for 2006 (Jemal et al. 2005). This accounts for 11% of all cancers, and is preceded only by prostate, breast, and lung cancers. In addition, it is estimated that 50% of the population will develop an adenomatous polyp by the age of 70 (Jemal et al. 2005).

Colon cancer has multiple etiological variables including diet, lifestyle, and contributing physiological disorders such as inflammation and obesity. Genetics also plays a role, and a common form of cancer known as familial adenomatous polyposis coli involves a mutation of the adenomatous polyposis coli (APC) gene (Cotran et al. 1991). Current treatment strategies of colon cancer include combinations of chemotherapy, radiation therapy, and surgery (Martinez 2005).

A multi-step, multi-factorial process, colon carcinogenesis involves the clonal selection and propagation of initiated colonic epithelial cells, which progress from normal to precancerous to malignant states over a span of 5-40 years (Curtis 1991, Roncucci et al. 1991, Cheng and Lai 2003). The sequential events of colon carcinogenesis concerning genetic and phenotypical changes are very well characterized by the adenoma-carcinoma model first described by Fearon and Vogelstein (1990). In this model, inactivation of tumor-suppressor genes APC, DCC and p53, and activation of oncogene K-*ras* are corresponded to morphological changes in colonic epithelia (Figure 1-3).
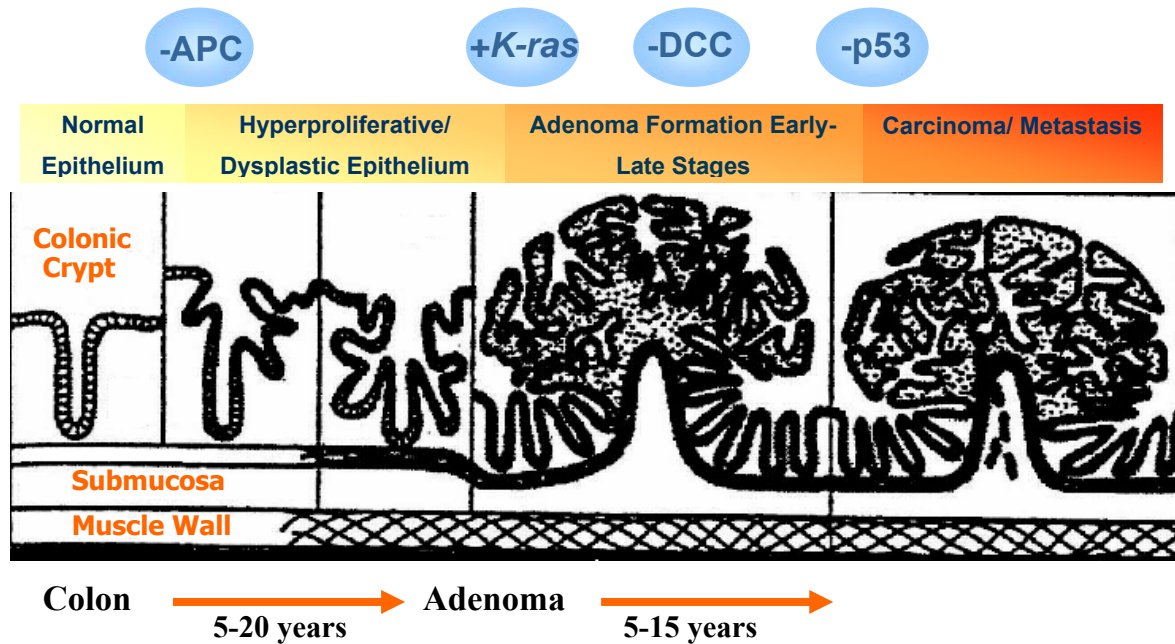
Figure 1-3: Vogelstein model of colon carcinogenesis.

Morphological changes in colonic epithelium may be correlated with genetic alterations during carcinogenesis. Progression from normal colonic epithelia to tumor formation is shown.

1.2.2 Aberrant Crypt Foci

Proliferation of initiated colonic cells leads to microscopic alterations to the normal histology of the colon, resulting in aberrant crypt foci (ACF) formation (Bird 1987). ACF, now well recognized as putative preneoplastic lesions, act as diagnostic biological markers for the process of colon carcinogenesis (Bird 1987).

As these preneoplastic lesions develop, they acquire novel genotypic and phenotypic features (morphology and number of crypts) which correspond to their ability to develop, survive and combat negative growth signals. Evaluation of ACF number, crypt multiplicity, location, and growth properties are common characteristics used to assess disease status, and effects of potential preventative agents (McLellan et al. 1991).

ACF have potential to undergo additional genetic alterations and progress into intra-epithelial benign structures known as polyps or adenomas, which may further advance to malignant lesions having the capacity to metastasize (Roncucci et al. 1991).

1.4 Colon Cancer and Obesity

Obesity is a premorbid condition and rising epidemic in North America, with both environmental and genetic etiological factors (Formiguera and Canton 2004). There is especially a well established epidemiological association between obesity and an increased risk for colon cancer (Rapp et al. 2005). While the biochemical and molecular links between the two physiological disorders are still under review, the interconnected roles of insulin resistance, adipose tissue, and inflammation are repeatedly observed throughout the literature (Figure 1-4).
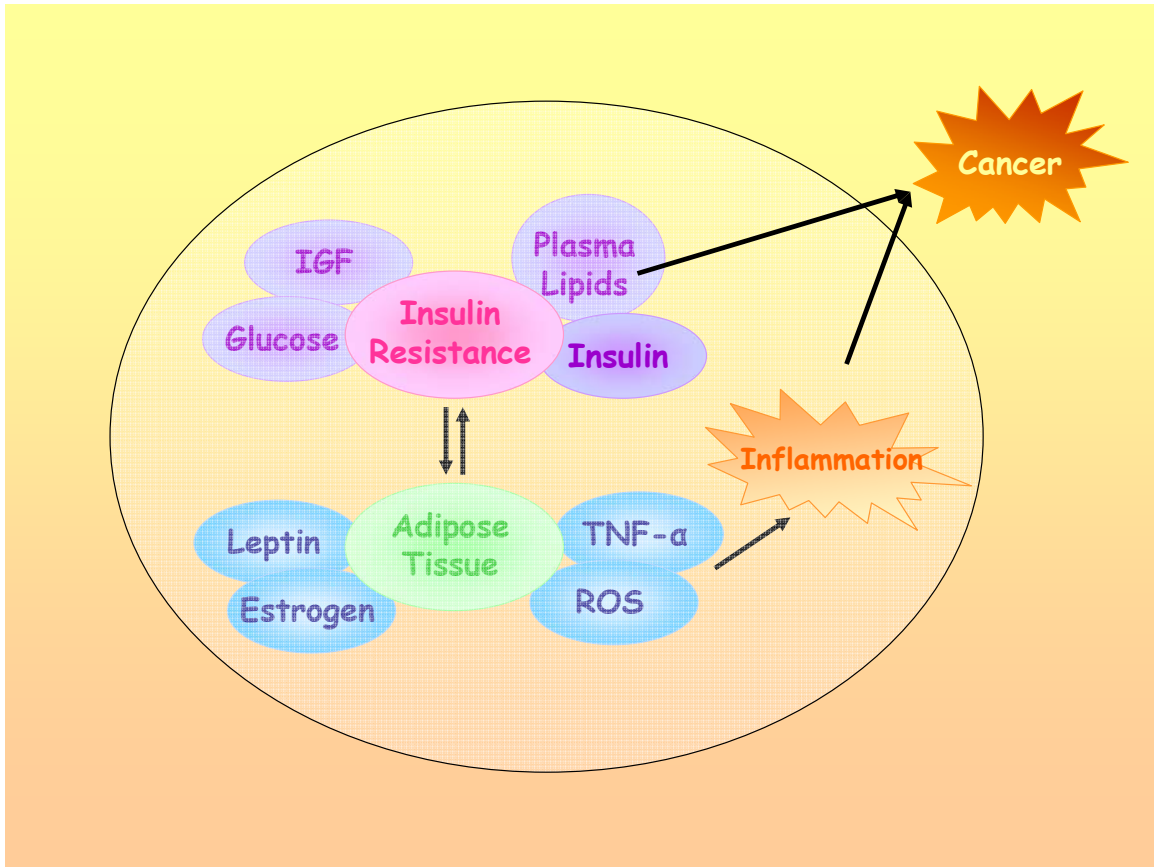
Figure 1-4: Pathogenic mechanisms linking obesity and colon cancer.

Pathogenesis of obesity is attributed to multiple factors such as inflammation, insulin resistance, and constituents secreted by adipose tissue. The combination of these variables influence and augment each other, creating a favorable environment for carcinogenesis.

Insulin resistance implies a cells inability to respond to normal levels of insulin, thus requiring abnormally high amounts of hormone for glucose metabolism. This condition further leads to irregular triglycerides, fatty acids and glucose levels, all metabolic aberrations that also correlate with an increased risk of colorectal cancer (Gunter and Leitzmann 2006). An emerging body of evidence emphasizes three possibilities that associate insulin resistance with colon cancer risk (reviewed in Gunter and Leitzmann 2006). Firstly, insulin itself is a growth factor, and exposure of high amounts to parts of the body that are otherwise not accustomed can interfere with normal cell signaling and promote cell proliferation. Insulin is observed to promote cell growth and proliferation in colon cancer cells (Gunter and Leitzmann 2006). Additionally, Kiunga et al. (2004) demonstrated elevated protein levels of insulin and insulin receptor in tumors compared to normal colonic mucosa.

Secondly, an insulin resistant state also promotes high levels of circulating insulin-like growth factor (IGF), which can also promote colonocyte division and block apoptosis by receptor binding (Giovannucci 2001). Increased IGF-1-receptor (IGF-IR) also stimulates cell division in intestinal epithelial cells (Ma et al. 1999), and several epidemiological studies have shown positive correlation between IGF and IGF-IR levels and colon cancer risk (Komninou et al. 2003).

Finally, the high circulating plasma glucose and lipids associated with insulin resistance serve as a reservoir for reactive oxygen species (ROS) generation, known contributors to carcinogenesis. High visceral abdominal fat found in obese individuals is especially a critical source for ROS (Furukawa et al. 2004, Frezza et al. 2005).

Along with oxidative stress, increased amount of fat tissue promotes a pro-inflammatory environment, also strongly correlates with increased cancer risk. Cytokines/adipokines such as tumor necrosis factor-α are readily secreted by adiopcytes, and further enhance inflammation, insulin resistance, impaired glucose metabolism, and ROS production (Furukawa et al. 2004, Sonnenberg et al. 2004).

Leptin, the hormone for satiety, has also been implicated in obesity associated colon cancer. Leptin has been shown to increase proliferation of HT-29 cells, and promote ACF formation *in vivo* (Liu et al. 2001). Conversely, F344 rats administered continuous leptin injections had reduced number of ACF in comparison to the controls (Aparicio et al. 2004). Leptin secreted from adipose tissue has also

been shown to enhance insulin resistance (Matsuzawa 2006). Thus, the role of leptin is not fully known, and under active review.

1.4.1 Metabolic Syndrome X

Metabolic syndrome, or syndrome X, first termed by Reavan in 1988 coins together physiological disorders associated with obesity, and specifically abdominal/visceral obesity. Although there is debate on the exact parameters, conditions such as insulin resistance and resulting dyslipidaemia (including hypercholesterolemia and hypertriglycerolemia), hyperglycemia, and hypotension are inclusive to this definition (Shaw et al. 2005, Sorrentino 2005). These abnormalities are further associated with physiological aberrations such as cancer, diabetes, and heart disease.

The concept of the metabolic syndrome allows for a comprehensive approach towards obesity in terms of investigating pathogenic relationships (Shaw et al. 2005). It may also be used as a preliminary diagnostic to determine the risk for heart disease and diabetes, thus facilitating implementation of appropriate treatment plans of which diet and exercise are important components (Stone and Saxon 2005, Sorrentino 2005).

Pathological origin of this condition is yet to be determined as the many complex relationships between several disorders seemingly precede one another, although insulin signaling pathways are a convincing common point (Shaw et al. 2005). From here, metabolic dysfunctions cascade and upregulate each other, creating favorable circumstances for carcinogenesis. From a single cell perspective, physiological disorder affects functioning of signaling pathways, ultimately disrupting the balance between proliferation and apoptosis.

1.5 Animal Models

Animal models provide the opportunity to study the biology of disease processes in a physiologically relevant state to humans. Along with the disease pathology itself, cellular and molecular events may be targeted in a somewhat environmentally and genetically controlled system (Green and Hudson 2005). Moreover, animal models offer valuable preliminary data upon which human clinical trials can be based. Further advantage of using an *in vivo* model is that tumor biology with regards to three-

dimension morphology, angiogenesis, metastasis, and tissue interaction may be studied in a relevant physiological setting (van Weerden and Romijn 2000). Although, animal studies should always be evaluated with regards to how relevant they are to human conditions, and how predictive they can be for the disease process (Green and Hudson 2005).

With regards to colon carcinogenesis, molecular and pathological similarities to the human condition should be observed in order to have an effective model (Reddy 2004). Among the most widely used, include the carcinogen injected azoxymethane rodent model and *Apc*Min mice model. Zucker obese rats, traditionally used to study obesity and related metabolic disorders, offer a novel way of studying the progression of cancer in an altered physiological state.

Azoxymethane Model

Malignant transformation of cells may be induced by a variety of agents such as irradiation, oncogenic manipulation and chemical carcinogens, the latter of which are commonly used for animal studies (Corpet and Pierre 2003). These may act directly to either initiate carcinogenesis, or require *in vivo* metabolism for activation (Cotran et al. 1999). Procarcinogen 1,2-dimethylhydrazine (DMH) and its metabolite, azoxymethane (AOM), (Figure 1-5), are commonly used hydrazine carcinogens that are metabolized into methylazoxymethanol (MAM), first identified and isolated from the cycad flower by Laquer and Spatz (1963). In turn, MAM is converted to methyldiazonium which can induce neoplastic transformation via methylation of DNA, RNA and proteins of colonic epithelial cells (Greene et al. 1987).

AOM and MAM are conveniently used colon specific carcinogens of choice that are easily prepared in saline solutions, and injected into rats subcutaneously at optimal dosages of 10-20mg/kg body weight (Bird 1998). Rats are the species of choice for these studies as they are more responsive to the carcinogen than mice which require several administrations to develop colonic tumors. Sprague-Dawley and Fischer F344 rats are common strains to study AOM initiated colon cancer (Nauss et al. 1987).

Historically the AOM model has provided valuable information on colon cancer, and has been used in numerous studies testing different chemopreventative agents (Reddy 2004). Furthermore, AOM-induced ACF and tumors exhibit similar histopathological characteristics to those found in humans

(Franks and Teich 2001). Moreover, tumors induced by AOM similar have mutations in *K-ras* and β-catenin genes, but seldom in the *Apc* gene, and almost never at p53 (Green and Hudson 2005). A limitation of the AOM model is that the cancer itself is of murine origin, rather than human, and it is specifically induced by a chemical (Pocard et al. 1996).

Studies looking at ACF as an endpoint biomarker require a duration of 8 weeks after AOM injection, while a 24-52 week period is sufficient to observe tumor formation. About 5-10 animals per group are desirable to achieve statistical significance, and adequately study characteristics of the colonic lesions (Bird 1997).

$$\overset{\displaystyle O}{\underset{\displaystyle \uparrow}{}}$$

CH3N=NCH
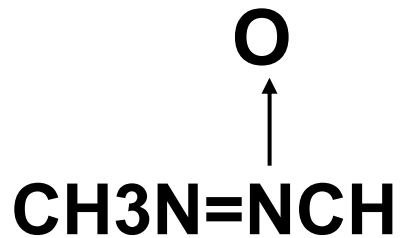
Figure 1-5: Chemical structure of AOM.

Colon specific carcinogen AOM is metabolized into methyldiazonium, which induces neoplastic transformation of colonocytes via methylation of DNA, RNA and proteins.

Zucker-Obese Animal Model

There is substantial epidemiological evidence supporting a strong correlation between obesity associated metabolic disorders with an increased risk of colon cancer (Giovannucci 2001, Gerber and Corpet 1999). Zucker obese (Zk-Ob) rats are an excellent model of human obesity, and provide an ideal opportunity to study colon carcinogenesis in an altered physiological state (Figure 1-6).

The journey of the Zucker or "fatty" rat began as a spontaneous mutation in a single recessive gene (*Fa* allele is designated as normal, while *fa* is the fatty mutation) in the laboratory of Zucker and Zucker (1961). Zk-Ob rats inherit obesity as an autosomal Mendelian recessive trait, fa/fa homozygous for nonfunctional leptin receptors, in comparison to their lean (Fa/fa or Fa/Fa) counterparts (Bray 1977). Leptin, a peptide hormone produced by adipocytes, regulates body weight and fat metabolism by sending signals to the hypothalamus to suppress appetite (Moore and Dalley 1999). Obesity in these rats is associated with metabolic dysfunction of fat as seen by lactescence and an increased amount of adipose tissue (Zucker and Zucker 1962). Genetic association of *fa* gene to obesity is confirmed as Zk-Ob rats on low fat or energy restricted diet also exhibit these symptoms. Interestingly, female Zucker rats are sterile, which has implications for breeding programs.

Average weights of these animals at 40 weeks is 800g and 625g for Zk-Ob, and 480g and 295g for Zucker lean (Zk-Ln), males and females respectively (Zucker and Zucker 1962). Zk-Ob rats exhibit hyperphagia, hypertriglyceridemia, hypercholesterolemia, hyperinsulinaemia and mild hyperglycemia at about six weeks of age. Pathological findings at death often include hydronephrosis and polycystic kidneys, as well as fatty livers (Zucker and Zucker 1962). It has been shown that Zk-Ob rats are more sensitive to chemically induced colon carcinogenesis in comparison to their lean counterparts (Raju and Bird 2003). Since there is little difference in ACF number between Fa/fa and Fa/Fa animals, the recessive gene linked to leptin receptor deficiency is not solely responsible to higher susceptibility of colon cancer (Weber et al. 2000). Use of this animal model will help to understand carcinogenesis in relation to obesity and associated metabolic disorders, providing valuable information for treatment and prevention strategies.

Figure 1-6: Zucker obese rat and its lean counterpart.

Zk-Ob rats inherit obesity as an autosomal Mendelian recessive trait, fa/fa homozygous for nonfunctional leptin receptors, as compared with their lean (Fa/fa or Fa/Fa) counterparts. Zk-Ob rats are an excellent model of human obesity, and provide an ideal opportunity to study colon carcinogenesis in an altered physiological state

Chapter 2

Tumor Necrosis Factor-α

2.1 Background

Tumor necrosis factor-α (TNF-α), a pleiotropic, pro-inflammatory cytokine part of the TNF ligand superfamily, is produced primarily by immune cells such as macrophages, neutrophils, natural killer cells, T and B lymphocytes, as well as tumor cells (Anderson et al. 2004). TNF-α plays a key role in the inflammatory process and modulates tissue damage and restoration via different mechanisms including chemokine and cytokine promotion, as well as extravasation of leukocytes (Varfolomeev et al. 2004, Balkwill 2002).

Excessive levels of TNF-α are associated with pathological disorders related to pro-inflammatory conditions such as arthritis and inflammatory bowel disease (Wajant et al. 2003). Inhibition of this cytokine in these circumstances has been observed to be beneficial. Additionally, TNF-α plays pivotal roles in cell death and survival signaling mechanisms, and is a key target for understanding cancer progression and related treatment strategies.

History

Coley's observation of tumor regression in patients when injected with bacterial cultures contributed to the concept of the immune response towards cancer (Coley 1906). Upon further study, TNF-α was identified and associated as one of the key molecules involved in this observation. cDNA of TNF-α was cloned in 1984, upon which its structural similarity to lymphotoxin was demonstrated (Pennica et al. 1985).

Since then, much attention has been focused on the potential of TNF-α as a possible cancer therapeutic as exogenous treatment with this cytokine has potent anti-tumor properties (reviewed in Balkwill 2002). Direct injection of TNF-α is associated with necrosis and vascular damage to xenograft tumors in mice, effects which are amplified with the addition of interferon (IFN). Induction of apoptosis, mediation of CD8+ T cells, and inhibition of angiogenesis in tumors are further consequences of TNF-α therapy (Balkwill 2002).

However, the highly toxic side effects of TNF-α such as organ failure and hypotension, in addition to the effective dose being much higher than the tolerated dosage, limit the usage of this cytokine in cancer therapy (Lejeune et al. 1998). Currently, TNF-α treatment involving hemorrhagic necrosis of tumors is approved for soft tissue sarcomas and superficial lesions in Europe (Anderson et al. 2004).

2.2 TNF-α and Cancer

TNF-α has contradictory effects with regards to cancer therapy; tumor regression is observed with exogenous administration of high doses, while endogenous levels of TNF-α is associated with promotion of tumor growth (Anderson et al. 2004). This is perhaps one of the most interesting aspects of the TNF-α and cancer relationship, and has been subject to great scientific controversy. The dual effects of TNF-α may be correlated to its signaling pathways which mediate both cell death and survival, and will be discussed further on.

High levels of TNF-α present in the tumor microenvironment promote conditions conducive to inflammation and cancer. Interestingly, TNF-α mediates changes in tumor architecture in a manner similar to the inflammatory response, and stimulates fibroblast production and changes to tumor angiogenesis (Balkwill 2002). TNF-α also induces DNA damage through inhibition of DNA repair enzymes and stimulation of inducible Nitric Oxide synthase (iNOS). Continuous exposure of HT-29 colon adenocarcinoma cells to TNF-α results in increased production of ROS via iNOS, an effect that is known to augment tumor development (Seidelin and Nielson 2005).

Tumor cells can contribute to TNF-α production and manipulate surrounding cells to secrete more cytokines, facilitating tissue damage (Dranoff 2004). The communication between cancer and normal cells further plays critical roles in initiating signaling pathways that may result in cell death or survival.

TNF-α mRNA has been detected in a variety of cancers, and clinical observations have demonstrated high protein levels in the plasma of cancer patients (Balkwill 2002). In addition, individuals having an advanced stage of disease have higher levels of TNF-α in comparison to those at earlier phases (Anderson et al. 2004). Interestingly, the association between malignancies and high plasma cytokine

levels has been substantiated by the increased frequency of a single nucleotide polymorphism at TNF-308 (Warzocha et al. 1998).

The role of TNF-α as a pro-cancerous cytokine has also been extensively studied in mice models using DMBA as a DNA damaging tumor inducer, and TPA/okadaic acid as a tumor promoter (Suganuma et al. 1999). TNF-α deficient mice had only 10% tumor incidence and delayed onset of tumors in comparison to the 100% incidence in control mice. TNF-α knockout mice being more resistant to tumor development further reinforces the pro-cancerous consequences of this cytokine (Suganuma et al. 1999).

Due to the role of TNF-α in cancer and inflammation related diseases, development and testing the efficacy of inhibitory drugs is of great interest. There are currently two TNF-α inhibitors that are licensed for clinical trials in the US for rheumatoid arthritis and Crohn's disease. Infliximab (also known as Remicade and Centocor) is a murine monoclonal antibody with a 75% humanized homology, and neutralizes human TNF-α by binding to it, and preventing receptor activation (reviewed in Braun and Sieper 2003). Etanercept (also known as Enbrel or Immunex), another TNF-α inhibitor, mimics solubilized human TNFR2 receptor - the Fc portion of human immunoglobulin is fused with extracellular portion of the receptor- and binds TNF-α (reviewed in Balkwill 2002). Safety and efficacy of this drug has been studied in phase II clinical trials for metastatic breast carcinoma, and the incorporation of Etanercept in chemotherapy is being considered (Madhusudhan et al. 2004).

These drugs are effective in alleviating symptoms of inflammation via inhibition of cytokine production, leukocyte infiltration, as well as angiogenesis (Charles et al. 1999). As inflammation and cancer share an intimate relationship, further investigation into using TNF-α inhibitors in a complimentary approach towards the two diseases is warranted.

2.3 TNF-α Structure

TNF-α is produced as a homotrimeric transmembrane protein, and then released in soluble homotrimeric form by TNF-α converting enzyme (TACE), a membrane bound metalloproteinase (MMP) (Wajant et al. 2003). Protomers of TNF-α are 17kDa each and composed of two anti-parallel beta sheets (Ecks and Sprang 1980). Both soluble and membrane bound forms of TNF-α exist, and

bind primarily with tumor necrosis factor receptor-1 (TNFR1) and tumor necrosis factor receptor-2 (TNFR2) receptors respectively (Varfolomeev and Ashkenazi 2004).

2.4 TNF-α Receptors

TNF-α mediates its effects through receptors TNFR1 (CD120a) and TNFR2 (CD120b) with molecular weights of 55-60 and 75-80 kDa respectively (Hohmann et al. 1989). The TNF-α receptors share very little homology, indicating that they may mediate different functions (Beyaert et al. 1994). Unlike TNFR1 which is commonly expressed in most cells, especially those of epithelial origin, TNFR2 is quite regulated and found mainly in immune and haematopoetic cells (Wajant et al. 2003). Interestingly, both receptors can bind lymphotoxin, most probably due to its structural similarity with TNF-α. Other cytokines such as interleukins (IL) and IFN can regulate TNFR expression as well (Higuchi and Aggarwal 1994a).

Signals mediated through TNFR are diverse, and may also have similar effects through distinct mechanisms. Depending on the outcome of the signaling pathway, activation of single or both receptors must occur (Thommesen and Laegeid 2005). Functional differences between TNFR1 and TNFR2 concerning cytotoxicity, DNA damage, and macrophage differentiation have been observed (Higuchi and Aggarwal 1994b). In some instances, the two receptors have opposing effects; while TNFR2 promotes cell survival, TNFR1 is more favorable towards mediating cell death (Fontaine et al. 2002). Cells lines expressing either TNFR1 or TNFR2 were used to confirm that cytotoxicity is mainly mediated through TNFR1 (Higuchi and Aggarwal 1994b). Lack of a cytoplasmic death domain in TNFR2 is attributed to its preferential cell survival signaling.

2.4.1 Soluble Receptors

While TNF-α receptors are mainly membrane bound, they can also be found in active soluble form, mimicking paracrine type actions (Lotz et al. 1996). Extracellular domains of receptors may be cleaved by TACE, leaving soluble fragments which have capacity to neutralize circulating TNF-α (Keith et al. 2000, Wajant et al. 2003). Soluble forms of both TNFR1 (sTNFR1) and TNFR2 (sTNFR2) have the ability to bind, as well as release TNF-α, although membrane bound TNF-α is more keen towards activating sTNFR2. (Teddy et al. 1994). This in turn can have two effects: 1)

soluble receptors act as inhibitors by binding to TNF-α, thus rendering it unavailable, or 2) they act as reservoirs for TNF-α, releasing it slowly and prolonging its biological effects. While response (1) is seen with high receptor concentrations, lower concentrations of soluble receptors stabilize the structure of TNF-α and actually augment its activity (Aderka et al. 1992). Unlike sTNFR2, sTNFR1 expression seems to be more indifferent towards responding to circulating TNF-α (Vandenabeele et al. 1995).

Usually the effects of soluble receptors are most critical in an environment of high cytokine production, as they can augment the biological activity of TNF-α (Rojas-Cartagena et al. 2005). Increased numbers of soluble receptors in colitis for example, increase and prolong TNF-α activity, thus enhancing the detrimental effects to the colon. Interestingly, the shedding of TNFR2 was more closely associated with colonic damage rather than TNFR1 in mice with colitis (Rojas-Cartagena et al. 2005).

Desensitization of receptors towards TNF-α is also possible, and occurs through internalization of TNFR1 and shedding of TNFR2 (Higuchi and Aggarwal 1994a). Prolonged exposure to TNF-α in U-937 cell line downregulated receptor expression in a time and concentration dependant manner. Number of receptors, but not their affinity, was decreased. Why the TNFR2 is shed as opposed to TNFR1 is not known. Evaluating levels of both membrane bound and soluble receptor forms is important when investigating the biological function of TNF-α (Higuchi and Aggarwal 1994a).

Soluble receptors are regarded as potential indicators of cancer due to high amounts shed by tumors, and may be correlated to disease progression (Langkopf and Atzpodien 1994). Levels of soluble receptors are increased in patients with ovarian cancer in comparison to those with benign lesions (Gadducci et al. 1995). Furthermore, patients with melanomas also showed high levels of sTNFR1, while a predominant amount of sTNFR2 was observed especially in metastatic lesions (Viac et al. 1996).

2.5 TNF-α Signaling Pathways

Upon binding to its receptors, TNF-α initiates signaling cascades mediating both cell death and survival. This dual effect of TNF-α has been under great speculation, and is particularly of interest in

conditions such as cancer where dysregulation of cell death contributes to disease progression. TNFR1 and TNFR2 can initiate both apoptotic and cell survival signaling cascades, and are discussed below.

TNFR1 Signaling Pathway

A model of the TNF-α signaling pathway mediated through TNFR1 is extensively described by Ashkenazi and Dixit (1998) and describes the formation of two intracellular complexes upon ligand-receptor binding (Figure 2-1). A cell survival signal is elucidated via stimulation of NF-κB by the first complex, while the second induces apoptosis through caspase activation. If this second complex is removed from the initial receptor complex, its effects may be counteracted via signaling of other anti-apoptotic gene products from the NF-κB pathway (Micheau and Tschopp 2003).

Formation of complex 1, which is plasma membrane bound, involves the death domains (DD) of TNFR1 to recruit TNF Receptor 1 associated death domain (TRADD) adapter molecules. TRADD then activates receptor interacting protein (RIP), which can activate the MAPK/JNK pathway via TNF Receptor Associated factor 2 (TRAF2) activation. The NF-κB pathway may also be initiated at this point, and induce a cell survival signal (Ashkenazi and Dixit 1998, Micheau and Tschopp 2003).

Complex 2, a cytoplasmic complex, originates when complex 1 starts to dissociate. As the TRADD and RIP detach, their DD are fee to bind with other molecules such as Fas associated death domain (FADD). Joining of FADD with TRADD enables caspase 8 recruitment, resulting in apoptosis (Micheau and Tschopp 2003). Importantly, complex 2 formation is dependant on FADD, which can also be recruited to the membrane by Fas ligand (Fas$_L$) (Ashkenazi and Dixit 1998). Apoptosis may be also initiated via caspase 2 through the binding of RIP associated Ich-1/CED with death domain (RAIDD) to the RIP and TRADD complex, further emphasizing that different components of DD and adaptor molecules may mediate the signal to be elicited (Duan and Dixit, 1997).

Thus, the outcome of the TNF-α signaling pathway is dependant on the modification of the initial TNF-α/TNFR1 complex 1; dissociation of this complex results in apoptosis, while the intact complex mediates cell survival though the NF-κB pathway. While factors affecting this decision are still being speculated, a possible influence is the Fas$_L$ which facilitates the migration of FADD to the plasma

membrane. Downregulation of the Fas_L has also been associated with enhanced cancerous growth *in vivo* (Philips et al. 2004).

The FLICE inhibitory protein ($FLIP_L$) switch, a potent inhibitor of TNF-α mediated apoptosis via blocking caspase 8, is another candidate that may affect the outcome of the signaling pathway (Micheau and Tschopp 2003). Complex I stimulates increased expression of $FLIP_L$ along with inhibitor of apoptosis proteins (IAP) via NF-κB transcriptional activity. If NF-κB pathway is not initiated however, the $FLIP_L$ activity diminishes and is not able to prevent caspase activation and resultant cell death. $FLIP_L$ production and availability is dependant on the activation of NF-κB, thereby creating a checkpoint in the signaling pathway (Micheau and Tschopp 2003). In addition, cells that cannot produce $FLIP_L$ may eventually be eliminated via TNF-α mediated apoptosis. It should be noted that the NF-κB can also mediate cell death, and this is discussed further in Chapter 3.
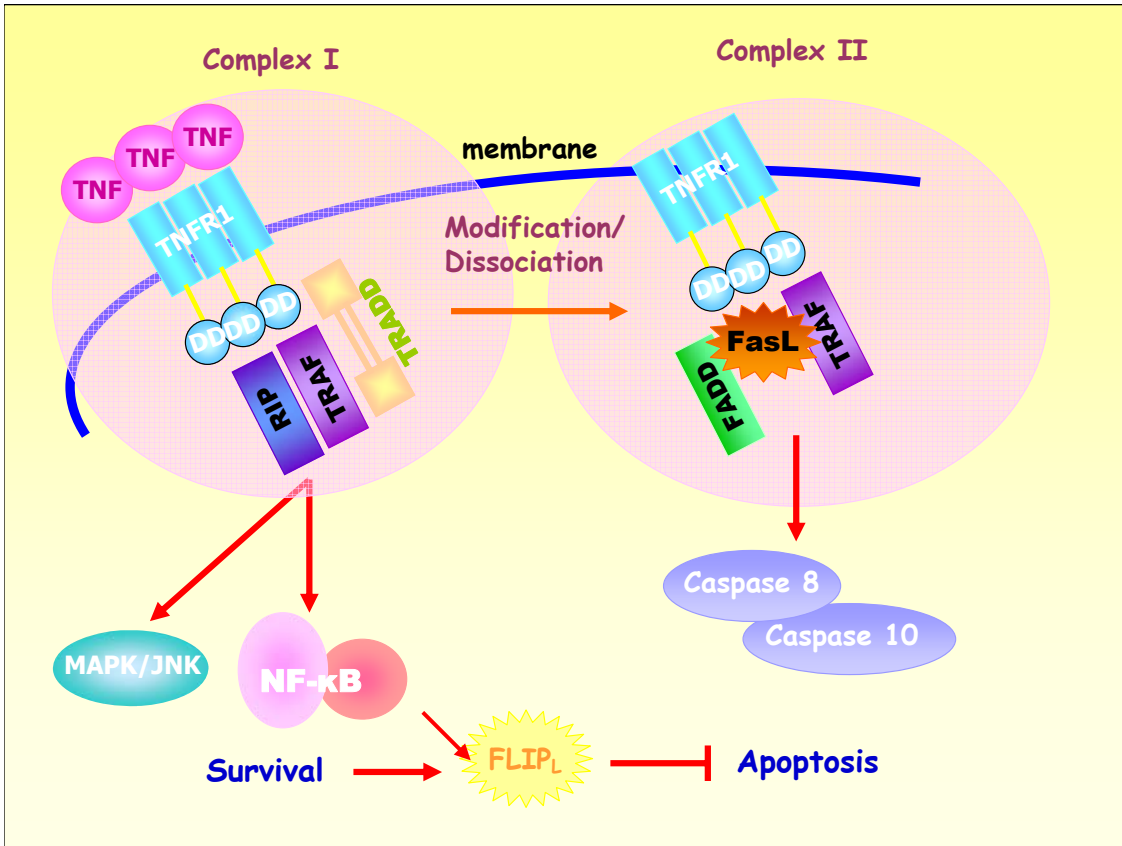
Figure 2-1: TNF-α signaling pathway via TNFR1.

Schematic representation of pathways initiated by the TNF-α and TNFR1 complex: Complex 1 initiates a cell survival pathway via NF-κB and MAPK/JNK activation. Dissociation of Complex 1 leads to formation of Complex 2, which is conjugated with Fas$_L$ recruited FADD. As a result, caspase 8 and 10 are recruited to induce apoptosis. FLIP$_L$, transcribed by NF-κB, is a potent inhibitor of caspase 8 mediated apoptosis and acts as a checkpoint in the signaling pathway.

TNFR2 Signaling Pathway

TNFR2 receptor lacks death domain complexes, thus activation of NF-κB is usually associated with TRAF1, 2, 3, and upregulation of cIAP. Conversely, TNFR1 interacts with death domains of TRADD, FADD and RIP adapter molecules. Signals elicited by the two receptors with regards to NF-κB activation are distinct, and inhibitors of TNFR1 mediated NF-κB activation have no effect on TNFR2 signaling (Thommesen and Laegeid 2005). TNFR2 may also mediate TRAF2 degradation, favoring the apoptotic outcome (Varfolomeev and Ashkenazi 2004). This may be confirmed with the earlier stated observation that occurrence of TNF-α associated DNA fragmentation requires a signal from TNFR2 (Higuchi and Aggarwal 1994b). Although the mechanisms of the pathway elicited through TNFR2 are still being clarified, it has been observed that activation of both receptors increases the apoptotic effect of TNF-α (Wajant 2003).

Thus, the TNF-α stimulus and resultant complex formation may interact and affect the final outcome of cell death or survival, demonstrating the importance of signaling and communication within the cell. Once stimulated, TNF-α can initiate a negative feedback signal to terminate the pathway via downregulation or solubilization of receptors (Balkwill 2002). Continuous binding of TNF-α to its receptors in aberrant physiological circumstances can promote inflammation and cancer.

Sphingo-ceramide Pathway

The sphingo-ceramide pathway initiates upon TNF ligand-receptor binding and involves activation of phosphatidylcholine-specific phospholipase C, leading to the production of 1,2-diacylglyercol (DAG). In turn, DAG stimulates the production of ceramide via acidic sphingomyelinases present in cell endosomes (Schutze 1995). Ceramide may then induce NF-κB activation via IκB degradation (Yang et al. 1993).

2.6 TNF-α and Obesity

Obesity, associated with a number of diseases such as cancer and heart disease, is also accompanied by physiological dysfunctions such as abnormal metabolism and elevated productions of hormones and pro-inflammatory molecules (Galisteo et al. 2005).

Chronic elevation of TNF-α, TNFR1, and TNFR2 in an obese physiological state have been observed in both obese human and animal studies (Samad et al. 1999, Hotamisligil et al. 1993). High plasma concentrations of TNF-α determined by ELISA, and mRNA expression in adipocytes via Northern blot (Hotamisligil et al. 1993), and RT-PCR (Hoffman et al. 1994) are documented. Furthermore, these studies have established that elevated levels of TNF-α in an obese state contribute to insulin resistance (Samad et al. 1999). Interestingly, an increased responsiveness to insulin was seen upon neutralization of TNF-α, and animals injected with a recombinant, soluble TNFR presented a two to three fold increase in insulin mediated glucose metabolism (Hotamisligil et al. 1993). Additionally, treatment of animals with an insulin sensitizer decreased TNF-α and TNFR mRNA expression, suggesting a working relationship between TNF-α and insulin resistance (Hoffman et al. 1994).

Effects of TNF-α on lipid metabolism have also been studied, yet results are conflicting. Although a high TNF-α level may be associated with cachexia, it is also known to stimulate lipogenesis, and modulate lipid and glucose metabolism (reviewed in Hotamisligil et al. 1993). Conversely, TNF-α can also mediate apoptosis in adipocytes of obese mice (Nelson-Dooley et al. 2005).

2.7 TNF-α and HT-29 Colon Cancer Cells

One of the first colon adenocarcinoma cells lines, HT-29, was developed in 1964 by Jorgen Fogh from the Memorial Sloan-Kettering Cancer Center, New York (Fogh and Trempe 1975). This cell line offers a valuable model system to study colon carcinogenesis, and is used extensively to screen and evaluate the efficacy of chemopreventative agents. Response of HT-29 cells to TNF-α is similar to those of freshly isolated intestinal epithelial cells, making them relevant for studying actions of this cytokine (Jung et al. 1995).

HT-29 cells are relatively resistant to TNF-α mediated cytotoxicity unless exposed to extremely high concentrations, or prolonged exposure times in comparison to other colon cancer cell lines (Vaculova et al. 2002). When exposed to 10ng/mL TNF-α during a 3 week time period to look at chronic effects, no obvious morphological changes, and marginal decline in cell growth was observed (Bruno and Kaetzel 2005). In general, effects of TNF-α on other cancer cells are usually seen either very quickly (minutes to an hour) or after a long duration (hours to days) (Beyaert et al. 1994).

Apoptosis due to extensive TNF-α treatment in a reduced serum environment is accompanied by poly (ADP ribose) polymerase (PARP) cleavage (Vaculova et al. 2002). PARP, a 113 kDa DNA repair enzyme cleaves into 85 and 25 kDa fragments during apoptosis.

Cancer cell lines become more responsive to TNF-α mediated cytotoxicity with the addition of other agents like IFN-γ and α (Kimura et al. 2003). IFN-γ also augments TNF-α impairment of the epithelial barrier functionality in HT-29 cells (Schimtz et al. 1999). Additionally, TNF-α and IFN-α have been shown to enhance expression of the Fas_L, which may contribute to their strong cytotoxic effect. Interestingly, this combination also activates NF-κB more strongly than the individual compounds themselves (Kimura et al. 2003).

Chapter 3

Nuclear Transcription Factor-κB

3.1 Background

Upon environmental stimuli, cells recognize and activate intrinsic pathways, creating a response appropriate for maintaining a homeostatic balance. In order for this biological consequence to succeed, transcription factors controlling gene expression play a significant role in regulating communication between the stimulus and final outcome.

Nuclear transcription factor-κB (NF-κB) is a transcription factor having multiple roles in different biological processes (Figure 3-1). Genes transcribed by NF-κB have numerous functions and dysregulation results in physiological impairments such as inflammation and cancer (Lin and Karin 2003). In addition, crucial roles of NF-κB in the regulation of cell death and survival have been linked to carcinogenesis, thus making the many components of the NF-κB signaling pathway targets for cancer therapies.

Ubiquitous cytoplasmic expression of dormant NF-κB is found in all cell types. Upon activation of the signaling pathway, NF-κB translocates to the nucleus and binds to the promoter region of target genes to induce transcription (Viatour et al. 2005). Gene products that are generated by NF-κB activation are diverse, and further influence cell death and survival (Lin and Karin 2003). As discussed, the outcome of TNF-α pathway is also intimately affected by NF-κB.
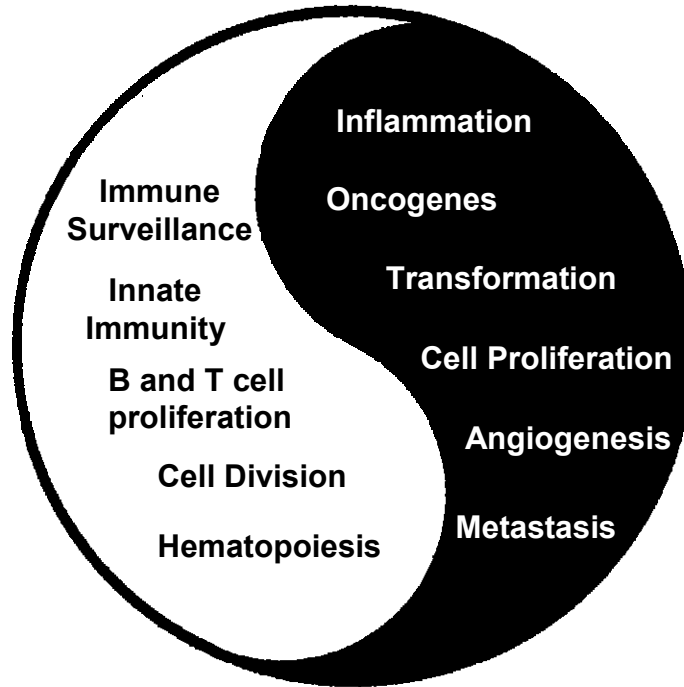
Figure 3-1: Multiple Roles of NF-κB.

Under normal circumstances, NF-κB regulates immune activity and cell division. Conversely, dysregulation is associated with inflammation and cancer promotion via cell proliferation, transformation, metastasis etc. (adapted from Shishodia and Aggarwal 2004).

History

NF-κB and DNA binding was first observed in 1986 in murine B cells (Sen and Baltimore 1986). Soon after, the inhibitor of NF-κB (IκB) subunit was identified as a inhibitory molecule which localizes NF-κB in the cytoplasm, and could be dissociated by treatment with certain detergents (Baeuerle and Baltimore 1988). Gene cloning of different NF-κB subunits such as p50/p105 took place in the1990s in different laboratories, and paved the way for identifying other parts of NF-κB family (reviewed in Seibenlist et al. 1994).

3.2 Components of NF-κB Pathway

NF-κB Subunits

NF-κB exists as dimers consisting of the following subunits: RelA (p65), RelB, c-Rel, NF-κB1 (p105/p50), and NF-kB2 (p100/p52). All subunits have Rel homology domains (RHD), a common, conserved sequence of 200 amino acids involved in binding the subunits together, as well as with DNA, and the inhibitory IκB molecule (Viatour et al. 2005). Only the RelB subunit does not form homodimers, while the p105 and p100 are processed into p50 and p52 DNA binding subunits post translation. The mechanism of p105 and p100 processing is unclear, although the N terminus containing the RHD binds to DNA while the C terminus is degraded (Siebenlist et al. 1994).

Properties of the NF-κB dimers vary depending on their composition, and can either activate or suppress gene transcription, or both (Bonnizi and Karin 2005, Perkins and Gilmore 2006). For example, homodimers of p50 or p52 subunits are weak gene activators in comparison to their heterodimerized form with p65 (Siebenlist et al. 1994). Additionally, characteristics such as expression, rate of nuclear translocation and location of κB binding sites are influenced by dimer composition (Molitor et al. 1990).

IκB

NF-κB dimers are bound at the RHD to IκB inhibitor molecules which prevent nuclear translocation. IκB also works by inhibiting the extrinsic nuclear localizing signal of NF-κB, thus further preventing its migration to the nucleus (Foo and Nolan 1999).

IκB exists in different forms (IκBα, β, γ, ε, and ζ, and BCL3), all of which have ankyrin repeats that facilitate binding to the RHD (Nakanishi and Toi 2005). Interestingly, the p105 and p100 NF-κB subunits also have these same ankyrin repeats, and can function as inhibitors of NF-κB as well (Bonizzi and Karin 2005). Different forms of IκB may preferentially interact with specific dimers; IκBα and β combine with p65/p50 and Rel/p50 subunits, while BCL3 joins with p50 and p52 (Foo and Nolan 1999).

Upon activation of the signaling pathway, IκB is phosphorylated and the NF-κB subunits migrate to the nucleus where they can transcribe genes for IκB. As a result, cytoplasmic levels of IκB are replenished. This negative feedback contributes to inhibiting further NF-κB activation (Foo and Nolan 1999). The newly transcribed IκB can also bind to nuclear NF-κB and re-shuttle it back to cytoplasm, thus terminating transcriptional activity (Hayden and Gosh, 2006). IκBβ and ε are not transcribed by NF-κB, and can also contribute indirect to negative feedback (Hoffman et al. 2002).

The role of IκB is not essential in all cell types. In B lymphocytes for example, levels of NF-κB in the nucleus are constitutive, thus making IκB degradation non-essential for NF-κB activation (Doerre and Corley 1999).

IKK

IκB kinase (IKK) is important for the phosphorylation of IκB-NF-κB complex, thereby freeing NF-κB and facilitating its move to the nucleus. Previous studies have demonstrated that out of the three kinds of kinases, α, β, and γ, IKKβ is more functional in the cytokine induced pathway, IKKα in the alternative pathway, while IKKγ (also referred to as NF-κB essential modulator, NEMO) regulates the other two kinases (Russo et al. 2002, Hayden and Ghosh 2006). Dominant negative expression of IKK has been demonstrated to block the NF-κB signaling cascade (Russo et al. 2002). Interestingly, IKK can also affect other transcription factors and pathways involving histones, and estrogen receptors (reviewed in Perkins and Gilmore 2006).

3.3 NF-κB Signaling Pathways

There are two NF-κB pathways, Classical/Canonical and Alternative, which are thought to be distinctly involved in innate or adaptive immunity respectively. The classical pathway is stimulated by cytokines such as TNF-α, while the alternative pathway involves activation by members of TNF-α

superfamily (excluding TNF-α) and receptors such as lymphotoxin-β and C-cell activating factor (Bonnizzi and Karin 2004). The sequential steps of these pathways are observed to be cell specific, and continue to be explored and verified.

Different components of the NF-κB pathway are observed to be essential for the outcome of cell death or survival. For example, presence of the NF-κB p65 subunit is necessary for cells to resist toxicity from TNF-α (Beg and Baltimore 1996).

Classical Pathway

The classical/canonical pathway of NF-κB is associated with innate immunity, and results in transcription of molecules such as chemokines, cytokines, and cell adhesion molecules (Viatour et al. 2005). Along with pro-inflammatory cytokines such as TNF-α, pathogens may also initiate this pathway, and stimulate the production of mediator molecules directing phagocytosis (Bonnizi and Karin 2005).

Upon the binding of TNF-α and TNFR1, the silencer of death domain (SODD) is released and transfers adapters TRADD, RIP and TRAF2 onsite. This in turn stimulates the recruitment and modification of the IKK complex consisting of IKKα and β conjugated with NEMO/IKKγ (Perkins and Gilmore 2006). Phosphorylation of IKKγ and IKKβ initiates phosphorylation of IκB at Ser residues 32 and 36. Ubiquitinized proteosome degradation of IκB enables the dissociation of the NF-κB/IκB complex, allowing the free NF-κB dimer to migrate into the nucleus and stimulate gene transcription (Figure 3-2) (Viatour et al. 2005). NF-κB may upregulate its own expression, which is often seen in pathological dysfunctions such as inflammation and cancer. Conversely, negative feedback may occur via cytoplasmic re-shuttling of the NF-κB dimers by IκB.
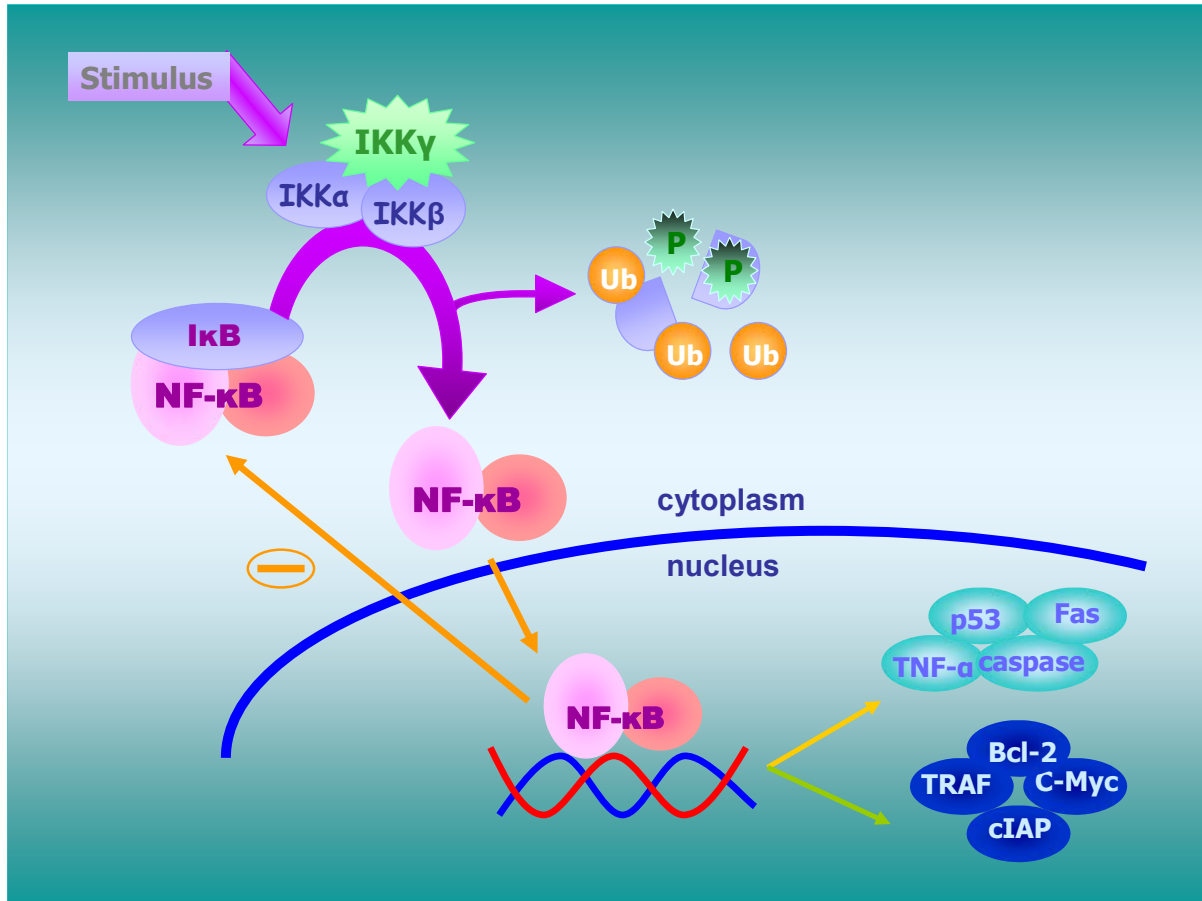
Figure 3-2: Simplified representation of the classical NF-κB Pathway.

Upon a stimulus from TNF-α, the IKK complex is recruited and phosphorylated, leading to phosphorylation and proteosome degradation of IκB. NF-κB dimers are then free to migrate into the nucleus and initiate transcription of genes important for cell death or survival. Negative feedback occurs through cytoplasmic re-shuttling of NF- κB dimers via IκB.

Alternative Pathway

The alternative or CD40 pathway is associated with adaptive immunity as well as development and maintenance of lymphoid organs. This pathway is triggered by lymphotoxin β and TNF homologues, and involves the phosphorylative activity of IKKα (Lin and Karin 2003).

Binding of the CD40 ligand to its receptor results in the recruitment of TRAF, and activation of NF-κB-inducing kinase (NIK), a serine/threonine kinase which stimulates IKKα. The inhibitory subunit p100 is then processed at the c terminus into the p52 subunit. Subsequently, the N terminal consisting of the RHD becomes available to bind with RelB to form a dimer and translocate to the nucleus (Bonnizi and Karin 2004). This pathway is NEMO independent, and requires the presence of IKK homodimers (Viatour et al. 2005).

A third pathway, referred to as the Atypical pathway, has also been described, and is triggered by DNA damage. This pathway is IKK independent, and relies on proteosomes to degrade IκB directly (Viatour et al. 2005).

3.4 NF-κB and Pro-Apoptosis

NF-κB signaling pathways are generally associated with cell survival. Anti-apoptotic genes that are induced include IAP, cFLIP, A1, Bcl-2, TRAF1 and 2, while pro-apoptotic Bax gene may be inhibited (Lin and Karin 2003). Continual activation of these in tumor cells further promotes tumorigenesis, metastasis, angiogenesis (as reviewed in Perkins and Gilmore). Upon entering the nucleus however, NF-κB can also induce transcription of several pro-apoptotic genes such as p53 tumor suppressor gene, Fas, and caspases (Ryan et al. 2000).

This dual effect of NF-κB is a result of many factors including the stimulus that initiates the pathway (Perkins and Gilmore 2006). Additionally, the same gene may be stimulated or inhibited depending on the activity and phosphorylation of the subunits (Viatour et al. 2005). Once cleaved, p65 can modulate gene expression by recruiting histone acetylases which promote gene activation, or deacytlases, which inhibit gene expression. Phosphorylation of NF-κB subunits is critical for the outcome of the signal pathway, and research into the dual action of p65 is ongoing (Viatour et al. 2005).

Dimer composition itself plays a significant role in influencing gene transcription (Perkins and Gilmore 2006). While p65 NF-κB increases expression of cIAP proteins and decreases caspase and death receptor expression, the c-Rel subunit has opposing effects (Chen et al. 2003). Therefore, p65 acts as a survival subunit, while c-Rel is favorable towards apoptosis. Modulating the activity of NF-κB subunits is a useful strategy to understand physiological implications of this pathway.

Therefore, the results of NF-κB signaling pathways, whether cell survival or apoptosis, are dependant on many factors such as subunit properties and type of external stimuli. Regardless of outcome, if the activity of NF-κB is dysregulated, physiological aberrations result. Continuous activation of NF-κB for example, is well associated with chronic inflammation and cancer.

3.5 TNF-α and NF-κB Crosstalk

The TNF-α and NF-κB pathways have much overlap in cell survival and apoptosis signaling. The apoptotic signal initiated by TNF-α is blocked by the cell survival signal by NF-κB. Inhibition of NF-κB in order to facilitate TNF-α mediated cytotoxicity is therefore of considerable interest. Conversely, TNF-α itself may also stimulate the NF-κB pathway through various mechanisms, including dissociation of the IκB complex. Variant cells lines as well as animal models that are IκB deficient have been developed to study the effects and interaction of TNF-α and NF-κB (Van Antwerp et al. 1996). The following section will aim to summarize evidence using models of NF-κB inhibition in attempts to promote apoptosis in cancer cells.

The p65 subunit is of significant interest as p65 -/- mice have extensive liver apoptosis resulting in death at 15 days (Beg and Baltimore 1996). Cells isolated from these mice do not survive upon TNF-α treatment, while re-transfection of p65 subunit facilitates resistance to death. These results were not seen with the p50-/- cells. Thus, p65 is more essential than the p50 subunit in protecting cells from apoptosis mediated by TNF-α (Beg and Baltimore 1996).

A variant line of human fibrosarcoma cells otherwise resistant to TNF-α was designed in which NF-κB was repressed by expression of a super form of IκBα (Wang et al. 1996). Essentially, this variant prevented phosphorylation of IκB, thus inhibiting NF-κB from going into nucleus and binding to

DNA. Apoptotic cell death was observed upon TNF-α exposure to these cells, suggesting that NF-κB, when activated, had a protective effect (Wang et al. 1996).

Sensitivity of TNF-α mediated apoptosis is variable according to cell line; while HCT-116 is quite responsive to cytotoxicity, HT-29, WiDR, DLD-1 colon cancer cell lines are not as sensitive (Han et al. 2000, Zwacka et al.2000). When looking at apoptosis during treatment with TNF-α in these cell lines, TNFR1 and accessory molecules such as FADD, TRADD, FLICE expression remained relatively constant, indicating that they were not critical factors involved in the apoptotic pathway (Han et al. 2000). Treatment with TNF-α resulted in a decrease in NF-κB-DNA binding that was time dependant. Additionally, overexpression of IκB-α resulted in growth inhibition of cells treated with TNF-α, providing further evidence for the involvement of NF-κB in cell survival (Han et al. 2000). However, the effects are variable depending on the cell lines. Why certain cell lines more responsive than others, and how we can use this information to further understand the interaction between pathways leading to cell death or survival is of interest.

3.6 NF-κB and TNF-α Expression in Colon Cancer

Activation of TNF-α and NF-κB is associated with the pathobiology and clinical outcome of colon cancer, and observing the expression of key players in the pathways is an ideal way to elucidate mechanisms of action. Immunohistochemistry (IHC) is a valuable tool for identifying spatial expression of molecules of interest. Higher levels of NF-κB are reported in adenomatous polyps versus normal tissue from human colonic biopsies via IHC analyses (Hardwick et al. 2001). In addition, amplified NF-κB activation in colon carcinomas versus normal mucosa has been observed with electrophoretic mobility shift assay (EMSA) (Kojima et al. 2004). Advanced stage carcinomas are seen to have higher NF-κB expression than early stages. It has been hypothesized that high levels of LPS and inflammatory cytokines in the rich bacterial and pathogenic environment of the colon further facilitate NF-κB activation (Kojima et al. 2004).

Microenvironment of the tumor provides important clues as to the mechanism of disease as well as understanding tumor biology. Barth et al (1996) studied tumor infiltrating lymphocyte (TIL) expression of TNF-α, IFN, and IL in the tumor microenvironment of human colon carcinomas through IHC. Higher cytokine expression was seen in metastatic carcinomas versus primary tumors. It

may be that levels of cytokines within the tumor environment change as lesions develop and become metastatic, thus warranting investigation into studying successive stages of cancer for transient expression patterns.

In addition to protein levels, separate studies have shown rats injected with MAM and 1-hydroxyanthraquinone (HAQ) colon carcinogens to have significantly higher levels of TNF-α and IL-α mRNA in tumors (Yoshimi et al. 1994, Baier et al. 2005). These observations further support the critical role of these molecules in colon cancer.

Elevated expression of NF-κB and TNF-α are also linearly correlated with inflammation associated colon cancer (Li et al. 2005). When compared to control animals, a significant increase of active NF-κB levels were observed in tumor bearing rats. Tumor incidence in a separate mouse model of colitis associated colon cancer was decreased upon deleting the IKKβ, providing further evidence for linking the NF-κB pathway with inflammation and cancer (Greten et al. 2004).

3.7 Targeting NF-κB Pathway in Cancer Therapy

TNF-α has potential to be an effective treatment for cancer, however, it has been observed that that some tumors and cancer cell lines are resistant to its effects. Increasing the dosage for cytokine treatment translates to clinical toxicity. However, by manipulating the gene interactions involved in the signaling cascades, desirable effects may be achieved (Zwacka et al. 2000). Genetic manipulation has potential to sensitize cells to apoptosis, and may be combined with lower doses of exogenous TNF-α to maximize treatment. While this has yet to show relevance for clinical settings, models have been created to better understand the mechanisms involved.

A popular option has been to utilize super repressor forms of IκBα, which essentially inhibit NF-κB translocation to the nucleus. Cell death results as apoptotic genes override the inhibitory signal from survival genes activated by NF-κB (Zwacka et al. 2000).

Additionally, the different types of NF-κB dimers formed in colonocytes also affect cell death or survival outcomes. Immature colon cells at the bottom of crypts express higher levels of p65/p50 and p50/p50 subunits, whereas surface cells primarily express p50-p50 (Tong et al. 2004). The p50-p50

dimer is of special importance due to its ability of inhibiting gene expression. Interestingly, high levels of other subunits such as p65-p50 can compete with p50-p50 for binding sites on DNA (Tong et al. 2004). Thus, targeting specific NF-κB dimers is a potential strategy to regulate its effects.

NF-κB Pathway Inhibition

The promotion of cell proliferation and inhibition of apoptosis are characteristics that make NF-κB a key player in oncogenesis, and also an attractive target for therapeutics. Among others, different components that have been targeted include IκB, IKK, RIP and TRAF and it is attempted to sensitize cells to TNF-α mediated apoptosis through these targets. There is also evidence to suggest that inhibition of NF-κB via these molecules may be more effective in earlier rather than late stages of cancer (Lin and Karin 2003).

Due the involvement of NF-κB with the immune system, a concern with inhibitory drugs is excessive suppression of the immune system. Thus, attempts are made to design drugs to target specific components like IKKα that do not interfere with immune activity. As ROS also induce NF-κB via degradation of IκB, inhibitors of ROS can potentiate cell death, and are another possible drug target (Schreck 1991). The essential aim is to focus on NF-κB activity relating to cancer growth, but not other functions that are otherwise beneficial (Lin and Karin 2003).

Considering the duality of its responses, NF-κB inhibition may also promote tumor growth (Kim et al. 2006, Perkins and Gilmore 2006). Thus, interaction between cancer therapies and NF-κB, especially in downstream signaling must be carefully evaluated. Moreover, NF-κB inhibition is shown to have altered outcomes depending on whether the cancer is a result of a chronic condition such as inflammation, or acute carcinogen exposure (Pikarsky and Ben-Neriah 2006). In an acute phase, NF-κB is only activated for a short duration, and is involved in promotion of apoptosis. Thus, inhibition under these circumstances may not be ideal. Conversely, inhibition is beneficial when activation is continuous throughout chronic disease progression (Pikarsky and Ben-Neriah 2006).

3.7.1 NF-κB and Drug Therapy

Drugs often stimulate many different signals that can elicit a survival or death response in the cell. By manipulating the mechanism action of drugs, the response may be modified towards apoptosis, a desirable outcome for cancer treatment (Nakanishi and Toi 2005).

Conventional cancer therapeutics may promote NF-κB activation directly, as well as through secondary mediators such as ROS, IL and TNF-α. While this effect may be insignificant in comparison to the other mechanistic actions of the drug, overexpression and constant stimulation of NF-κB in tumors and many cancer cell lines have exhibited resistance towards cancer drugs (Nakanishi and Toi 2005). In other words, NF-κB can inhibit apoptosis attempted by cancer drugs, leading to resistance and further challenges for current treatment strategies (Bremner and Heinrich 2002).

Drugs which are inhibitors of NF-κB, and found as natural or synthetic compounds have shown some promise by facilitating cell death induced by another factor such as TNF-α. Concerns with these types of drugs include their suppressing effect on the immune system due to NF-κB inhibition. Thus, the goal is to design drugs that target cancer therapy, but do not interfere with immune or other functions of NF-κB that are otherwise beneficial (Li and Karin 2003).

Using specific inhibitors of NF-κB in combination with conventional cancer drugs have increased efficacy, especially for colon cancer (reviewed in Nakanishi and Toi 2005). Blocking of proteosomes, which rapidly degrade proteins through ubiquitous-proteosome pathway, is one strategy that has shown promise with regards overcoming resistance encountered with cancer therapeutics. These prevent the degradation of IκB and subsequent translocation of NF-κB to the nucleus (Nakanishi and Toi 2005). For example, Cusack et al. (2001) have shown increased apoptosis in colon cancer cell lines by treatments of lovostatin and proteosome inhibitor PS-341. These synergistic effects were also observed *in vivo* where a 94% decrease in tumor size was seen along with an increased number of apoptosic cells (Cusack et al. 2001). The combination of butyrate and TNF-α also inhibits IκB degradation via proteosome inhibition, and is though to be mediated through inhibition of histone deacetylation (Yin et al. 2001, Luhrs et al. 2002).

3.7.2 NF-κB and St. John's Wort

Natural products are under key investigation for their potential as cancer therapeutics. A wide variety of compound from natural sources have been identified as NF-κB inhibitors and include flavonoids, isoprenoids, and phenolics (Bremner and Heinrich 2002, Nakanishi and Toi 2005). Commonly seen mechanistic actions for these drug types include inhibition of IKK activity, nuclear translocation of NF-κB, and DNA binding of NF-κB (Bremner and Heinrich 2002).

St. John's Wort (*Hypericum perforatum* L.) is a top selling herbal medicine in North America, used primarily for its therapeutic role in depression. Recent investigations have established potential of St. John's Wort (SJW) as a novel cancer therapeutic. The two main constituents of SJW are hypericin and hyperforin, which are naphthodianthrone and phloroglucinol derivatives respectively, are attributed to medicinal properties of SJW (Figure 3-3). Both hypericin and hyperforin are lipophilic, bioavailable compounds, and hypericin has a tendency to concentrate in the Golgi complex and endoplasmic reticulum (Agostinis et al. 2002).

Hypericin has been shown to play a role in the NF-κB pathway, and may be a used as a potential agent to block the cell survival signal induced by this transcription factor. Specifically, hypericin inhibits proteosome 26S and 20S function in glioma and mammary carcinoma cells, thus preventing the degradation of the inhibitory IκB subunit (Pajonk et al. 2005). This was correlated to NF-κB inhibition in a dose dependant manner, accompanied by an increase in phosphorylated forms of IκBα. Consequently, hypericin prevented NF-κB binding of DNA, thus enabling pro-apoptotic stimuli such as TNF-α to initiate cell death signaling. Addition of caspase inhibitor z-VAD-fmk was seen to counteract hypericin activity (Pajonk et al. 2005).

In a separate study, inhibition of NF-κB was observed in HeLa and TC10 mouse endothelial cells pre-incubated with hypericin, and then stimulated by phorbol ester phorbol 12-myristate 13-acetate (PMA) and TNF-α respectively (Bork et al. 1999). TNF-α, H_2O_2, and PMA are stimulants of NF-κB, leading to initiation of signaling cascades, and eventual gene expression via NF-κB translocation to the nucleus (Bork et al. 1999). Effective inhibition of NF-κB when cells were stimulated by TNF-α was seen with 3.96μM of hypericin. This concentration is much lower in comparison to other tested compounds such as curcumin or parthenolide (Bork et al. 1999). Interestingly, no effect was seen

when cells were stimulated by H_2O_2, thus indicating hypericin was not acting as an antioxidant. Inhibition of IL-6 expression was also seen upon exposure to hypericin and TNF-α, and thought to be attributed to the lack of signal for IL-6 gene transcription by NF-κB (Bork et al. 1999).

The effect of hyperforin on NF-κB inhibition is not yet known. Whether hypericin and hyperforin influence NF-κB activation in HT-29 cells, and their combined effects with TNF-α were investigated in this study.
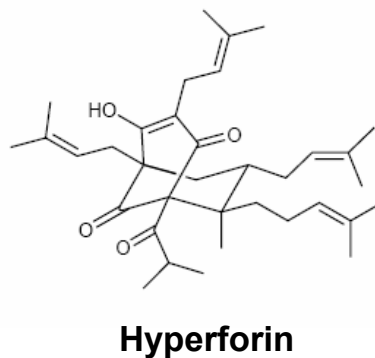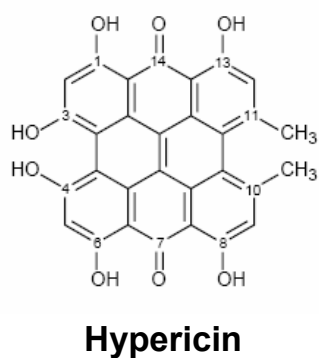
Figure 3-3: Chemical structures of hypericin and hyperforin.

Hypericin and hyperforin are naphthodianthrone and phloroglucinol derivatives respectively. Medicinal properties of SJW with regards to cancer and depression are attributed to these two active constituents.

Chapter 4
Materials and Methods

Unless otherwise stated, all chemicals and reagents were purchased from Sigma Chemical Co. (Mississauga, ON). Primary and secondary antibodies were obtained from Santa Cruz Biotechnology (Santa Cruz, CA, USA).

4.1 Study 1: Effects of TNF-α and NF-κB inhibitors on HT-29 colon cancer cells

4.1.1 Cell Culture

HT-29 colon adenocarcinoma cells were obtained from American Type Culture Collection (Manassas, VA), and grown in McCoys 5A medium supplemented with 10% fetal bovine serum and 1% penicillin/streptomycin (HyClone, Logan, UT). Cells were maintained in a humidified atmosphere of 5% CO_2, at a temperature of 37ºC. All studies were done at a cell confluency of 80% using cell passages 4-14.

4.1.2 Cytotoxicity and Cell Growth Assay

Compounds of interest were assessed for cytotoxic potential using the 3-(4,5-dimethylthiazol-2-yl)-2,5-diphenyltetrazolium bromide (MTT) assay. This assay evaluated cell viability by measuring the ability of the mitochondrial dehydrogenase enzyme from viable cells to cleave tetrazolium rings of the MTT, forming purple formazen crystals (Mueller et al. 2004). Absorbance was measured upon dissolving these crystals with solubilizing agent DMSO, and correlated to the percentage of surviving cells in comparison to the control.

Hypericin (HY) and hyperforin (HP) standards were obtained from Chromadex (Santa Ana, CA). Methanol in these solutions were evaporated under a stream of liquid nitrogen, and reconstituted in ethanol. Hypericin rich (HYex) and hyperforin rich (HPex) whole plant extracts were kindly provided by collaborators at the University of Guelph (Guelph, ON). Recombinant human TNF-α was purchased from Sigma (Mississauga, ON), and reconstituted in ddH_20.

HT-29 cells were seeded in 96 well plates at a concentration of 5×10^4 cells/well. Following cell adhesion, old media was removed, and replaced with serum-free media. Cells were then exposed to different concentration ranges of treatments (TNF-α: 10, 20, 40, 50, 60, 80, 100ng/mL, HPex and HYex: 1.25, 2.5, 5, 10, 15, 20, 25 μL/mL, HY and HP: 0, 2.5, 5, 7.5, 10, 12.5, 15 μM), and control lanes were exposed to corresponding concentrations of 80% ethanol. Combination treatments of SJW and TNF-α used the following concentrations: 10ng/mL TNF-α, 2.5 μL/mL HPex, HYex, and 2μM HP and HY. Upon treatment periods of 24 and 48h, 20μL of MTT (5 mg/mL stock in PBS) was added in each well, and plates were further incubated for 5h. Subsequently, media was gently removed, and 200μL of DMSO was added to each well to dissolve purple formazen crystals. Plates were stirred on a shaker for 5min, and absorbance was recorded at 570nm using Asys UVM 340 spectrophotometer (Montreal Biotech, Montreal, QB). As extracts were colored compounds, parallel blank tests were run with only media and extracts to exclude possible interferences in absorbance readings. The % survival was calculated as follows: % Survival: (A570 of test sample*100)/(A570 of control sample). All tests were performed in triplicates, repeated thrice, and expressed as means ± SE.

4.1.3 Morphological Assessment

Cells were plated in 6-well Petri dishes at 1×10^6 cells/well. Upon 80% confluency, media was replaced with serum-free medium containing either 2.5 μL/mL HPex, HYex, or 2μM HP and HY, or each treatment in combination with 10ng/mL TNF-α for 24h. Following a wash with PBS, cells were incubated for 1 min with 10μL of combined stain of 1 part each of 100μg/mL ethidium bromide (EtBr) and 100ug/mL acridine orange (AO) in PBS. Stains were discarded, and coverslips were placed in each well. Cells were viewed under the blue light filter using the Zeiss Axioport epi-flouresence microscope (Quorom Technologies Inc., Guelph, Canada) connected to digital imaging system software Openlab.

4.1.4 Sample Preparation

Whole cell lysates

HT-29 cells seeded in 20mm petri plates (BD Falcon, Mississauga, ON) at a concentration of 1×10^6 cells/mL were grown to confluence, washed in PBS, and treated with compounds in fresh serum-free

media. After a 24h treatment period, media were removed and cells were washed with PBS, and scraped with sterile cell scrapers (BD Falcon). Cell were then pelleted at 2000rpm for 10min and resuspended in 500μL ice-cold RIPA buffer (50mM Tris HCl, 1%NP-40, 0.25% Sodium deoxycholate, 150mM Nacl, 1mM EDTA, 1mM NaF) and freshly added protease inhibitors (1ug/mL of Aprotinin, Leupeptin, Trypsin Inhibitor, Pepstatin, Sodium Orthovanadate) for 15minutes with vigorous shaking. Following centrifugation for 15min at 15K rpm, supernatant was aliquoted in pre-chilled tubes and stored at -80ºC for further analysis.

Nuclear rich fractions

Cells were seeded, treated, scraped and washed with PBS as above. Pellets were then resuspended in 500 μL Buffer A (1M HEPES pH 7.9, 1M KCl, $1MMgCl_2$, 1M DTT, 100mM PMSF, and 10μL/mL each of freshly added aproptinin, leupeptin, pepstatin A protease inhibitors) and incubated on ice for 15min. Following, 1% NP-40 was added and cells were vortexed, and then centrifuged for 5min at 13K rpm. Supernatent (cytoplasmic fractions) were aliquoted and stored at -80ºC. Remaining pellets were further resuspended in 175 μL Buffer B (1M HEPES pH 7.9, 1 M $MgCl_2$, 1M DTT, 100mM PMSF, 1M NacL, 20% Glycerol, and 10μL/mL each of freshly added aproptinin, leupeptin, pepstatin A protease inhibitors). Pellet was shaken vigorously on a rocker for 30min at 4ºC, and then centrifuged for 15min at 13K rpm. Supernatant (nuclear fraction) was aliquoted in pre-chilled tubes and stored at -80ºC for further analysis.

4.1.5 Protein Assay

Total protein content of samples was determined according to the Bradford assay, using a protein assay dye reagent (Bio-Rad Laboratories, Hercules, CA) and bovine serum albumin as a standard. Duplicates of each sample were analyzed in a 96 well plate, and absorbance measured with Bio-Rad 3550-UV Microplate Reader at 595nm (Bio-Rad Laboratories).

4.1.6 Western Blot Analyses

Whole cell lysates and nuclear rich extracts were analyzed for protein expression by western blotting. Samples with consistent protein content, 10μg per sample, were mixed with equal amount of Laemmli 2xSDS buffer, and heated for 4min at 90ºC. Resolving gels were made with Acrylamide-Bis

45

(30% T, 2.67% C), 1.5 M Tris-HCL (pH 8.8), 10% SDS (Fisher Scientific), 10% Ammonium persulphate, and 0.05% TEMED. Stacking gels were made similarly, with the exception of Tris-HCL buffer, which was 0.5 M with pH 6.8. The percentage of acrylamide in each gel was used according to the kDa weight of the protein to be detected. In addition, one molecular weight marker per gel was loaded to track protein separation. Proteins were then separated by Sodium Dodecyl Sulfate Polyacrylamide Gel Electrophoresis (SDS-PAGE) at 120V for 90min using the Mini-Protean-BioRad II apparatus (Bio-Rad Laboratories). Subsequently, the protein gel was placed on the top of a filter paper pre-soaked in transfer buffer, which was then overlaid with a 0.45μm PVDF membrane (Pall Corp., FL) pre-soaked in methanol for 15min. Another filter paper was placed on top to complete the membrane sandwich which then placed in the Trans-Blot Semi-Dry transfer cell (Bio-Rad Laboratories Ltd, Canada) at 20V, for 30min. Equal loading and adequate transfer was visualized by soaking membranes in Ponceau-S stain, followed by washing of membranes in several changes of dH$_2$O (Appendix C). At this point, gels were stained with Coomassie Blue solution to ensure proper separation of proteins (Appendix C). Membranes were then blocked for 1h at room temperature in 5% skim milk powder in TBS-T and subsequently probed with primary antibody for 1h at room temperature, followed by overnight incubation at 4ºC. Following three times wash in TBS-T for 10min each, blots were probed with appropriate horse radish peroxidase (HRP) or alkaline phosphatase (AP) conjugated secondary antibodies for 2h at room temperature, and once again washed in TBS-T for three washes, 10min each. Blots were incubated for 5min with SuperSignal West Pico Chemiluminescent substrate (Pierce) and exposed in FluorChem™ Imaging Systems (Alpha Innotech Corporation, CA, USA) for peroxidase conjugated antibodies. Blots probed with AP secondary antibody were developed with 5-Bromo-4-Chloro-Indolyl-Phosphatase/ Nitroblue tetrazolium (BCIP/NBT) solution, and the reaction was stopped with distilled water once bands became visible.

Optimal amount of protein for loading was determined by performing a linear range western blot; increasing amount of protein was loaded in successive lanes of one gel and probed with housekeeping protein antibody for β-actin to determine saturation point of protein (Appendix C). All subsequent western blots were performed with protein amounts within the tested range. In addition, equal loading and constant protein expression of β-actin was determined (Appendix C). Each western blot is representative of one gel.

46

4.1.7 NF-κB Activity Assay

Activation of NF-κB, p65 subunit, was measured in ELISA format according to manufacturer's protocol for the commercially available TransAM kit (Active Motif, Carlsbad, CA). Briefly, 5µg of nuclear or whole cell extracts in lysis buffer were loaded in wells coated with oligonucleotide with the 5´-GGGACTTTCC-3´ sequence recognized by active NF-κB. Incubation with primary antibody specific to the p65 subunit was followed by exposure to HRP-conjugated secondary antibody and developing solution. Absorbance was read at 450nm along with a reference at 655nm. Samples were tested in triplicate and expressed as mean absorbance ± SE.

4.1.8 Statistical Analysis

Statistical analyses was carried out using the t-test, or ANOVA in conjunction with Tukey post-hoc test, using SPSS 13.0 statistical software (Chicago, IL). For all tests, $p \leq 0.05$ was considered significant.

4.2 Study 2: Tumor incidence and phenotype in Zk-Ob, Zk-Ln, and SD rats

4.2.1 Animals

Female Zk-Ob, Zk-Ln and SD rats (n=30/group) at 5 weeks of age, weighing approximately 153, 88 and 126g respectively were obtained from Charles River (Montreal, QB). Animals were housed in plastic cages lined with woodchip bedding and stainless steel wire mesh lids in the Biology Animal Facility, with controlled environmental conditions (22ºC temperature, 50% humidity, 12hr light/dark photoperiod). Standard labchow (Rodent Diet 5001, Labdiet, MO, USA) and water was provided *ad libitum*. Animal care and all investigative procedures adhered to guidelines of the Office of Research Ethics, University of Waterloo (AUPP:04-17) and the Canadian Council of Animal Care. Body weights of animals were monitored bi-weekly for the initial 15 weeks of the study, and finally at termination.

Following a 1 week acclimatization period, animals were injected subcutaneously with colon specific carcinogen AOM diluted in 0.9% saline at a dose of 10mg/kg body weight, once a week for two weeks. Animals were terminated at 30 weeks by CO_2 asphyxiation. After recording body weight, blood was obtained in heparinized or EDTA vacutainer tubes (BD Vacutainer Systems, NJ) from a

cardiac puncture using a multiple sample Luer adapter. Weights of heart, liver, spleen, kidney, adipose and muscle tissues were recorded, and specimens were frozen for future analysis.

4.2.2 Blood Analysis

Blood samples were centrifuged for 10min at 2000rpm to separate plasma, which was then aliquoted. Samples were either stored for further analysis at -80ºC, or sent to Animal Health Laboratories (University of Guelph, Guelph, ON) for complete blood count (CBC) and biochemical (TG: triglycerides, HDL: high density lipoprotein, CK: creatinine kinase, ALT: alanine aminotransferase, AST: aspartate aminotransferase, CB: conjugated bilirubin, TB: total bilirubin) analysis using rat specific parameters. Heparinized and EDTA plasma was used for biochemical and CBC assays respectively.

Additionally, plasma levels of insulin and leptin (Linco Research Inc., St. Charles, MS), TNF-α (Pierce Endogen, Rockford, IL), and sTNFR1 and sTNFR2 (R&D Systems, Minneapolis, MN) were assessed using commercially available sandwich enzyme linked immunosorbent assay (ELISA) kits, according to manufacturer's protocol. Briefly, standards, blanks and prepared samples diluted with assay buffer were incubated in a 96-well plate pre-coated with antibody of interest. Wells were then aspirated, washed, and further incubated with conjugated antibody. Following another aspiration and wash step, substrate solution was added to each well, and color development was monitored and terminated with stop solution. Absorbance was read at 450nm with a correction reading set at 540nm using Asys UVM 340 spectrophotometer.

A four parameter logistic curve fit was applied to the standard curve, and averages of sample absorbance values were compared to determine protein concentrations using GraphPad Prism Software (San Diego, CA). Values were multiplied with the dilution factor when applicable, and expressed as averages of n=8 at the least, ±SE.

Plasma was further assayed for levels of o-tyrosine and 8-OH-DGnc markers of ROS, and free 3-nitrotyrosine marker of reactive nitrogen species (RNS) at the Ottawa Health Research Institute (Ottawa, ON). Analyses was carried out via a novel, highly sensitive, non-radioactive HPLC method allowing simultaneous measurement of multiple oxidative stress markers (Kumarathasan and Vincent 2003).

4.2.3 Colon Preparation

Colon from each animal was removed, flushed with ice-cold PBS, and placed on a cold plate set at 4ºC. A longitudinal cut was made from the rectal to the ceacal end. Colons intended for morphological or immunohistochemistry analyses were spread flat between two filter papers, and fixed in either 10% neutral buffered formalin, or Carnoy's fixative (3:1 Ethanol and Glacial Acetic Acid). Mucosa from the remaining colons was scraped separately according to proximal and distal regions, snap frozen in liquid nitrogen, and stored at -80ºC for biochemical analyses.

4.2.4 Tumors

Tumors were recorded for size and location from the rectal end of the colon, and either excised and snap-frozen in liquid nitrogen, or fixed in place in 10% neutral buffered formalin for histological analyses. All tumors used for analyses in this study ranged from 20-50 mm^2 in size.

Calculation of Tumor Parameters

The following tumor parameters were assessed:

- Tumor incidence (% of total animals with tumors/group)
- Total number of tumors
- Tumor multiplicity (Average number of tumors per tumor bearing rat)
- Average tumor size (mm^2)/tumor- bearing rat
  - (Total of average size (mm2) of tumor in each tumor bearing rat/Number of tumor bearing rats in the group)
- Average tumor size (mm^2)/group
  - (Total size (mm2) of all tumors in the group/number of tumors in the group)
- Tumor Burden
  - (Total of Total Tumor area in each tumor bearing rat in group/Total number of tumor bearing rats in the group)
- Total Number of Microadenomas

4.2.5 Sample Preparation

Colon scrapings (from distal half of the colon) and distally located tumors (within 0-8cm of the colon, measured from the rectal end) were homogenized in 1mL of ice-cold RIPA buffer over an ice-bath using a polytron homogenizer. Samples were then rinsed with an additional 500μL of RIPA buffer along with 10 μL PMSF protease inhibitor. Following centrifugation for 15min at 10K RPM, and then

again for 5min at 15K RPM, aliquots of the supernatant were collected and stored at -80˚C. Total protein was quantified using the Bradford assay, as described previously (section 4.1.4).

4.2.6 Western Blot Analyses

Colon and tumor homogenates were analyzed for protein expression via western blotting techniques as described (section 4.1.5). Equal amount of protein, 100µg and 300µg per tumor and colon samples respectively, were loaded in each lane. All membranes were probed with AP conjugated secondary antibodies at 1:1000 dilutions, and developed with BCIP/NBT solution. As before, linear range westerns for colon and tumor samples were probed with β-actin to determine protein saturation points (Appendix C). In addition, equal loading and constant protein expression of β-actin was determined (Appendix C). Densitometric analyses was carried out using AlphaEase®FC Image Analyses Software (Alpha Innotech). A common sample of rat liver homogenate was used in each blot to account for gel-to-gel variability when comparing results from two different blots. For example, each densitometric value of interest was adjusted to the ratio of common samples between the two blots under comparison. Each western blot is representative of one gel, and each band indicates a colon or tumor sample from one individual animal.

Amount of protein loaded for colonic mucosae was three times more than tumor samples. Thus, densitometric data was adjusted by multiplying tumor values by three in order to present results on an equal protein basis when comparing between colon and tumor protein expression.

4.2.7 NF-κB Activity Assay

Measurement of active form of p65 NF-κB in colon and tumor homogenates was performed with the TransAM kit as described (section 4.1.7).

4.2.8 Immunohistochemical Analyses

Semi-quantitative assessment of spatial expression of specific proteins was conducted by IHC analyses. Selected tumors were placed in formalin and sent to Animal Health Laboratories (University of Guelph) for sectioning. Briefly, specimens were embedded in paraffin wax, sectioned

into 4-6μm thick pieces, and mounted onto slides. One section from each tumor was stained with hematoxylin and eosin (H&E), while the rest were processed for IHC analyses.

Tumor sections were deparaffinized in xylene, and rehydrated in a series of 100%, 70%, and 50% ethanol, followed by several washes in dH_2O. As preservation of samples in formalin often results in conformational changes of epitopes and subsequent loss of antibody reactivity, an antigen retrieval procedure using Citrate buffer (BioGenex, San Ramon, CA) was performed. Slides were submerged in 1X Citrate buffer and brought up to a rapid boil in a conventional microwave oven. Next, samples were simmered at a low power setting for an additional 4 minutes, and allowed to cool in the buffer for another 15-20min. Slides were rinsed with several changes of dH_2O to complete antigen retrieval procedure.

Samples were then incubated in 3% H_2O_2 to quench any endogenous peroxidase activity, rinsed with dH_2O, and then dipped in 2N HCl for 30sec, followed by additional washes in dH_2O. Blocking serum from Rabbit Histostain® Bulk Kit (Zymed Laboratories, San Francisco, CA) was added to completely cover the tissue, and slides were incubated in a humid chamber at ambient temperature for 20min. Subsequently, primary antibodies for TNF-α, TNFR1, TNFR2, NF-κB, and IκBα were prepared in dH_2O at a dilution of 1:200, applied to labeled sections, and incubated for 2 hours in the humid chamber. Sections were then rinsed in dH_2O and incubated for an additional 30min with biotinylated secondary antibody (linking reagent), followed by incubation with an enzyme conjugate (labeling reagent) for 10min. The 3,3-diaminobenzidine tetrahydrochloride (DAB) chromagen was prepared using a DAB substrate kit (Zymed) and applied to sections to initiate peroxidase reaction. Upon visualizing color formation, slides were washed several times in dH_2O and counterstained with Hematoxylin. Following sequential dehydration of section in ethanol, slides were immersed in xylene and mounted with glass coverslips using Permount. Control slides with either no primary or secondary antibodies were included in the analyses to ensure specificity of the reaction (Appendix C).

4.2.9 Statistical Analysis

Statistical analyses was carried out using ANOVA in conjunction with Tukey and LSD post-hoc tests where appropriate, using SPSS 13.0 statistical software (Chicago, IL). For all tests, $p \leq 0.05$ was considered significant.

4.3 Study 3: Differences in protein expression patterns in distal and proximal tumors of Zk-Ob rats

Tumors were procured as described previously (section 4.2.4) and selected for protein analyses based upon their location. Specifically, distal and proximal tumors located at 0-8cm and 8-16cm from the rectal end respectively were chosen from Zk-Ob rats.

4.3.1 Sample Preparation

Tumors were homogenized in 1mL of ice-cold RIPA buffer over an ice-bath using a polytron homogenizer. Samples were then rinsed with an additional 500μL of RIPA buffer along with 10 μL PMSF protease inhibitor. Following centrifugation for 15min at 10K RPM, and then again for 5min at 15K RPM, aliquots of the supernatant were collected and stored at -80˚C. Total protein was quantified using the Bradford assay, as described previously (section 4.1.4).

4.3.2 Western Blot Analyses

Tumor homogenates were analyzed for protein expression via western blotting techniques as described (section 4.1.5). Equal amount of protein, 100μg per sample, were loaded in each lane. All membranes were probed with AP conjugated secondary antibodies at 1:1000 dilutions, and developed with BCIP/NBT solution. Densitometric analyses was carried out using AlphaEase®FC Image Analyses Software (Alpha Innotech). In addition, equal loading and constant protein expression of β-actin was determined (Appendix C). A common sample of rat liver homogenate was used in each blot to account for gel-to-gel variability when comparing results from two different blots. For example, each densitometry value was adjusted to the ratio of common samples between the two gels under comparison. Each western blot is representative of one gel, and each band indicates a tumor sample from one individual animal.

4.3.3 Statistical Analysis

Statistical analyses was carried out via the t-test, using SPSS 13.0 statistical software (Chicago, IL). For all tests, $p \leq 0.05$ was considered significant.

Chapter 5

Study 1:Effects of TNF-α and NF-κB inhibitors on HT-29 colon cancer cells

5.1 Study Background and Objectives

Cell culture model systems are a valuable tool for providing insight into disease mechanisms and identifying potential chemopreventative agents. HT-29 colon adenocarcinoma cells have been shown to be relatively resistant to TNF-α mediated apoptosis in comparison to other colon cancer cell lines. Thus, they are ideal to investigate the interaction between TNF-α and NF-κB pathways with regards to cell survival signaling.

The central theme of this thesis project is that tumorigenesis noted in Zk-Ob rats is due to the ability of preneoplastic lesions, and therefore tumors, to resist the pro-apoptotic effects of TNF-α. In order to test this hypothesis, it was essential to determine the changes associated with the TNF-α resistant phenotype from cellular and molecular perspectives. Thus, Study 1 utilized HT-29 cells that exhibit resistance to TNF-α mediated cytotoxicity to further investigate responses to exogenous TNF-α treatment, and involvement of NF-κB, which is known to transcribe survival genes.

General objectives of this study were to:

- acquire experience with experimental techniques
- assess the treatment effect of TNF-α and NF-κB inhibitors on HT-29 colon cancer cells

In the present study, HT-29 cells were exposed to TNF-α, and alterations in protein levels of key players in TNF-α and NF-κB pathways were assessed by western blot. In addition, active form of NF-κB was assessed in the nuclear rich fractions of HT-29 cells.

To assess the involvement of NF-κB in rendering protection against TNF-α mediated cytotoxicity, cells were treated with NF-κB inhibitors. Hypericin has been shown to block NF-κB via proteosome inhibition of the IκB subunit, making SJW an ideal candidate. Thus, two novel, chemically standardized SJW whole-plant extracts with optimized chemical profiles for either hypericin or

hyperforin content were utilized (Plant Cell Technology Lab, University of Guelph). Commercially available hypericin and hyperforin standards were used as an additional comparison.

Specific aims of this study were:

- To determine changes at protein levels of TNFR1, TNFR2, NF-κB, IκBα, and IKKβ in HT-29 cells treated to exogenous TNF-α.
- To assess whether inhibition of NF-κB via SJW extracts and standards augment TNF-α mediated cytotoxicity in otherwise resistant HT-29 cells.

5.2 Results

5.2.1 Methodological Approach

Details of experimental procedures are provided in Chapter 4 Materials and Methods. Briefly, HT-29 cells were grown and treated with TNF-α and/or SJW extracts and standards upon confluency. Treatment effects were assessed by MTT cytotoxicity assay, and morphological analyses via EtBr and AO staining. Cells were processed for whole cell and nuclear rich fractions, and levels of specific proteins of interest were determined by western blot. Active levels of p65 NF-κB were further evaluated by the TransAM kit.

5.2.2 Cytotoxicity Assay

HT-29 cells exhibit cytotoxic resistance to TNF-α treatment, but not SJW

In order to confirm the resistant phenotype of HT-29 cells towards TNF-α mediated cytotoxicity, cells were treated with increasing concentrations of TNF-α, and viability was assessed with MTT assay. Results indicated the percentage of cell survival to fluctuate around 100%, while 50% survival was observed at the highest concentration of 100ng/mL (Figure 5-1A). Toxicity resulting from extremely high concentrations of TNF-α treatment has been documented in previous studies (Vaculova et al. 2002).

Conversely, treatments of SJW extracts, HYex, HPex and standards HP and HY resulted in dose dependant cytotoxic responses at 24 and 48h (Figure 5-1B). LD_{50} doses for HY and HP were ~7.5 µM and 10µM respectively, while those for HYex and HPex were ~10µL/mL.

HPLC analyses of extracts confirmed total amount of active constituent of HY and HP present (data provided by University of Guelph). Relative amounts of HY and HP constituents in both extracts were compared to amounts of HY and HP in commercially available standards, using LD_{50} values from the MTT assay as a reference point (Appendix C).

Combination treatment of TNF-α and SJW sensitizes HT-29 cells to cytotoxic response

Cells were treated to dosages of SJW compounds that were previously seen to have low toxicity via MTT assay in combination with a constant concentration of 10ng/mL of TNF-α. Combination treatments had significantly more cytotoxicity than standard, extract, or TNF-α by itself, indicating a synergistic mechanism at play (Figure 5-2).
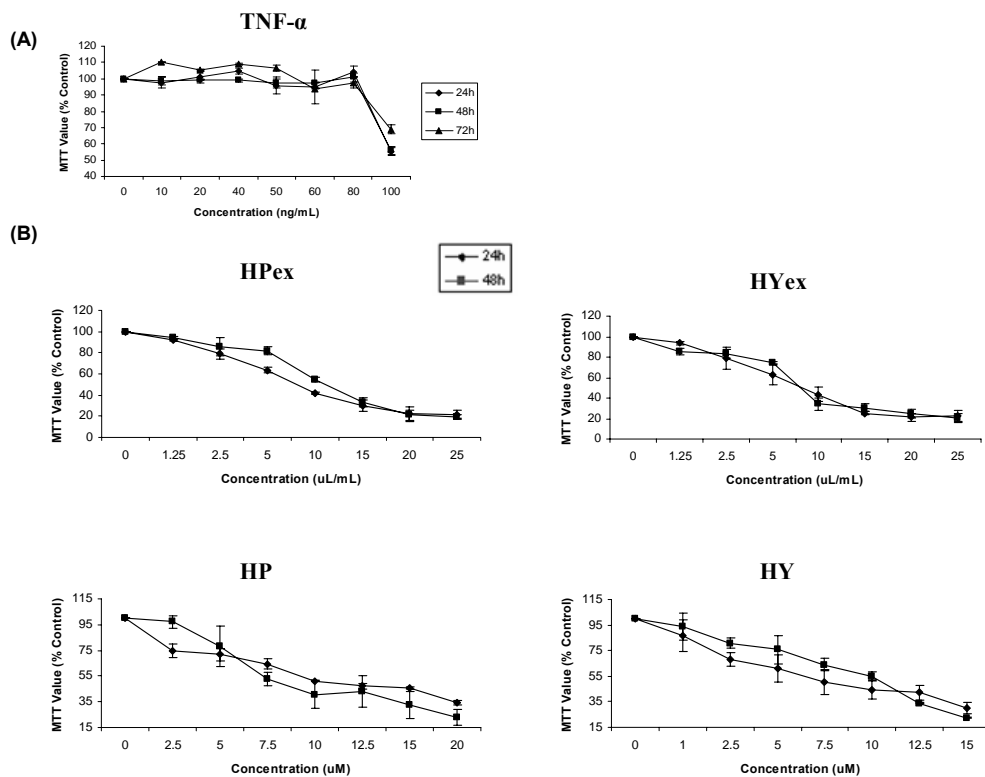
Figure 5-1: Effects of (A) TNF-α and (B) SJW extracts and standards on cell viability of HT-29 cells.

HT-29 cells were seeded in 96 well plates, and treated upon confluency with increasing concentrations of TNF-α for 24, 48, and 72h, or HYex, HPex, HY, and HP for 24 and 48h in fresh serum-free media. Following treatment periods, cells were incubated with MTT for 5h, and purple formazen crystal formation was measured at 570nm. Results are expressed as percentage of the control and indicate mean of triplicates ± SE from at least three independent experiments. HY: hypericin, HYex: hypericin extract, HP: hyperforin, HPex: hyperforin extract.
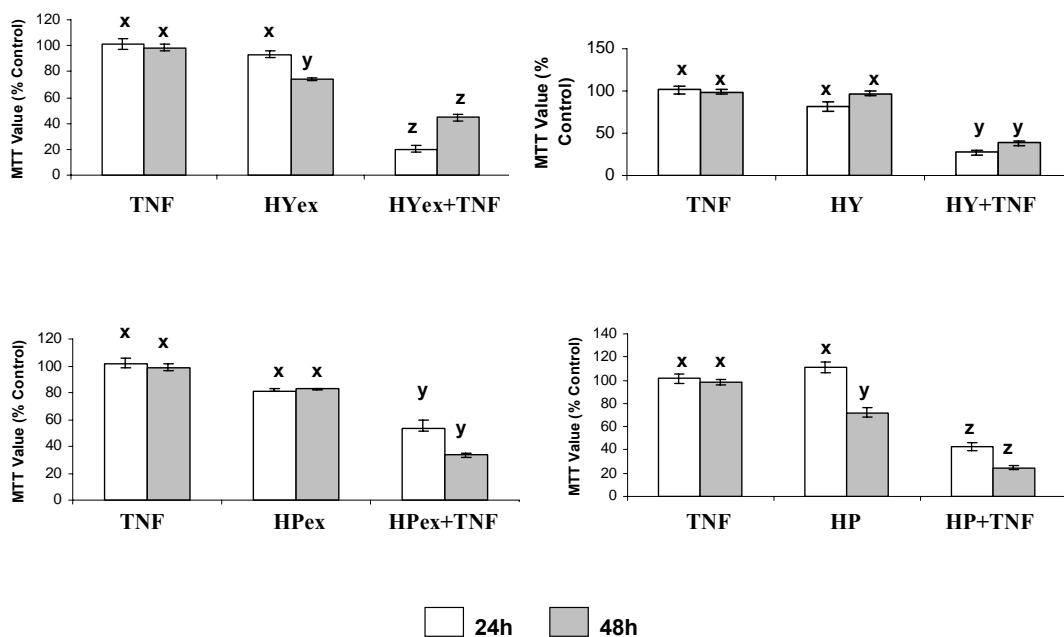
Figure 5-2: Combination treatment effects of TNF-α and SJW extracts and standards.

HT-29 seeded in 96 well plates were treated with either TNF-α (10ng/mL), HYex, HPex (2.5µL/mL), HY,HP (2µM), or in combination of each individual SJW compound with TNF-α for 24 and 48h. Following treatment periods, cells were incubated with MTT for 5h, and purple formazen crystal formation was measured at 570nm. Results indicate mean of triplicates ± SE. from at least three independent experiments. Values with different superscripts are significantly different via t-test, p<0.05. HY: hypericin, HYex: hypericin extract, HP: hyperforin, HPex: hyperforin extract.

5.2.3 Morphological Analyses

Cells treated with TNF-α and SJW were stained with a combination of AO and EtBr dyes. AO fluoresces green and stains both live and dead cells, while also fluorescing orange when binding with RNA. In contrast, EtBr fluoresces red/orange and only penetrates cells with compromised membranes. Depending on the degree of dye penetration, cells will stain from yellow, to orange and red in color, giving an indication of cellular integrity (Figure 5-3).

Control and TNF-α treatment (Figure 5-3:A1,A2) show a healthy population of cells with organized structure, and intact membranes and nuclei. Overall, cells treated with just extract or standards at low concentrations (Figure 5-3:B1,C1,D1,E1) have fewer necrotic and apoptotic cells (with an exception of HY treatment, D1, showing cell shrinkage and extensive necrosis) in comparison to cells exposed to a combination of SJW and TNF-α (Figure 5-3:B2, C2, D2, E2).

Figure 5-3: EtBr and AO staining of treated HT-29 cells treated with TNF-α and/or SJW (200x).

HT-29 cells were seeded in 6-well plates and treated at confluency with either 2.5 μL/mL HPex, HYex, or 2μM HP and HY, or each treatment in combination with 10ng/mL TNF-α for 24h. Following, cells were incubated with a combined stain of EtBr and AO, and viewed under a blue light filter. A1:control, A2: TNF-α, B1: HYex, B2: HYex+TNF-α, C1: HPex, C2: HPex+TNF-α, D1: HY, D2: HY+TNF-α, E1:HP, E2:HP+TNF-α. Arrows indicate distinct necrotic and apoptotic cells with fragmented nuclei. HY: hypericin, HYex: hypericin extract, HP: hyperforin, HPex: hyperforin extract.
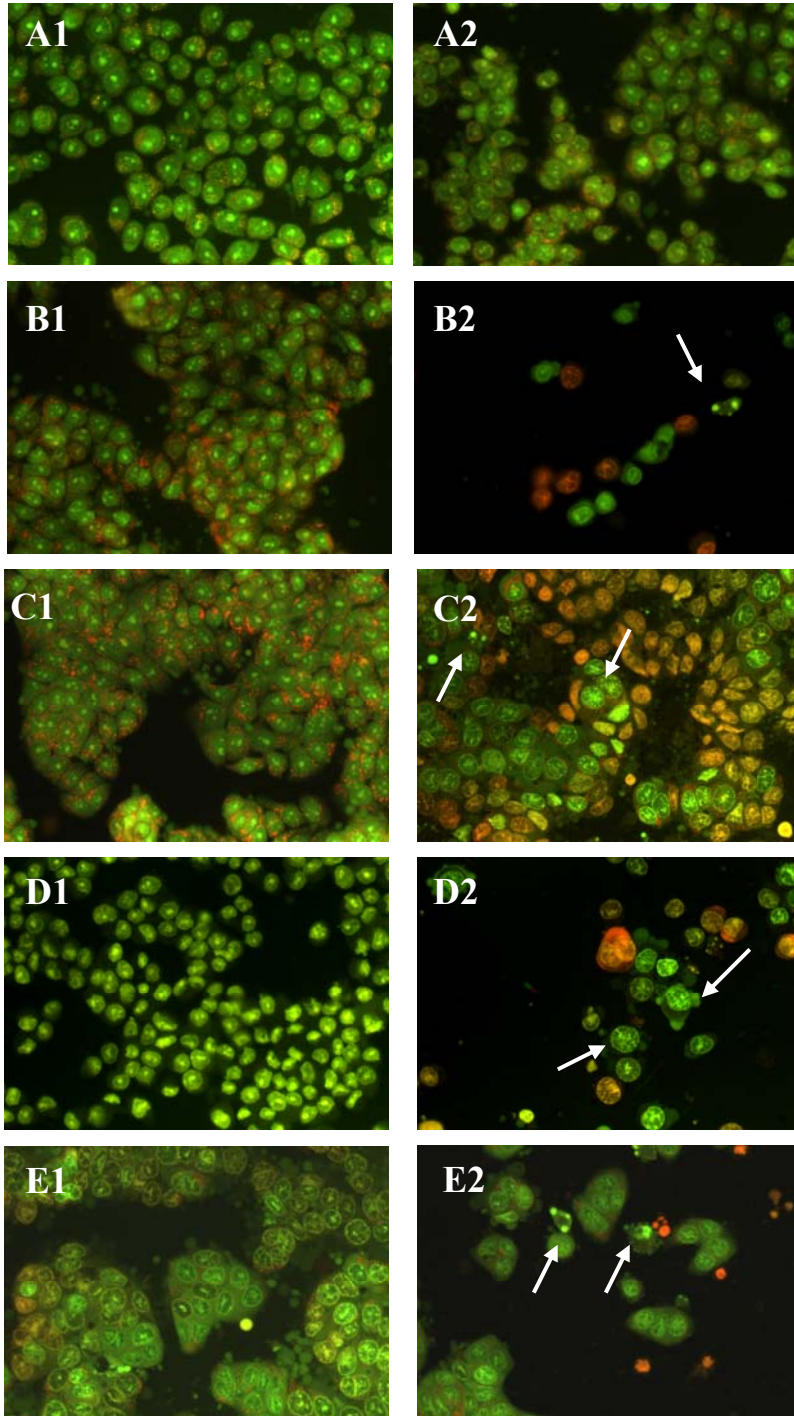
5.2.4 Western Blot Analyses

TNF-α stimulates, while SJW inhibits NF-κB protein expression

Western blots of HT-29 cells treated with increasing concentrations of TNF-α, as well as two concentrations each of SJW standards and extracts showed conflicting patterns of NF-κB expression (Figure 5-4). Higher levels of NF-κB were seen in both whole cell and nuclear rich fractions (used to determine levels of potentially active NF-κB) from cells treated with TNF-α, while inhibitory action was demonstrated by SJW. Among the standards however, HP appeared to stimulate NF-κB in comparison to the strong inhibitory effect of HY, a known NF-κB blocker. In contrast to HP, HPex did inhibit NF-κB, demonstrating a difference between standard and extract treatment.

Synergistic effects of SJW and TNF-α on NF-κB expression

Cells treated with combinations of TNF-α and SJW compounds were analyzed for changes in NF-κB levels (Figure 5-5). Similar patterns were observed between whole cell and nuclear rich fractions. Combination treatments inhibited NF-κB expression in comparison to TNF-α or SJW exposure alone. In contrast to HPex, the HP standard, with or without TNF-α had no detectable effect on NF-κB level. Additionally, HYex was observed to have a stronger effect than HPex.

Treatment effects on active NF-κB levels

Active p65 NF-κB levels in nuclear rich lysates was measured using the TransAM transcription factor ELISA kit (Figure 5-6). A significant increase in active NF-κB from 5 to 10ng/mL TNF-α treatment was detected. The combination of TNF-α and SJW showed a decrease in active form in comparison to individual treatments. HP on its own, or in combination with TNF-α did not cause a significant decrease in active NF-κB level.
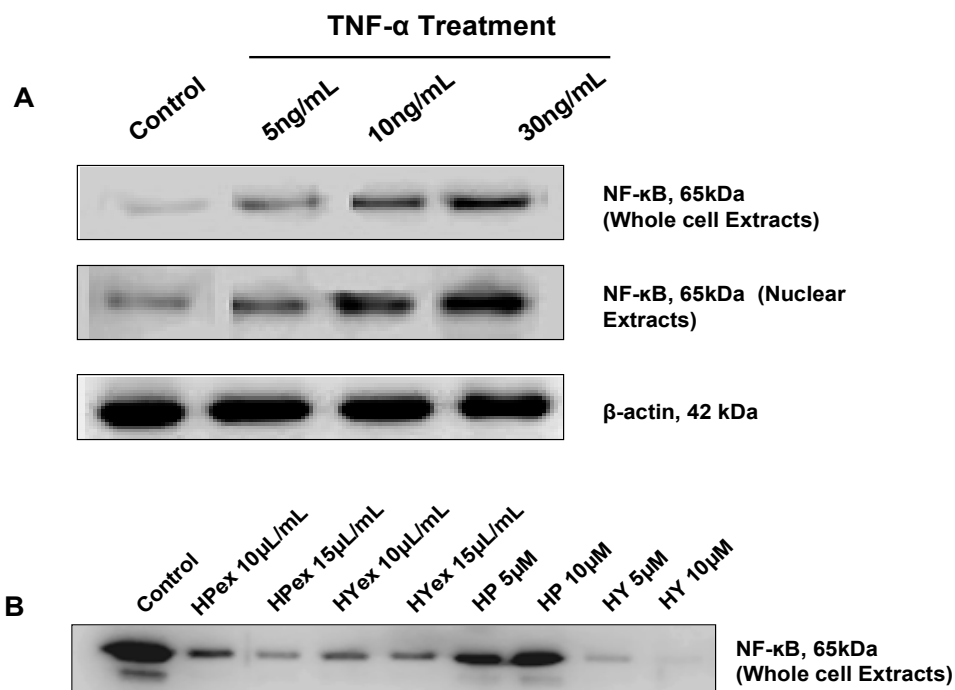
Figure 5-4: Individual effects of TNF-α and SJW on NF-κB protein expression.

Western blots of cells treated with A:TNF-α (5, 10, and 30ng/mL), or B:HYex, HPex (10 and 15μL/mL) and HY, HP (5, 10μM) for a 24h treatment period are shown. Whole cell or nuclear lysates, 10μg of protein per sample, were processed and separated through SDS-PAGE. Following transfer, membranes were probed with primary antibody for p65 NF-κB, followed by rabbit HRP-conjugated secondary antibody, and exposed in FluorChem™ imager. HY: hypericin, HYex: hypericin extract, HP: hyperforin, HPex: hyperforin extract.
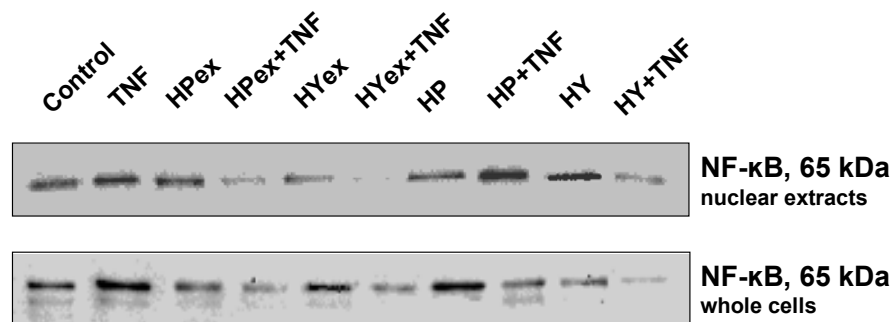
Figure 5-5: Synergistic effects of TNF-α and SJW treatment on NF-κB expression.

Western blots of cells treated with HPex, HYex (2.5 μL/mL), or HP, HY (2μM), as well as in combination with 10ng/mL TNF-α for 24h are shown. Whole cell and nuclear rich lysates, 10μg of protein per sample, were processed and separated by SDS-PAGE. Following transfer, membranes were incubated with primary antibody for p65 NF-κB followed by rabbit HRP conjugated secondary antibody, and exposed in FluorChem™ imager. HY: hypericin, HYex: hypericin extract, HP: hyperforin, HPex: hyperforin extract.
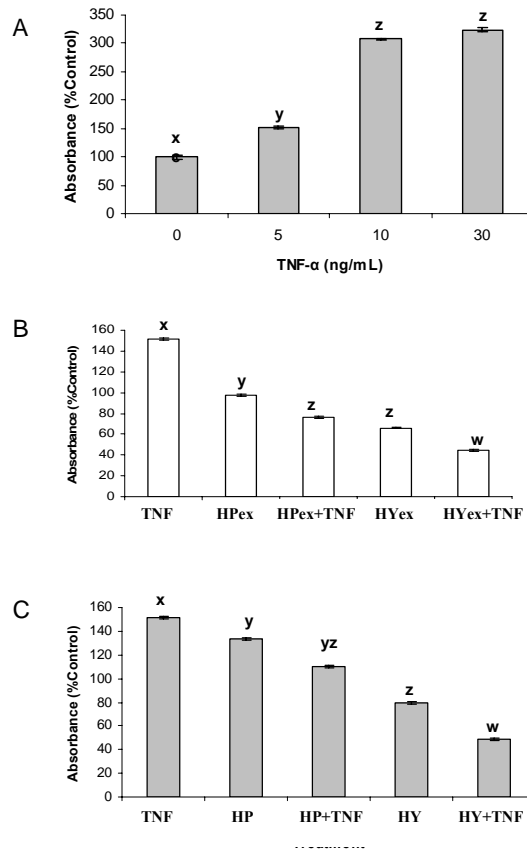
Figure 5-6: Measurement of active NF-κB levels in nuclear rich extracts of TNF-α and SJW treated cells.

Nuclear rich lysates were extracted from cells treated with 5, 10, and 30ng/mL TNF-α (A), 2.5 μL/mL HPex, HYex, (B), or 2μM HP and HY (C), with each SJW compound also combined with 10ng/mL TNF-α for 24h. Active levels of p65 NF-κB were measured by a transcription factor ELISA (Active Motif) by loading nuclear rich extracts, 2 μg of protein per sample, in a 96 well plate coated with 5´-GGGACTTTCC-3´ oligonucleotide sequence. Incubation with primary antibody specific to the p65 NF-κB subunit was followed by exposure to HRP-conjugated secondary antibody and developing solution. Absorbance was read at 450nm along with a reference at 655nm. Samples were tested in triplicate and expressed as percentage of control (untreated cells) means ± SE. Values with different superscripts are significantly different via ANOVA in conjunction with Tukey post-hoc test, p<0.05. HY: hypericin, HYex: hypericin extract, HP: hyperforin, HPex: hyperforin extract.

64

Treatment effects of SJW and TNF-α on protein expression of key players in of TNF-α/ NF-κB pathways

Whole cell extracts treated with TNF-α and SJW were analyzed for changes in expression of TNFR1, TNFR2, IκBα, and IKKβ proteins. With increasing concentrations of TNF-α treatment, TNFR2 and IKKβ were upregulated, while TNFR1 and IκBα protein expression decreased (Figure 5-7A). Cells treated with both SJW and TNF-α resulted in a significant reduction of IκBα and IKKβ (Figure 5-7B). Additionally, combination treatments appeared to downregulate TNFR2, and upregulate TNFR1, responses opposite to TNF-α exposure alone.
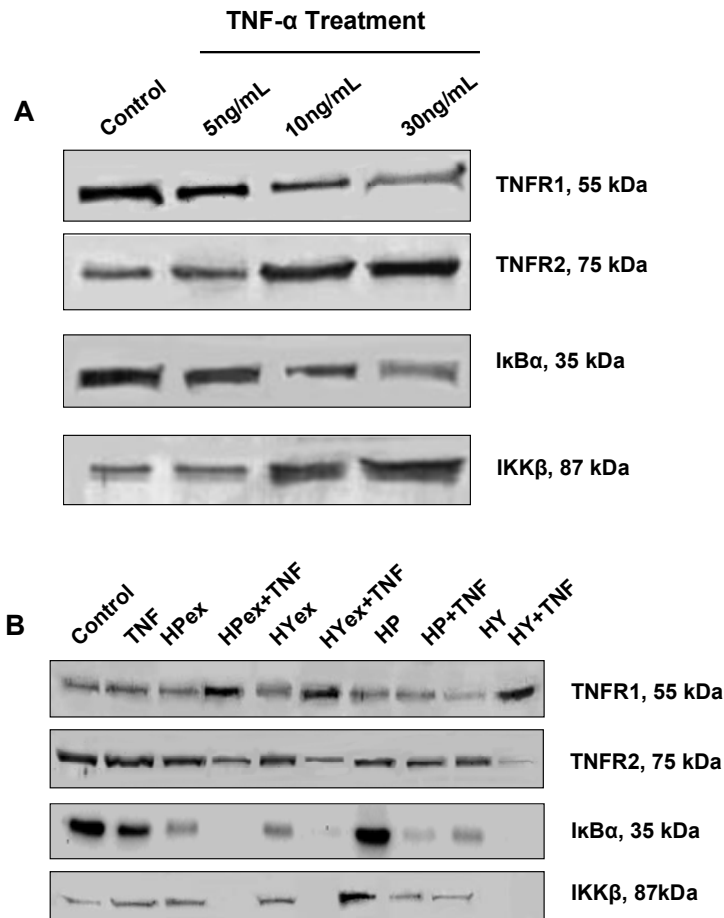
Figure 5-7: Treatment effects of TNF-α and SJW on TNFR1, TNFR2, IκBα, and IKKβ protein expression.

Western blots of cells were treated with A: TNF-α (5, 10, and 30ng/mL) or B: HPex, HYex (2.5 μL/mL), or HP, HY (2μM), as well as in combination with 10ng/mL TNF-α for 24h are shown. Following extraction, 10 μg of protein per sample was loaded, separated with SDS-PAGE, and transferred on membranes for immunoblotting. Following incubation with primary antibodies to TNFR1, TNFR2, IκBα and IKKβ membranes were exposed to corresponding AP conjugated secondary antibodies and developed with BCIP/NBT solution. HY: hypericin, HYex: hypericin extract, HP: hyperforin, HPex: hyperforin extract.

66

5.3 Discussion

The dual nature of TNF-α and NF-κB pathways in mediating cell death and survival signals pose many questions as to their involvement during carcinogenesis. Preneoplastic lesions and tumors have been shown to exhibit resistance to TNF-α mediated cell death. To better understand this response from a cellular and mechanistic approach, HT-29 cells otherwise resistant to cytotoxicity by TNF-α, were treated with this cytokine, and expression of key proteins was analyzed. As NF-κB is thought to contribute to this resistant phenotype by initiating a survival signal, protein levels relevant to the NF-κB pathway were also examined. Subsequently, inhibition of NF-κB by SJW treatments were investigated to further study potential effects on survival outcome.

TNF-α pathway modulation

TNF-α exerted little to no cytotoxicity to HT-29 cells. A relative increase in expression of NF-κB upon TNF-α treatment indicated its involvement in mediating cell survival. Moreover, levels of active p65 NF-κB in nuclear rich fractions also increased with exposure to TNF-α. There is a strong possibility therefore, that the amplified activity of NF-κB led to transcription of survival proteins counteracting the potential apoptotic effects of TNF-α. IKKβ is responsible for releasing NF-κB from its inhibitor subunit IκBα and initiating its migration to the nucleus for transcription. Higher and lower levels of IKKβ and IκBα proteins respectively supported the contention that this pathway was activated in HT-29 cells in response to exogenous TNF-α.

The expression patterns of these key proteins identify the NF-κB pathway as critical in the survival response in HT-29 cells, possibly contributing to its resistant phenotype towards TNF-α. To further substantiate these conclusions, it would be important to look at expression patterns of survival proteins associated with NF-κB transcriptional activity.

Downstream signaling mediated by TNFR1 and TNFR2 is complex, and not yet fully explored. TNFR1 is generally recognized to contribute to death signals whereas TNFR2 favors a survival signal (Higuchi and Aggarwal 1994b). In this study, upregulation of TNFR2 and inhibition of TNFR1 in HT-29 cells was observed upon treatment of TNF-α. It may be speculated that receptor modulation is also a contributing factor for resistance of HT-29 cells towards TNF-α mediated cytotoxicity.

Although TNFR2 can also play a role in death signaling, there seems to be preferential tendency towards the survival outcome in the presence of exogenous TNF-α.

NF-κB inhibition sensitizes HT-29 cells to TNF-α mediated cell death

The role of SJW as a NF-κB inhibitor was confirmed by the decreasing levels of protein in whole cell and nuclear rich fractions of treated cells. While components of SJW have been shown to independently induce apoptosis through various mechanisms such as caspase cleavage (Hostanska et al. 2003), the correlation of protein expression patterns and cytotoxicity assays indicate NF-κB inhibition to also play a role in mediating cell death.

The combination of TNF-α and SJW significantly increased the cytotoxic response, as determined by MTT assay as well as morphological analyses demonstrating higher numbers of necrotic and apoptotic cells. Since this occurred with low doses of SJW that were otherwise non-toxic to HT-29 cells, it may be speculated that this response was due to synergistic activity of the treatments, and not SJW alone. Lower levels of NF-κB p65 subunit determined by western blot and NF-κB activation assay suggest that downregulation of NF-κB plays a role in augmenting a cell death signal. Biologically, TNF-α could stimulate both cell death and survival. Inhibition of NF-κB via SJW appears to augment TNF-α mediated cell death and a subsequent switch in downstream signaling in the presence of exogenous cytokine. Thus, in circumstances where resistance to TNF-α is seen, as with HT-29 cells, the strategy of NF-κB inhibition holds potential for achieving the desired outcome of cell death.

Evidence that NF-κB pathway is being downregulated by the combination treatment is substantiated by the decrease in IKKβ level. However, expression of IκBα was virtually non-existent in the cell extracts, and was opposite to what was expected. It is possible that low expression of IκBα was due to proteosomal degradation, or a decrease in its transcription by lower levels of active NF-κB. It would be pertinent to analyze IκBα expression in nuclear fractions as IκBα can also enter the nucleus and bind NF-κB, inhibiting its activity.

Combination treatments of SJW and TNF-α resulted in higher and lower expression of TNFR1 and TNFR2 respectively, opposite trends seen from TNF-α exposure alone. As discussed, TNFR appear to

play differential roles in cell death signaling, and their expression may be modulated by the cell to achieve a desired outcome. Upregulation of TNFR1 in combination with NF-κB inhibition presents a mechanism by which the two TNF-α and NF-κB pathways are oriented towards cell death outcome.

Questions that remained unanswered in this study include how NF-κB promotes cell survival in HT-29 cells upon treatment with TNF-α. Further study into transcription of survival proteins is warranted. Moreover, substantial evidence exists for the pro-apoptotic effects of NF-κB, and it would be interesting to investigate how this aspect would come into play in the proposed mechanisms.

Due to its extensive role in promoting carcinogenesis, NF-κB inhibition is a popular strategy from treatment perspectives (Perkins and Gilmore, 2006). As seen by this study, inhibition of NF-κB via SJW increases cytotoxicity on its own, and augments the cell death signal initiated by TNF-α in cells that otherwise exhibit resistance. However, the multiple effects of NF-κB and interplays with other signaling pathways are reasons to approach the inhibition strategy with caution. Considering the inherent duality of NF-κB itself, blocking it may also weaken the pro-apoptotic responses, and potentially promote tumor growth (Kim et al. 2006). Thus, careful consideration must be given to the interaction between cancer therapies and NF-κB activity, and its subsequent effects on downstream signaling.

Most importantly, these findings confirmed that the ability of HT-29 cells to resist TNF-α induced cytotoxicity is due to augmented expression of NF-κB.

Chapter 6

Study 2: Tumor incidence and phenotype in Zk-Ob, Zk-Ln, and SD rats

6.1 Study Background and Objectives

Obesity associated pathological abnormalities such as high levels of plasma insulin and lipids are coined as the metabolic syndrome, and are considered a key link with many other physiological disorders such as cancer, diabetes, and cardiovascular disease (Shaw et al. 2005, Sorrentino 2005).

The TNF-α and NF-κB pathways are observed to play significant roles in the manifestation of obesity and metabolic syndrome. High levels of adipokines such as TNF-α produced by adipocytes mediate insulin resistance, and stimulate leptin production, among other hormones. TNF-α also contributes to a pro-inflammatory environment by initiating ROS and RNS production leading to oxidative stress (Sonnenberg et al. 2004). Activation of NF-κB by TNF-α further contributes metabolic disorder and cell cycle disturbance via transcription of survival proteins. Insulin resistance and oxidative stress are few of the consequences of NF-κB activation, establishing a central role of this transcription factor in the manifestation of metabolic syndrome (Gunter and Leitzmann 2006, Sonnenberg et al. 2004).

Unlike the epidemiological associations, the mechanistic link between obesity and cancer is still under investigation. Both TNF-α and NF-κB pathways, which are also significant for metabolic disorders, play controversial roles in carcinogenesis. Genes transcribed by NF-κB have multiple functions, leading to apoptosis or survival. Physiologically elevated TNF-α could induce cell death, whereas in the same organism it is suggested that neoplastic tissue could take advantage of TNF-α activated NF-κB for growth. At present, very little is known how elevated TNF-α affects tumor phenotype.

Zk-Ob rats are an ideal model system for this investigation due to their inherent characteristics of metabolic dysregulation and elevated levels of plasma TNF-α. Previous studies found Zk-Ob rats to have an increased number of ACF in comparison to their lean counterparts, along with higher plasma levels of insulin, cholesterol, triglycerides, and lactate (Raju and Bird, 2003). In addition to ACF, higher incidence of adenocarcinomas in Zk-Ob versus Zk-Ln rats is also reported (Weber et al. 2000).

Furthermore, hyperinsulinaemia in these animals is observed to be strongly associated with colon cancer incidence (Lee et al. 2001). In this study, Zk-Ob rats, along with their lean counterparts, Zk-Ln rats, were used a model system. In addition, SD rats were used concurrently as an external comparison to the Zucker strain. It was thereby possible to determine if the differences in tumor outcome noted between Zk-Ob and Zk-Ln rats was not simply because Zk-Ln rats were resistant to colon carcinogenesis due to their genotype.

The primary objective of this study was:

To determine if tumors appearing in Zk-Ob rats are biologically different from those in Zk-Ln and SD rats. It is hypothesized that the physiological state of Zk-Ob rats will affect tumor phenotype. In particular, elevated levels of TNF-α in these animals exerts a tumor promoting effect by inducing increased expression of transcriptionally active NF-κB, which is known to transcribe genes crucial to cell survival.

In order to accomplish this objective, this study was divided into three components with the following aims:

Study 2A: Assessment of physiological, hematological, and biochemical parameters in Zk-Ob, Zk-Ln, and SD rats

Specific aims of this study were to determine effects of genotype of Zk-Ob, Zk-Ln, and SD rats on:
- Body and organ weights
- Complete blood count
- Plasma levels of TG, HDL, Cholesterol, Glucose, insulin, leptin, TNF-α, sTNFR1, and sTNFR2
- Plasma levels of oxidative stress markers

Study 2B: Assessment of tumor parameters in Zk-Ob, Zk-Ln, and SD rats

Specific aims of this study were to determine effects of genotype of Zk-Ob, Zk-Ln, and SD rats on:
- Tumor incidence, multiplicity, and distribution pattern along the colonic axis

Study 2C: Assessment of protein expression patterns in tumors and colonic mucosa of Zk-Ob, Zk-Ln, and SD rats

Specific aims of this study were to determine effect of genotype of Zk-Ob, Zk-Ln, and SD animals on tumors and colonic mucosae protein expression of the following:

- TNF-α, TNFR1, and TNFR2
- NF-κB, IκBα, and IKKβ
- IRα, IRβ, and IGF-IRα
- MAPK p42/p44

Results and discussion of study 2A, 2B, and 2C are presented together in the following sections. A general discussion highlighting and integrating main findings from all studies is included in the conclusion, page 122.

6.2 Results and Discussion, Study 2A: Assessment of physiological, hematological, and biochemical parameters in Zk-Ob, Zk-Ln, and SD rats

6.2.1 Methodological Approach

Details of experimental procedures are provided in Chapter 4 Materials and Methods. Briefly, Zk-Ob, Zk-Ln, and SD rats were designated as controls, or injected with AOM, and terminated after 30 weeks. Body and organ weights were recorded. Blood samples were collected and processed to determine CBC and biochemical parameters by automated procedures. Plasma was also analyzed for TNF-α, insulin, leptin, sTNFR1 and sTNFR2 by ELISA, as well as oxidative stress markers by HPLC.

6.2.2 Body and Organ Weights

Body and organ weights collected from animals terminated at 30 weeks are shown in Table 6-1. As expected, Zk-Ob animals had higher body and organ weights in comparison to Zk-Ln and SD rats. Overall, AOM injected animals had lower body and organ weights than their respective controls, possibly due to a decreased food intake related to presence of tumors. An exception was noted, however, with the spleen weight of injected Zk-Ob animals, which was significantly higher than the control group. Splenomegaly, an enlarged spleen, indicates an over-worked, diseased state of the

organ corresponding to increased production of immune cells (Moore and Dalley 1999). Possibly, a hyperfunctional immune system in these animals was responding to the presence of tumors. This notable difference was only present in Zk-Ob rats, perhaps due to their increased sensitivity to carcinogenesis in comparison to Zk-Ln and SD animals.

Table 6-1: Final body and organ weights of control and AOM injected Zk-Ob, Zk-Ln and SD animals[a].

	Zk-Obc	Zk-Lnc	SDc	Zk-Ob	Zk-Ln	SD
Body Weight (g)	706.3 ± 4.3^x	322.1 ± 5.9^y	473.4 ± 18.5^w	672.0 ± 15.4^x	280.9 ± 8.3^y	397.8 ± 9.2^z
Liver Weight (g)	34.2 ± 4.6^x	13.4 ± 0.8^w	19.5 ± 1.9^{xy}	29.9 ± 1.7^x	10.9 ± 0.5^z	16.8 ± 0.6^y
Heart Weight (g)	5.0 ± 0.5^x	3.5 ± 0.2^y	3.2 ± 0.3^y	3.5 ± 0.3^y	2.8 ± 0.2^y	3.3 ± 0.1^y
Kidney Weight (g)	4.7 ± 0.9^x	3.2 ± 0.3^x	3.0 ± 0.1^y	4.3 ± 0.6^x	2.6 ± 0.1^y	2.8 ± 0.1^y
Spleen Weight (g)	0.83 ± 0.09^x	0.58 ± 0.05^y	0.70 ± 0.04^x	1.30 ± 0.4^w	0.49 ± 0.03^y	0.69 ± 0.03^{xy}

[a]Zk-Ob, Zk-Ln, and SD animals were designated as control or injected with 10mg/kg body weight AOM, once a week for two weeks. Following 30 weeks, animals were terminated by CO_2 asphyxiation, and body and organ weights collected. Values expressed as mean $\pm$ SE, with at least n=10 per group. Values in a row without a common superscript[(w,x,y,z)] are significantly different, $p<0.05$ as determined by ANOVA analyses with LSD and Tukey post hoc tests. AOM: azoxymethane, Zk-Ob: Zucker obese, Zk-Ln: Zucker lean, SD: Sprague dawley, subscript c indicates control animals.

6.2.3 Hematological Analyses

CBC analyses was performed on blood samples collected upon termination (Table 6-2), and descriptions of parameter tests are included in Appendix B. Notable differences were seen in the WBC, segregated neutrophil, and monocyte count for Zk-Ob rats in comparison to Zk-Ln and SD, and were significantly higher in the AOM injected Zk-Ob group. The WBC accounts for different types of white blood cells, including neutrophils (immature band cells, and mature segregated neutrophils) T-type and B-type lymphocytes, monocytes, eosinophils, and basophils. Increased levels of these cell types indicate a hyperfunctional immune response, possibly due to presence of tumors in these animals. This observation further correlates with the significantly enlarged spleen in injected Zk-Ob animals.

The individual monocyte count was significantly higher in AOM injected Zk-Ob rats than the control group. Monocytes also have a critical role in the immune response, and develop into macrophages upon entering tissues where they ingest foreign particles through phagocytosis (Goldsby et al. 2003). Monocytosis, excess monocytes in the blood, is indicative of diseased states such as chronic inflammation and stress responses, physiological aberrations also characteristic of Zk-Ob rats. As with the elevated WBC, monocytosis in these animals may be acting in response to tumors. Moreover, elevated monocytes may also correspond to an increased number of macrophages, primary secretors of TNF-α, and further contribute to inflammation, oxidative stress, and tumor promotion.

With regards to red blood cells, the RBC and Hb levels were lower in injected Zk-Ob animals versus their control group. Conversely, both control and injected Zk-Ob rats had significantly higher RDW percentages, indicating an increased size of red blood cells. This may be due to a compensation for the lower number of red blood cells. The spleen also filters, recycles, and stores blood (Moore and Dalley 1999). Thus, the abnormal size of red blood cells may have further contributed to the splenomegaly in these animals.

Interestingly, the platelet count in Zk-Ob animals was noticeably high, and even more so in the AOM injected group. Involved in blood clotting, platelets also secrete many growth factors and are physiologically linked to chronic illnesses such as cancer, heart disease, and inflammation (Adam et al. 2000). It is a likely possibility the high platelet count in these animals was also contributing to tumorigenesis.

Table 6-2: Complete blood count analyses of control and AOM injected Zk-Ob, Zk-Ln and SD animals[a].

	Zk-Obc	Zk-Lnc	SDc	Zk-Ob	Zk-Ln	SD
RBC (10^{12}/L)	7.5 ± 0.2^x	7.5 ± 0.4^x	6.8 ± 0.2^y	6.2 ± 0.4^y	7.6 ± 0.3^x	7.1 ± 0.1^x
Hb (g/L)	132.3 ± 3.8^x	135.4 ± 4.1^x	129.8 ± 3.9^x	111.5 ± 4.3^y	129.9 ± 3.4^x	132.8 ± 1.9^x
HCT (L/L)	0.4 ± 0.04^x	0.4 ± 0.04^x	0.4 ± 0.01^x	0.4 ± 0.03^x	0.4 ± 0.01^x	0.4 ± 0.01^x
Platelets (10^9/L)	914.0 ± 4.6^x	799.4 ± 65.7^y	691.6 ± 65.9^z	1107.0 ± 56.5^v	689.9 ± 75.6^z	547.0 ± 86.8^w
RDW (%)	15.4 ± 0.3^x	13.4 ± 0.3^y	12.7 ± 0.2^y	15.9 ± 0.5^x	12.8 ± 0.2^y	12.7 ± 0.2^y
MCH (pg)	17.7 ± 0.9^{xy}	18.2 ± 1.0^{xy}	19.6 ± 0.4^x	18.4 ± 0.6^{xy}	17.9 ± 0.5^y	18.6 ± 0.2^{xy}
MCHC (g/L)	341.7 ± 12.5^x	351.0 ± 24.2^x	345.0 ± 4.2^x	323.4 ± 9.2^x	322.6 ± 2.3^x	331.3 ± 1.8^x
MCV (fL)	52.3 ± 0.3^x	50.2 ± 1.2^x	56.0 ± 0.7^y	56.1 ± 0.1^y	53.8 ± 1.8^y	56.5 ± 0.5^y
WBC (10^9/L)	7.2 ± 0.6^x	6.0 ± 1.1^y	7.6 ± 0.4^x	9.4 ± 0.4^w	6.3 ± 0.6^y	9.0 ± 0.9^w
Segregated Neutrophils (10^9/L)	2.7 ± 0.5^x	1.7 ± 0.5^x	1.8 ± 0.2^x	4.8 ± 0.3^y	2.4 ± 0.3^x	1.8 ± 0.2^x
Lymphocytes (10^9/L)	3.8 ± 0.2^y	3.8 ± 0.8^y	5.5 ± 0.3^x	3.7 ± 0.3^y	3.4 ± 0.4^y	$6.6\pm0.8z$
Monocytes (10^9/L)	0.41 ± 0.07^y	0.2 ± 0.03^x	0.3 ± 0.04^x	0.6 ± 0.04^z	0.2 ± 0.04^x	0.3 ± 0.03^x
Eosinophils (10^9/L)	0.3 ± 0.1^x	0.2 ± 0.04^x	0.2 ± 0.009^x	0.3 ± 0.08^x	0.2 ± 0.05^x	0.2 ± 0.03^x

[a]Blood samples were collected at termination of 30 week old control and AOM injected Zk-Ob, Zk-Ln, and SD animals. CBC was analyzed by automated procedures, where RBC: red blood cell count, Hb: hemoglobin, HCT: hematocrit, RDW: red cell distribution width, MCH: mean corpuscular hemoglobin, MCHC: mean corpuscular hemoglobin concentration, MCV: mean corpuscular volume. Values expressed as mean ± SE, with at least n=8 per group. Values in a row without a common superscript [(v,w,x,y,z)] are significantly different, $p<0.05$, as determined by ANOVA analyses with LSD and Tukey post hoc tests. AOM: azoxymethane, Zk-Ob: Zucker obese, Zk-Ln: Zucker lean, SD: Sprague dawley, subscript c indicates control animals.

6.2.4 Clinical and biochemical assessments

Plasma was isolated by centrifugation of blood samples, and analyzed for key biochemical parameters (Table 6-3) described in detail in Appendix B. As expected, Zk-Ob animals had higher TG and cholesterol levels in comparison to other groups. LDL levels could not be calculated due to abnormally high cholesterol and triglyceride levels. Glucose levels were notably higher in AOM injected Zk-Ob animals versus control. Zk-Ob rats have inherent hyperinsulinemia and insulin resistance, and presence of preneoplastic lesions and tumors may further contribute to the elevated glucose levels (Komninou et al. 2003). Variable differences were seen with kidney and liver function assays, and no consistent trend was apparent (Appendix C).

Plasma insulin, leptin, and TNF-α were determined using commercially available ELISA kits (Figure 6-1). Zk-Ob animals had significantly higher levels of insulin and leptin than the SD rats, which were subsequently higher than the Zk-Ln group. No differences were seen between control and AOM injected groups of each strain. Most changes in response to experimentally induced cancer occur in early stages, possible explaining the marginal differences between control and AOM groups. The notably high insulin levels in Zk-Ob rats may be further connected with the high glucose levels observed in Table 6-2, both of which contribute to insulin resistance in these animals. Dysregulation of the insulin pathway is shown to intricately promote carcinogenesis (Gunter and Leitzmann 2006).

Zk-Ob rats had significantly higher plasma TNF-α level than Zk-Ln and SD groups, and AOM injected Zk-Ob rats had higher levels than corresponding control animals. TNF-α has rapid clearance from plasma (Keith et al. 2000), thus the elevated levels in Zk-Ob rat plasma may be attributed to continuous cytokine production by adipocytes, macrophages and tumor cells among other potential sources. It is well established that high levels of TNF-α are associated with both cancer and obesity, possibly explaining why this trend is observed only in the Zk-Ob group.

Table 6-3: Biochemical analyses of plasma samples collected from control and AOM injected Zk-Ob, Zk-Ln and SD animals[a].

	Zk-Obc	Zk-Lnc	SDc	Zk-Ob	Zk-Ln	SD
TG (mmol/L)	24.6 ± 2.0^{x}	12.2 ± 5.2^{y}	$11.\pm2.6^{y}$	10.5 ± 4.2^{y}	4.9 ± 0.9^{z}	6.4 ± 1.2^{y}
HDL (mmol/L)	3.6 ± 0.8^{x}	2.2 ± 5.2^{y}	2.6 ± 0.4^{x}	4.2 ± 0.5^{x}	2.7 ± 0.2^{y}	2.7 ± 0.2^{y}
Cholesterol (mmol/L)	8.7 ± 0.5^{x}	4.4 ± 0.8^{y}	4.5 ± 0.2^{y}	7.1 ± 0.9^{x}	4.2 ± 0.5^{y}	3.9 ± 0.3^{y}
Glucose (mmol/L)	13.1 ± 1.3^{x}	12.2 ± 2.5^{x}	12.6 ± 0.4^{x}	16.8 ± 1.6^{y}	8.9 ± 1.9^{z}	11.1 ± 0.6^{x}

[a]Plasma was isolated from heparinized blood samples collected at termination of 30 week old control and AOM injected Zk-Ob, Zk-Ln, and SD animals. Biochemical parameters were tested by automated procedures, where TG: triglycerides, HDL: high density lipoprotein. Values expressed as mean ± SE, with at least n=8 per group. Values in a row without a common superscript [(w,x,y,z)] are significantly different, $p<0.05$, as determined by ANOVA analyses with LSD and Tukey post hoc tests. AOM: azoxymethane, Zk-Ob: Zucker obese, Zk-Ln: Zucker lean, SD: Sprague dawley, subscript c indicates control animals.
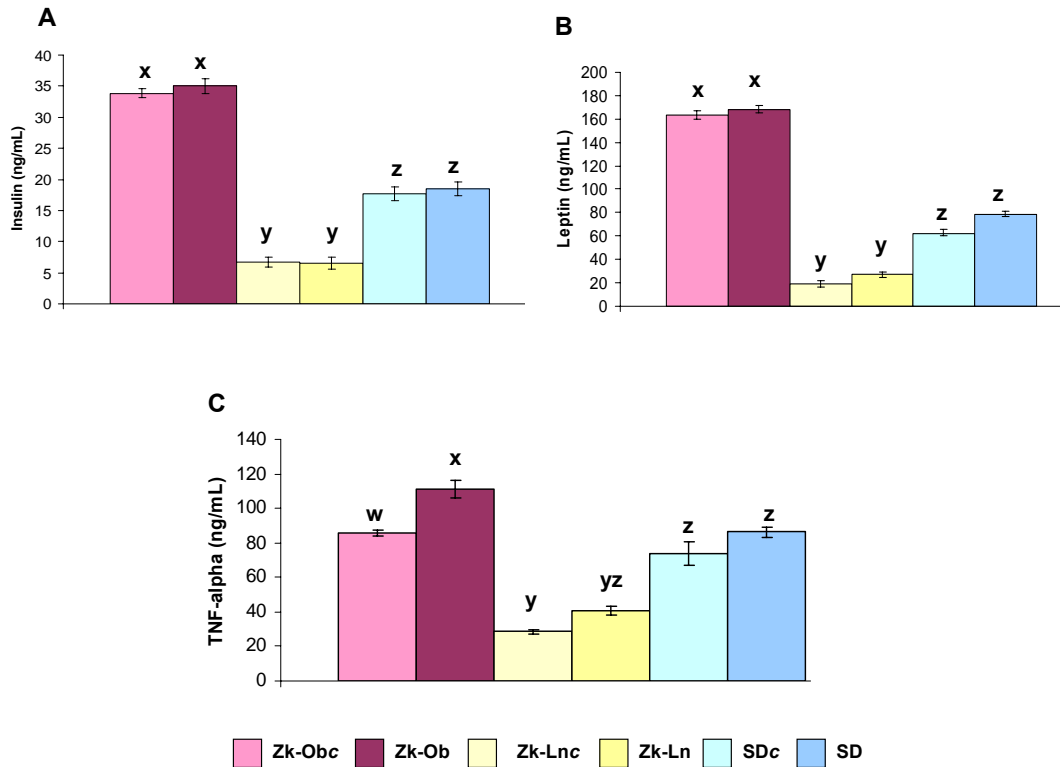
Figure 6-1: Plasma levels of (A) insulin, (B) leptin, and (C) TNF-α in control and AOM injected Zk-Ob, Zk-Ln, and SD rats.

Briefly, plasma samples were incubated in a 96 well plate pre-coated with antibody to insulin, leptin, or TNF-α. Wells were then aspirated, washed, and further incubated with corresponding conjugated secondary antibody. Reaction was monitored upon addition of substrate solution, and absorbance read at 450nm. Values were extrapolated from a four parameter logistic curve, and represent mean ± SE, n=9 animals per group. Bars without a common superscript[(w,x,y,z)] are significantly different, $p < 0.05$, as determined by ANOVA analyses with LSD and Tukey post hoc tests. AOM: azoxymethane, Zk-Ob: Zucker obese, Zk-Ln: Zucker lean, SD: Sprague dawley, subscript c indicates control animals.

Overall, all plasma samples had notably more sTNFR2 than sTNFR1 when compared on a weight basis (Figure 6-2). Little difference was observed for sTNFR1 among all animal groups with the exception of AOM injected Zk-Ob and control Zk-Ln animals which had lowest and highest levels respectively. AOM injected Zk-Ob rats had highest sTNFR2, followed by control Zk-Ob and SD groups. Soluble receptors may act as neutralizers or reservoirs for TNF-α, binding and releasing it into the plasma (Rojas-Cartagena et al. 2005). High TNF-α levels may therefore be attributed to increased sTNFR2, which could contribute to prolonged cytokine release in the plasma. TNFR2 is proposed to play a greater role in mediating cell survival signaling in comparison to TNFR1, possibly explaining the high sTNFR2 to sTNFR1 ratio in all groups (Higuchi and Aggarwal 1994b). Moreover, the AOM injected Zk-Ob group in particular shows lower and higher levels of sTNFR1 and sTNFR2 respectively in comparison to control rats. Soluble receptors are also shed by tumors, and may play a role in their growth promotion. Studies have shown that measurement of soluble receptors, and not plasma TNF-α, is a better indicator of disease status (Gadducci et al. 1995). Further implications of TNFR in tumorigenesis are discussed in Study 2C.

Plasma was also analyzed for o-tyrosine, n-tyrosine, and 8-OH-DGnc oxidative markers in collaboration with the Ottawa Health Research Institute (Ottawa, ON) (Figure 6-3). Relative amounts of ROS and RNS may be quantified by measuring respective reaction products such as tyrosine isomers via HPLC (Kumarathasan and Vincent 2003). Assessment of these gives further insight on physiological condition of the animal.

Zk-Ob rats had significantly higher o-tyrosine and n-tyrosine levels in comparison to other groups. Little difference was seen in the 8-OH-DGnc marker with the exception of AOM injected Zk-Ln group, which had the lowest level. ROS and RNS are key links between obesity and cancer by generation of a pro-inflammatory environment. High levels of oxidative markers in Zk-Ob rats are further consistent with a constant pro-inflammatory state in these animals.
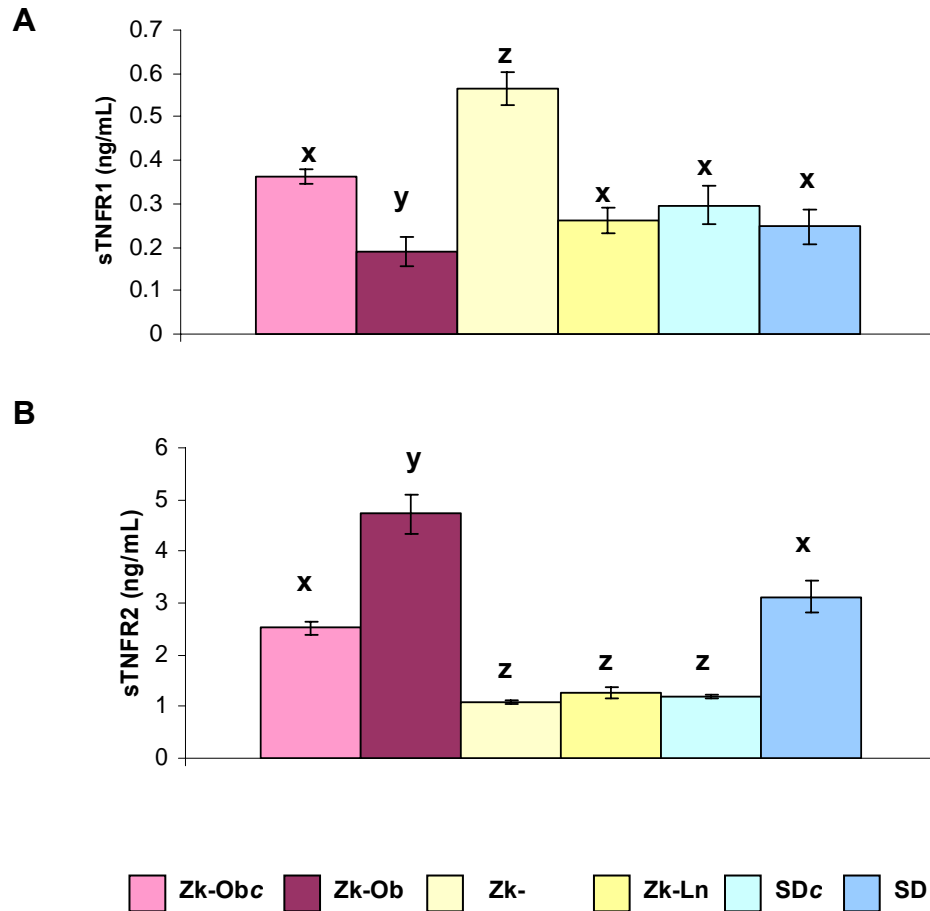
Figure 6-2: Plasma levels of (A) sTNFR1 and (B) sTNFR2 in control and AOM injected Zk-Ob, Zk-Ln, and SD rats.

Samples were incubated in a 96 well plate pre-coated with antibody to sTNFR1 or sTNFR2. Wells were then aspirated, washed, and further incubated with conjugated secondary antibody. Reaction was monitored upon addition of substrate solution, and absorbance read at 450nm. Values were extrapolated from a four parameter logistic curve, and represent mean ± SE, n=9 animals per group. Bars without a common superscript[(x,y,z)] are significantly different, p<0.05, as determined by ANOVA analyses with LSD and Tukey post hoc tests. AOM: azoxymethane, Zk-Ob: Zucker obese, Zk-Ln: Zucker lean, SD: Sprague dawley, subscript c indicates control animals.
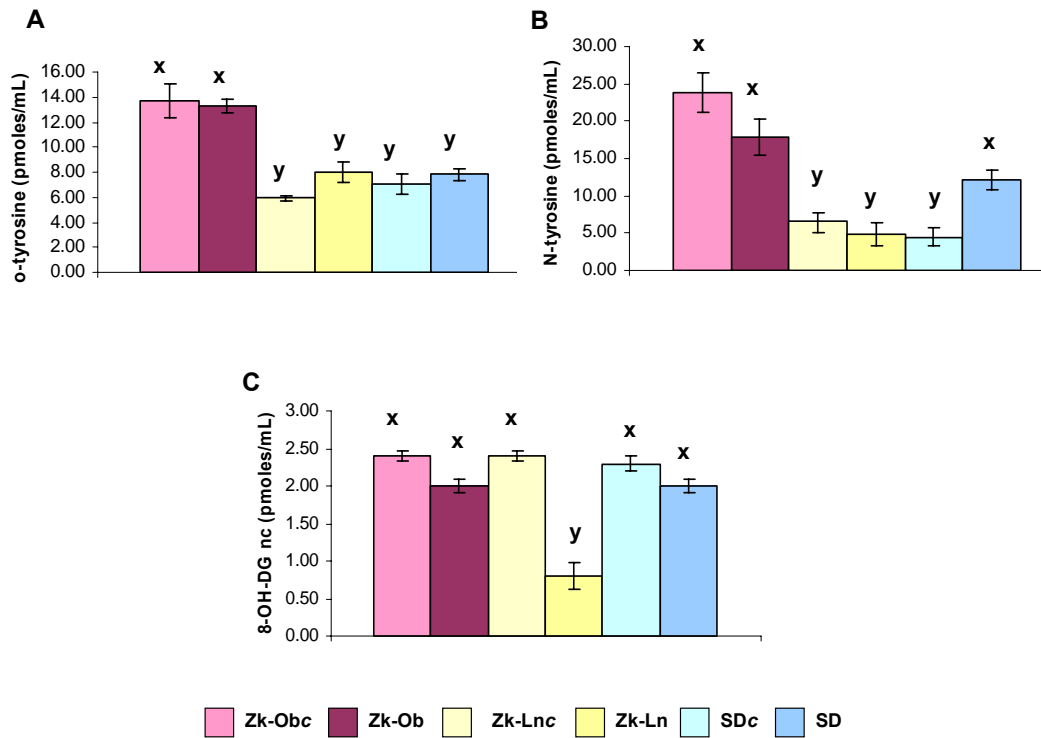
Figure 6-3: Plasma levels of (A) o-tyrosine, (B) n-tyrosine, and (C) 8-OH-DGnc in control and AOM injected Zk-Ob, Zk-Ln, and SD rats.

Plasma ROS and RNS levels were measured by a highly sensitive HPLC assay (Kumarathasan and Vincent 2003). Values are mean ± SE, n=6 animals per group. Bars without a common superscript[x,y] are significantly different, p<0.05, as determined by ANOVA analyses with LSD and Tukey post hoc tests. Zk-Ob rats had highest levels of o-tyrosine and n-tyrosine in comparison to other groups. AOM: azoxymethane, Zk-Ob: Zucker obese, Zk-Ln: Zucker lean, SD: Sprague dawley, subscript c indicates control animals.

6.3 Results and Discussion, Study 2B: Assessment of tumor parameters in Zk-Ob, Zk-Ln, and SD rats

6.3.1 Methodological Approach

Details of experimental procedures are provided in Chapter 4 Materials and Methods. Briefly, Zk-Ob, Zk-Ln, and SD rats were injected with AOM, and terminated after 30 weeks. Location and size of tumors and microadenomas along the colonic axis were recorded (Figure 6-4). Depending on their size, tumors were fixed in place with formalin, or excised and stored at -80°C or for further analyses. Tumor incidence, multiplicity, average size, and burden were calculated for all animal groups.

Figure 6-4: Presence of multiple colonic tumors in Zk-Ob rat.

Following removal, colons were flushed with PBS and slit lengthwise. Tumors were identified for size and location, and excised or fixed in place for further analyses. Four tumors located in the distal region from a Zk-Ob rat colon are shown. Note variable size of tumors, and highly vascularized tumor tissue as depicted by the red coloring.

6.3.2 Tumor Parameters

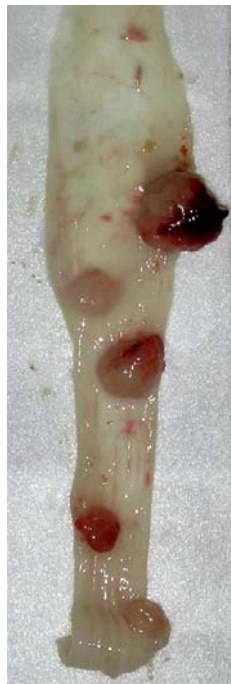Characteristics of tumor numbers and size are described (Table 6-4). Zk-Ob animals had 100% tumor incidence, confirming these rats are indeed an excellent model for investigating the augmented risk of obesity associated colon cancer. Zk-Ln rats had a higher incidence compared to SD, indicating that this genotype is not resistant, and simply less sensitive than the obese counterparts towards carcinogenesis. Tumor burden and tumor multiplicity representing average number of tumors per tumor-bearing rat was also highest in Zk-Ob rats. SD rats had highest size per tumor bearing rat and group, although size of SD tumors was marginally different compared to Zk-Ob tumors. The number of microadenomas was also highest in Zk-Ob rats, followed by SD and Zk-Ln groups respectively. These findings also demonstrate that preneoplastic lesions grew at different rates, and whether this phenomena is due to the different biological make-up of the groups, or microenvironment, remains to be determined.

Distribution of tumors along the colon is summarized in Table 6-5. Zk-Ob animals had greatest percentage of tumors along the most distal segment of the colon (0-4cm), while Zk-Ln and SD tumors were mostly located in the adjacent section (4-8cm). It was noted that tumors in the distal regions (0-8cm) also had a larger size than those in proximal regions. The distribution pattern and size of tumors along the colonic axis in all groups demonstrated that colon tumorigenesis is different depending on the region of the colon. Phenotypical differences between distal and proximal colonic tumors are further investigated in Study 3.

Table 6-4: Tumor Parameters of Zk-Ob, Zk-Ln and SD rats[a].

	Zk-Ob	Zk-Ln	SD
Total number of rats (AOM injected)	21	23	25
Tumor incidence (%)	100	47.8	20.0
Total number of tumors	78	15	5
Tumor multiplicity [a]	3.71 ± 1.92	1.36 ± 1.21	1 ± 0
Average tumor size (mm^2)/tumor-bearing rat	35 ± 0.17	17 ± 0.13	41 ± 0.28
Average tumor size (mm^2)/group	38 ± 0.38	22 ± 0.27	41 ± 0.28
Tumor Burden	1.31 ± 0.87	0.3 ± 0.5	0.41 ± 0.28
Total Number of Microadenomas	7	0	3

[a]Colonic tumors were collected upon termination of Zk-Ob, Zk-Ln, and SD animals. Calculation details of tumor parameters are given in Chapter 4 Materials and Methods. Values expressed as means ± SD. Zk-Ob: Zucker obese, Zk-Ln: Zucker lean, SD: Sprague dawley.

Table 6-5: Distribution and average size of tumors along the length of the colon in Zk-Ob, Zk-Ln, and SD rats.

	Colon Segment (cm length)			
	A (0-4)[a]	B (4-8)	C (8-12)	D (12-16)
Zk-Ob[d]	55.3[b] (30)[c]	34.0 (44)	8.5 (36)	2.1 (12)
Zk-Ln	13.3 (12)	60.0 (29)	20 (23)	6.7 (1)
SD	16.7 (16)	50.0 (45)	33.3 (29)	0 (1)

[a]A-D represent 16cm of the unfixed colon, in 4cm sections starting from the rectal end, where A is the most distal segment, and D is most proximal.

[b]Percentage of tumors present in the indicated colonic region.

[c]Values in brackets represent average tumor sizes (mm^2) in the corresponding colonic section.

[d]Zk-Ob: Zucker obese, Zk-Ln: Zucker lean, SD: Sprague dawley.

6.4 Results and Discussion, Study 2C: Assessment of protein expression patterns in tumors and colonic mucosa of Zk-Ob, Zk-Ln, and SD rats

Elevated NF-κB levels have been implicated in disease progression of both cancer and obesity. Additionally, downstream signaling mediated by TNFR1 and TNFR2 is complex, and not yet fully explored. TNFR1 is generally recognized to contribute to death signals whereas TNFR2 favors a survival signal. Considerable evidence also exists for insulin resistance acting as a critical link between obesity and cancer progression. Insulin, IGF-IR, and IR transduce survival signals that promote carcinogenesis, and may act synergistically with TNF-α to provide a growth and survival advantage for developing tumors. Evaluation of these pathways via protein expression analyses gave further insight into possible interplays occurring in obesity associated colon cancer.

6.4.1 Methodological Approach

Details of experimental procedures are provided in Chapter 4 Materials and Methods. Protein analyses was carried out in tumors of Zk-Ob, Zk-Ln, and SD animals. For comparison purposes colonic mucosae were also analyzed in a similar manner from six different groups of animals: Zk-Ob, Zk-Ln and SD groups injected with AOM, and Zk-Obc, Zk-Lnc and SDc non-injected, control groups. Briefly, tumors and mucosae were homogenized and proteins separated by SDS-PAGE. Following transfer, membranes were incubated with primary, then AP conjugated secondary antibodies, and developed with BCIP/NBT solution. Specific proteins analyzed in tumors and colonic mucosae included TNF-α, TNFR1, TNFR2, NF-κB, IκBα, IKKβ, IRα, IRβ, IGF-IRα, and MAPK p42/p44.

6.4.2 Protein Expression Patterns in Tumor Homogenates

Tumor homogenates were analyzed for proteins expression of key players in TNF-α and NF-κB pathways including TNF-α, TNFR1, and TNFR2, NF-κB, IκBα, and IKKβ. In addition, modulators of the insulin and glucose homeostasis pathways, IGF-IRα, IRα, and IRβ were examined. Finally, tumor tissue was also analyzed for MAPK p42/44 enzyme.

TNF-α, TNFR1, and TNFR2 protein expression

TNF-α, TNFR1, and TNFR2 protein expression in tumors were determined by western blot (Figure 6-5). Analyses of TNF-α and TNFR2 showed similar trends of Zk-Ob and SD tumors having higher expression than Zk-Ln. Two closely related bands were observed with TNFR1, and shared highest to lowest expression for Zk-Ob, SD, and Zk-Ln tumors respectively. Overall, there was higher protein expression for TNFR2 than TNFR1 in tumors from all groups.

Roles of TNFR are diverse and are important for both cell death and survival outcomes. However, some studies have shown TNFR1 to be more critical for apoptotic signaling due to the presence of death domains (Fontaine et al. 2002). Previous studies in our lab have further demonstrated TNFR2 to be preferentially associated with cell survival (Raju and Bird, 2006). It is therefore important to note that Zk-Ob and SD tumors exhibited a phenotype favoring survival by expressing higher levels of TNFR2. These findings suggests that in presence of high TNF-α, tumors maybe upregulating or downregulating TNFR2 and TNFR1 expression respectively as a strategy to direct TNF-α as an instigator of cell survival. Plasma analyses further showed higher levels of sTNFR2 than sTNFR1, corroborating protein patterns found in tumors.

Perhaps the physiological conditions and elevated TNF-α in Zk-Ob rats promoted increased levels of TNFR. Conversely, Zk-Ln tumors had lowest expression of TNFRs, indicating a decreased sensitivity of these lesions towards TNF-α.

Soluble forms of TNFR1 and TNFR2 were further analyzed in tumor homogenates via ELISA, demonstrating higher levels of sTNFR2 overall (Appendix C). Zk-Ob tumors had more soluble receptor than SD, which further had higher levels than Zk-Ln tumors. It is quite possible that receptors were solubilized during preparation and lyses of cells, thus questioning the validity of this assay. However, it is interesting to note the similar trends between both tumor and plasma samples.

Figure 6-5: Representative western blots of TNF-α, TNFR1, and TNFR2 protein expression in tumors of Zk-Ob, Zk-Ln, and SD animals (A), and (B) Bar graphs of mean densitometric values.

Tumor homogenates, 100 μg of protein per sample, were separated by SDS-PAGE, and transferred onto membranes. Following incubation with primary antibodies and corresponding AP-conjugated secondary antibodies, blots were developed with BCIP/NBT solution, and bands quantified by densitometric analyses. Values in (B) are pixels (arbitrary units) and are mean ± SE, n=6 per group. Each band represents a tumor from one animal, and groups are as indicated. Bars without a common superscript[(x,y,z)] are significantly different, $p<0.05$, as determined by ANOVA analyses with LSD and Tukey post hoc tests. Zk-Ob: Zucker obese, Zk-Ln: Zucker lean, SD: Sprague dawley.

NF-κB, IκBα, and IKKβ protein expression

NF-κB, IκBα, and IKKβ protein expression were determined by western blot (Figure 6-6). NF-κB and IκBα levels were significantly higher in Zk-Ob and SD tumors. An additional band was noted for IκBα, and showed no differences among the groups. IKKβ levels were highest in Zk-Ob tumors.

Active p65 NF-κB levels showed significantly higher levels in Zk-Ob tumors in comparison to Zk-Ln and SD tumors (Figure 6-7). These results correlated with protein expression patterns shown by western blot for both NF-κB and IKKβ, the enzyme responsible for releasing NF-κB in its active form. NF-κB activity associated with high levels of IκBα was unexpected due to its role as an inhibitor of NF-κB. However, IκBα is transcribed by NF-κB, and higher levels in Zk-Ob and SD tumors may be a result of the increased NF-κB activity, trying to initiate a negative feedback signal. Overall, analyses demonstrated increased activity of the NF-κB signaling pathway in Zk-Ob and SD tumors.
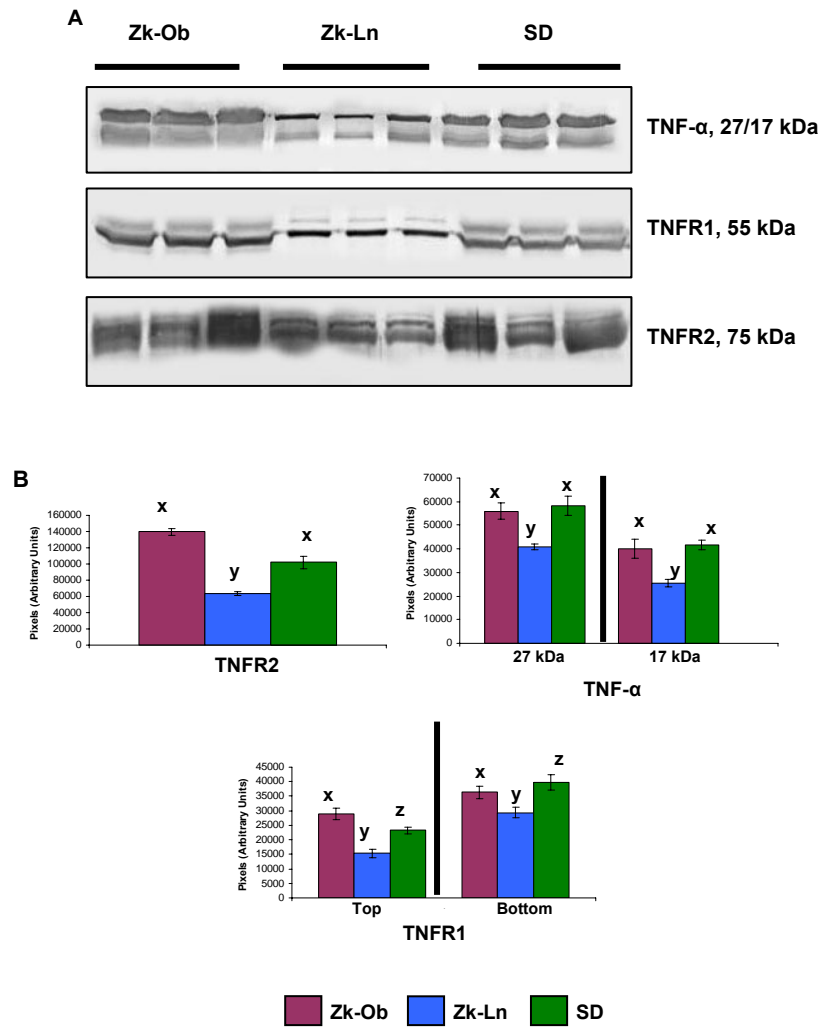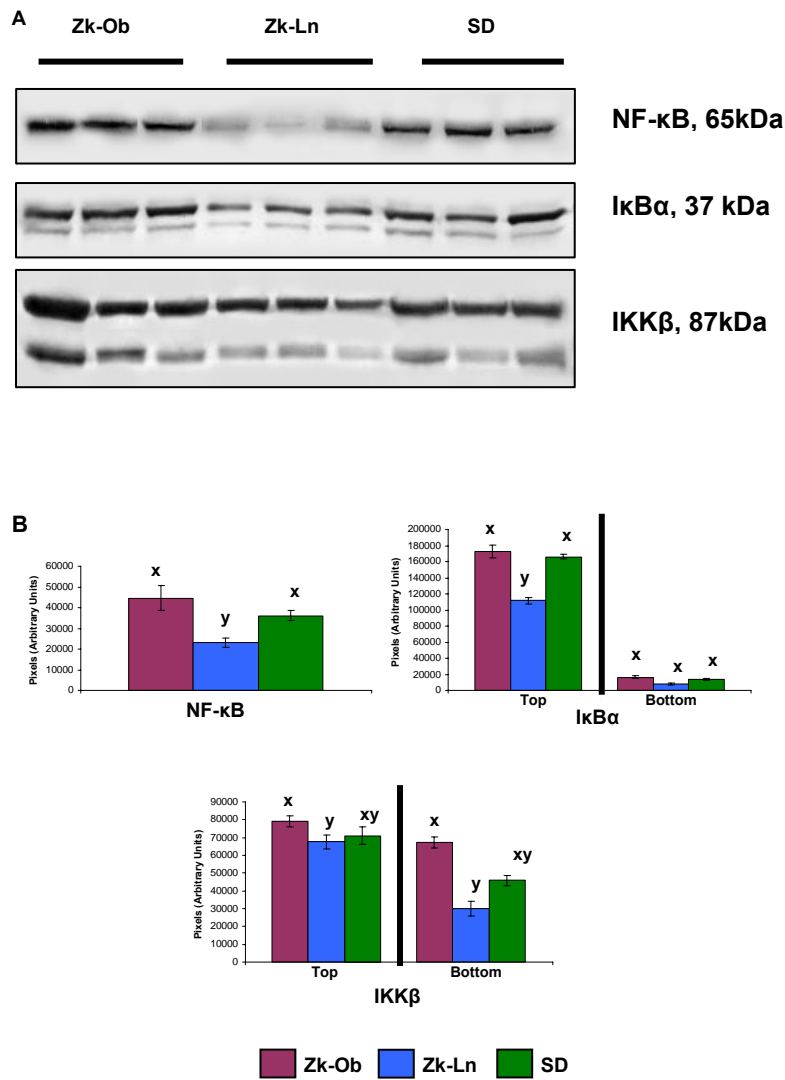
Figure 6-6: Representative western blots of NF-κB, IκBα, and IKKβ protein expression in tumors of Zk-Ob, Zk-Ln and SD animals (A), and (B) Bar graphs of mean densitometric values.

Tumor homogenates, 100 μg of protein per sample, were separated by SDS-PAGE, and transferred onto membranes. Following incubation with primary antibodies and corresponding AP-conjugated secondary antibodies, blots were developed with BCIP/NBT solution, and bands quantified by densitometric analyses. Values in (B) are pixels (arbitrary units) and are mean ± SE, n=6 per group. Each band represents a tumor from one animal, and groups are as indicated. Bars without a common superscript[(x,y,z)] are significantly different, $p<0.05$, as determined by ANOVA analyses with LSD and Tukey post hoc tests. Zk-Ob: Zucker obese, Zk-Ln: Zucker lean, SD: Sprague dawley.

Figure 6-7: Active p65 NF-κB levels in Zk-Ob, Zk-Ln, and SD tumors.

Assay was carried out using the TransAM kit as per manufacturer instructions (Active Motif). Briefly, tumor homogenates, 10μg of protein per sample, were incubated with an oligonucleotide specific to NF-κB. Subsequent incubation with primary antibody specific to the p65 subunit was followed by exposure to HRP-conjugated secondary antibody and developing solution. Absorbance was read at 450nm. Values are mean ± SE, n=6 per group. Bars without a common superscript[x,y,z] are significantly different, $p<0.05$, as determined by ANOVA analyses with LSD and Tukey post hoc tests. Zk-Ob: Zucker obese, Zk-Ln: Zucker lean, SD: Sprague dawley.
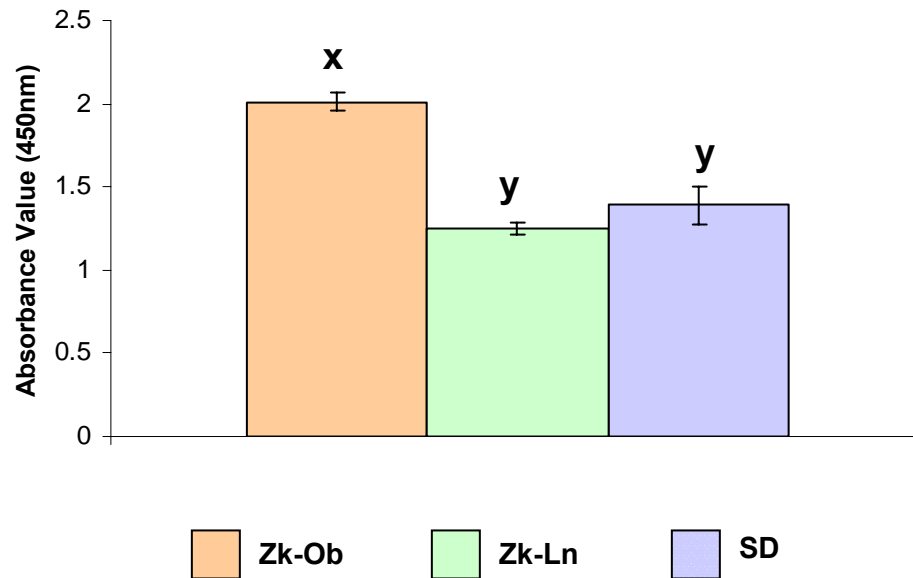
IGF-IRα, IRα, and IRβ protein expression

IGF-IRα, IRα, and IRβ protein levels were determined via western blot (Figure 6-8). Expression for all these proteins was significantly higher in Zk-Ob and SD tumors in comparison to Zk-Ln. Both IGF-IR and IR are associated with tumor promotion, and are considered important factors in obesity associated tumorigenesis (Giovannucci 2001, Ma et al. 1999). High levels of these proteins in Zk-Ob tumors also corroborated with hyperinsulinemia and insulin resistance observed in these animals, which further contribute to an increased risk for cancer.

MAPK p42/44 protein expression

MAPK p42/44 protein levels were analyzed by western blot, and were observed to be notably higher in Zk-Ob tumors for both forms (Figure 6-9). MAPK, a serine/threonine kinase, can initiate, or be activated by a number of signaling pathways, including NF-κB (Pearson et al. 2001). This enzyme family is multi-functional, influencing cell differentiation, proliferation, and death. MAPK is also implicated in increasing NF-κB transcriptional activity (reviewed in Perkins and Gilmore 2006). It is apparent that Zk-Ob tumors had higher levels of MAPK p42/44 than Zk-Ln tumors. This may be related to the elevated levels of NF-κB, IR, and IGF-IRα signaling leading to the augmented growth noted in Zk-Ob tumors.

Figure 6-8: Representative western blots of IGF-IRα, IRα, and IRβ protein expression in tumors of Zk-Ob, Zk-Ln, and SD animals (A), and (B) Bar graphs of mean densitometric values.

Tumor homogenates, 100 μg of protein per sample, were separated by SDS-PAGE, and transferred onto membranes. Following incubation with primary antibodies and corresponding AP-conjugated secondary antibodies, blots were developed with BCIP/NBT solution, and bands quantified by densitometric analyses. Values in (B) are pixels (arbitrary units) and are mean ± SE, n=6 per group. Each band represents a tumor from one animal, and groups are as indicated. Bars without a common superscript[(x,y,z)] are significantly different, p<0.05, as determined by ANOVA analyses with LSD and Tukey post hoc tests. Zk-Ob: Zucker obese, Zk-Ln: Zucker lean, SD: Sprague dawley.
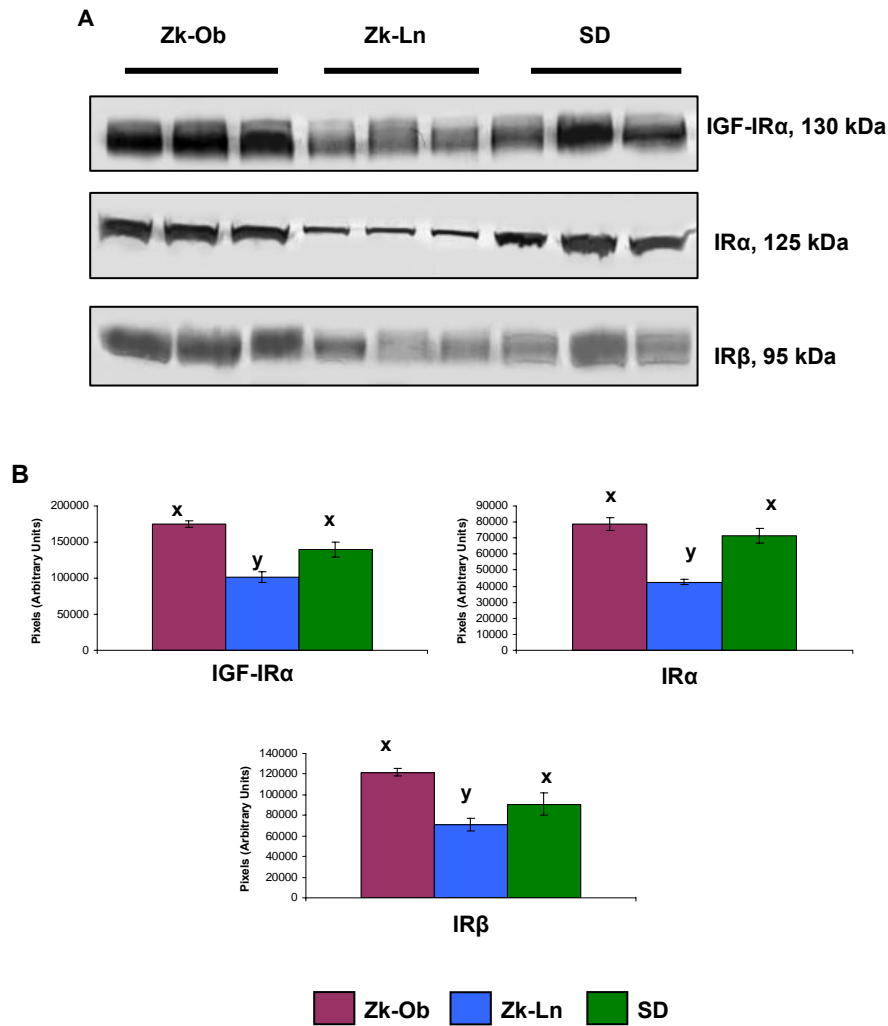
Figure 6-9: Representative western blot of MAPK p42/44 protein expression in tumors of Zk-Ob, Zk-Ln, and SD animals (A), and (B) Bar graphs of mean densitometric values.

Tumor homogenates, 100 μg of protein per sample, were separated by SDS-PAGE, and transferred onto membranes. Following incubation with primary antibodies and corresponding AP-conjugated secondary antibodies, blots were developed with BCIP/NBT solution, and bands quantified by densitometric analyses. Values in (B) are pixels (arbitrary units) and are mean ± SE, n=6 per group. Each band represents a tumor from one animal, and groups are as indicated. Bars without a common superscript[(x,y,z)] are significantly different, p<0.05, as determined by ANOVA analyses with LSD and Tukey post hoc tests. Zk-Ob: Zucker obese, Zk-Ln: Zucker lean, SD: Sprague dawley.
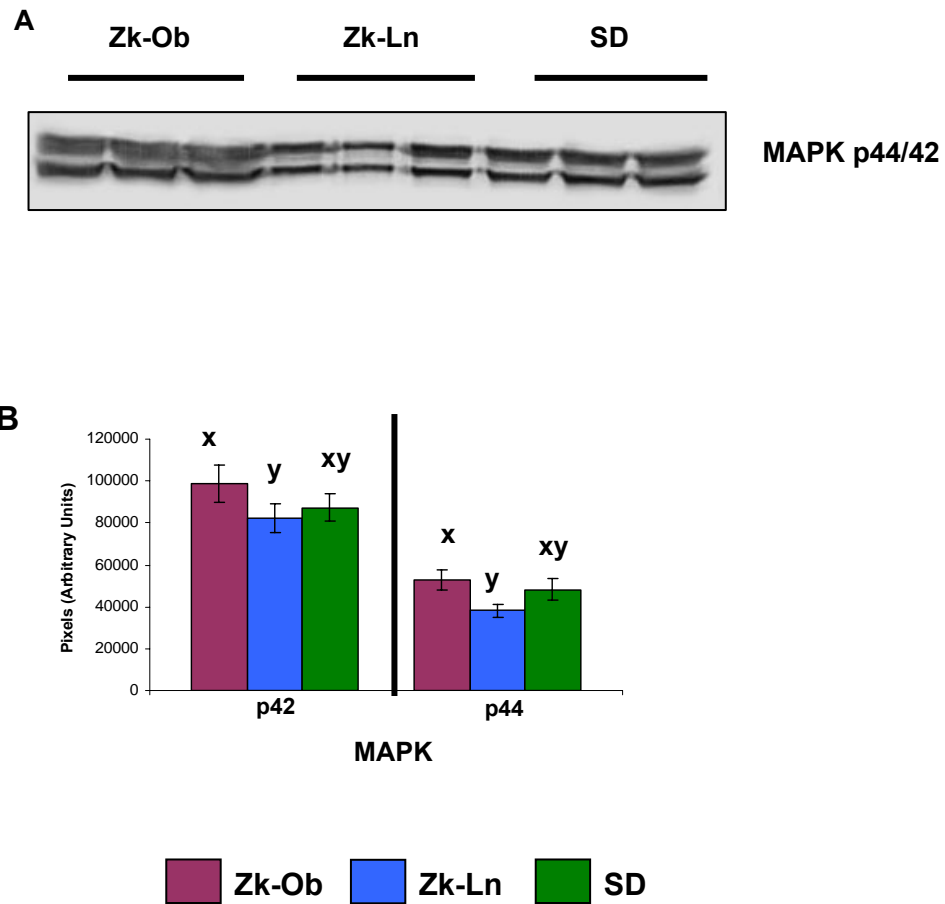
6.4.3 Protein Expression Patterns in Colonic Mucosae

Colonic mucosal homogenates from control and AOM injected animals were analyzed for proteins expression of key players in TNF-α and NF-κB pathways including TNF-α, TNFR1, and TNFR2, NF-κB, IκBα, and IKKβ. In addition, modulators of the insulin and glucose homeostasis pathways, IGF-IRα, IRα, and IRβ were examined. Finally, mucosal samples were also analyzed for MAPK p42/44 enzyme. Overall, insignificant differences were seen between control and AOM injected colonic mucosal samples.

TNF-α, TNFR1, and TNFR2 protein expression

TNF-α, TNFR1, and TNFR2 protein expression were determined by western blot (Figure 6-10). Protein bands at 27 and 17 kDa were observed for TNF-α, possibly corresponding to the transmembrane and soluble protein forms respectively. Zk-Ob and SD rats had significantly higher levels of the 27kDa protein than Zk-Ln animals, with no difference between respective AOM and control groups. Overall, there was more 27kDa than 17kDa TNF-α for all groups. Higher levels of soluble 17 kDa TNF-α were observed in the control than AOM injected groups collectively. Within the AOM injected animals, Zk-Ln rats had lowest expression of 17kDa TNF-α

Zk-Ob and SD rats had significantly higher levels of TNFR1 in comparison to Zk-Ln, while no difference was observed between AOM and control groups. Similarly, Zk-Ob and SD animals had higher TNFR2 expression in comparison to Zk-Ln, and no differences were seen between control and AOM groups.

Figure 6-10: Representative western blots of TNF-α, TNFR1, and TNFR2 protein expression in colonic mucosae of (A) control and (B) AOM injected Zk-Ob, Zk-Ln, and SD animals, and (C) Bar graphs of mean densitometric values.

Colonic mucosal homogenates, 300 μg of protein per sample, were separated by SDS-PAGE, and transferred onto membranes. Following incubation with primary antibodies and corresponding AP-conjugated secondary antibodies, blots were developed with BCIP/NBT solution, and bands quantified by densitometric analyses. Values in (C) are pixels (arbitrary units) and are mean ± SE, n=6 per group. Each band represents a colon sample from one animal, and groups are as indicated. Bars without a common superscript[(x,y,z)] are significantly different, p<0.05, as determined by ANOVA analyses with LSD and Tukey post hoc tests. Zk-Ob: Zucker obese, Zk-Ln: Zucker lean, SD: Sprague dawley, subscript c indicates control animals.

NF-κB, IκBα, and IKKβ protein expression

NF-κB, IκBα, and IKKβ protein expression were determined by western blot (Figure 6-11). NF-κB and IKKβ levels are elevated in Zk-Ob and SD groups significantly more than Zk-Ln animals. In addition to the 87 kDa IKKβ band, another closely related band was visualized. IκBα levels were significantly lower in all AOM injected groups in comparison to their controls, while no differences were observed between the genotypes.

Active NF-κB levels were significantly higher in Zk-Ob animals, and further increased in the corresponding AOM injected group in comparison to Zk-Ln and SD groups (Figure 6-12). No differences were found between Zk-Ln and SD control and AOM injected groups. High levels of active NF-κB in Zk-Ob rats corresponded to IKKβ protein levels as this enzyme is responsible for releasing NF-κB into its functional form (Hayden and Ghosh 2006).
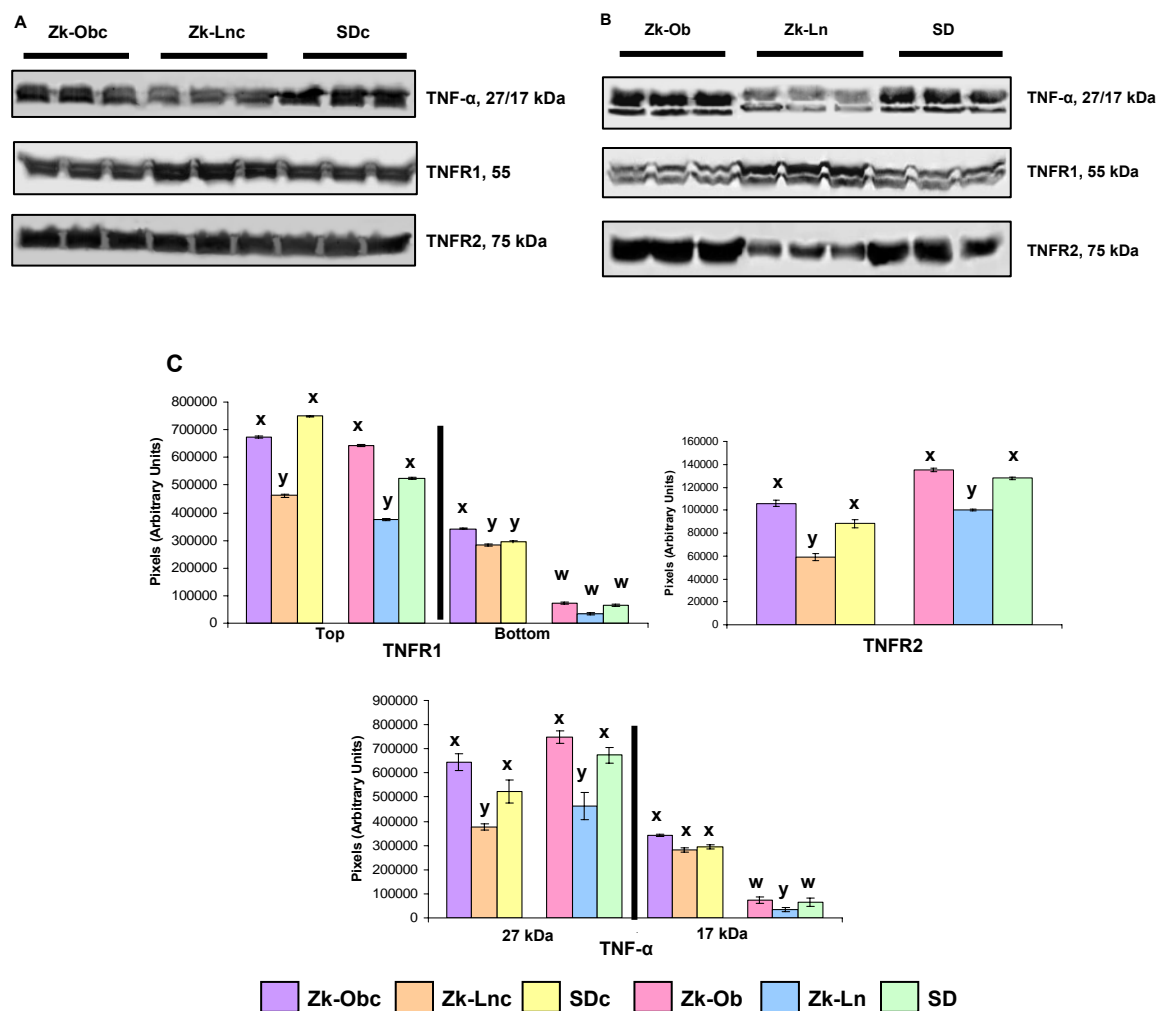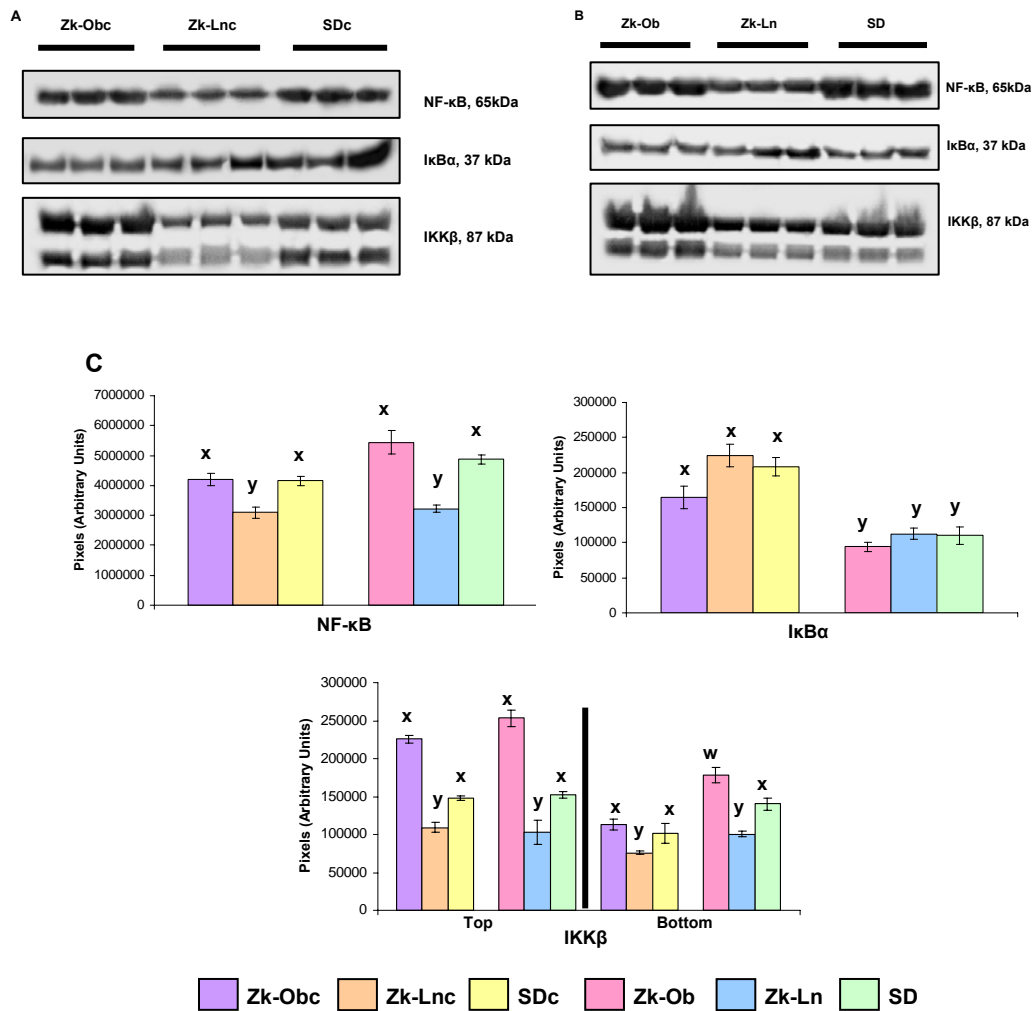
Figure 6-11: Representative western blots of NF-κB, IκBα, and IKKβ protein expression in colonic mucosa of (A) control and (B) AOM injected Zk-Ob, Zk-Ln, and SD animals, and (C) Bar graphs of mean densitometric values.

Colonic mucosal homogenates, 300 μg of protein per sample, were separated by SDS-PAGE, and transferred onto membranes. Following incubation with primary antibodies and corresponding AP-conjugated secondary antibodies, blots were developed with BCIP/NBT solution, and bands quantified by densitometric analyses. Values in (C) are pixels (arbitrary units) and are mean ± SE, n=6 per group. Each band represents a colon sample from one animal, and groups are as indicated. Bars without a common superscript[(x,y,z)] are significantly different, p<0.05, as determined by ANOVA analyses with LSD and Tukey post hoc tests. Zk-Ob: Zucker obese, Zk-Ln: Zucker lean, SD: Sprague dawley, subscript c indicates control animals.

Figure 6-12: Measurement of active p65 NF-κB levels in colonic mucosae of control and AOM injected Zk-Ob, Zk-Ln, and SD rats.

Assay was carried out using the TransAM kit. Briefly, colonic mucosal homogenates, 10 μg of protein per sample, were incubated with an oligonucleotide specific to NF-κB. Subsequent incubation with primary antibody specific to the p65 subunit was followed by exposure to HRP-conjugated secondary antibody and developing solution. Absorbance was read at 450nm. Values are mean ± SE, n=6 per group. Bars without a common superscript[(x,y,z)] are significantly different, p<0.05, as determined by ANOVA analyses with LSD and Tukey post hoc tests. AOM: azoxymethane, Zk-Ob: Zucker obese, Zk-Ln: Zucker lean, SD: Sprague dawley, subscript c indicates control animals.
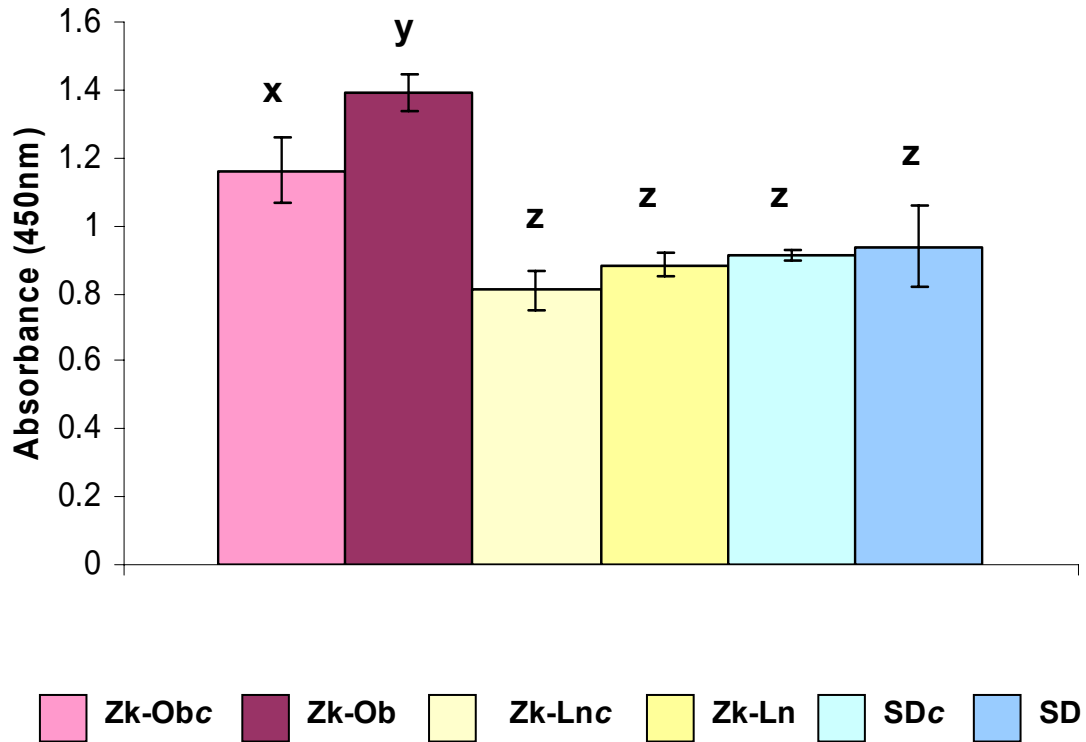
IGF-IRα, IRα, and IRβ protein expression

IGF-IRα, IRα, and IRβ protein levels were determined via western blot (Figure 6-13). IGF-IRα levels were significantly increased in AOM injected Zk-Ob animals in comparison to SD, which were also higher than Zk-Ln rats. All three AOM injected groups had higher IGF-IRα than their respective controls. IRα expression was also significantly higher in Zk-Ob and SD animals than Zk-Ln. The only notable difference between control and AOM injected groups was present in Zk-Ob animals, which had the highest expression. Zk-Ob rats had highest levels of IRβ followed by SD and Zk-Ln groups respectively. The only difference present between AOM and control groups was in Zk-Ln animals, where AOM injected rats had higher expression of IRβ.

MAPK p42/44 protein expression

MAPK p42/44 protein levels were analyzed by western blot (Figure 6-14). AOM injected Zk-Ob and SD groups showed increased expression of both MAPK p42 and p44 in comparison to Zk-Ln rats, while no differences were seen among all control groups for both forms. Higher levels of p42 than p44 were noted between AOM injected groups.

Figure 6-13: Representative western blots of IGF-IRα, IRα, and IRβ protein expression in colonic mucosae of (A) control and (B) AOM injected Zk-Ob, Zk-Ln, and SD animals, and (C) Bar graphs of mean densitometric values.

Colonic mucosal homogenates, 300 µg of protein per sample, were separated by SDS-PAGE, and transferred onto membranes. Following incubation with primary antibodies and corresponding AP-conjugated secondary antibodies, blots were developed with BCIP/NBT solution, and bands quantified by densitometric analyses. Values in (C) are pixels (arbitrary units) and are mean ± SE, n=6 per group. Each band represents a colon sample from one animal, and groups are as indicated. Bars without a common superscript[(x,y,z)] are significantly different, $p < 0.05$, as determined by ANOVA analyses with LSD and Tukey post hoc tests. Zk-Ob: Zucker obese, Zk-Ln: Zucker lean, SD: Sprague dawley, subscript c indicates control animals.
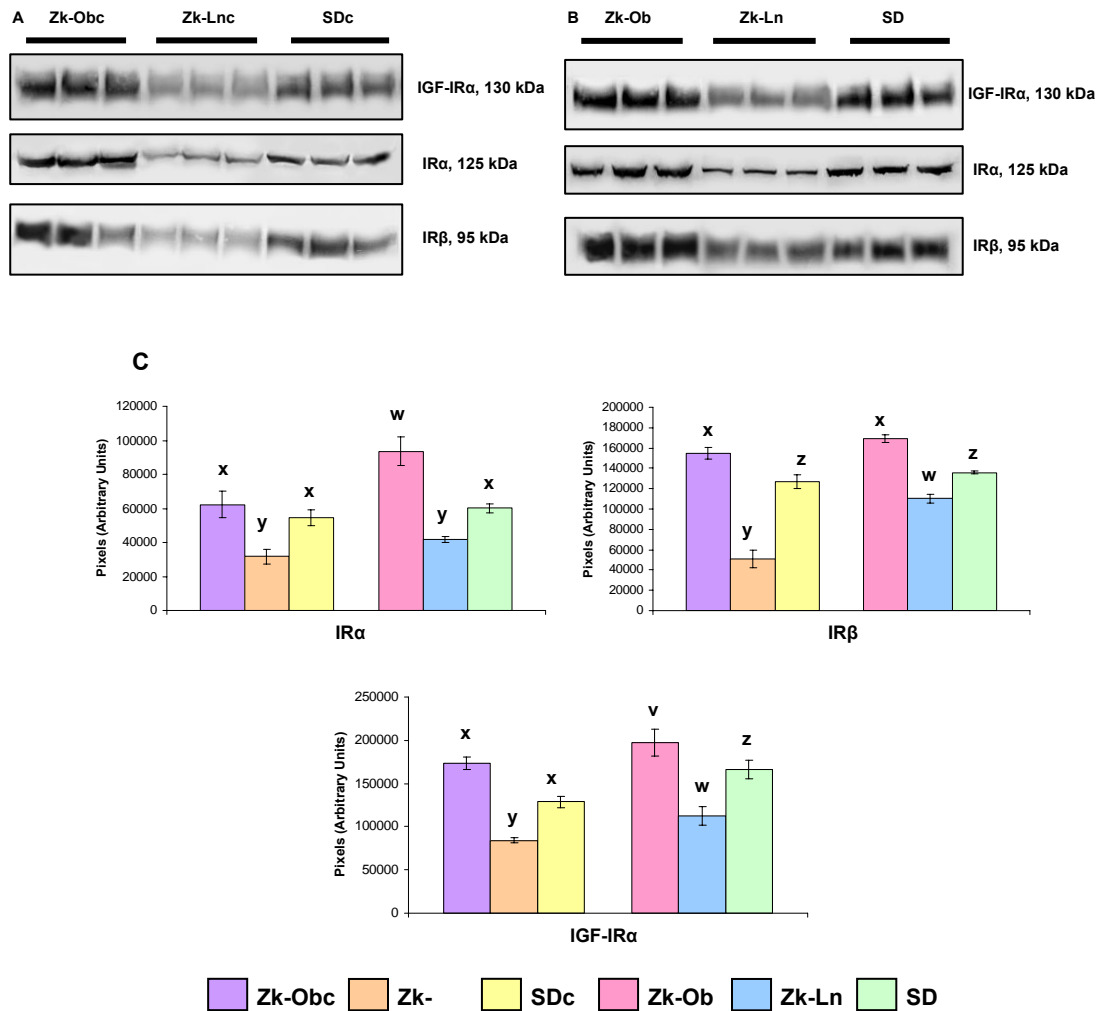
Figure 6-14: Representative western blots of MAPK p42/44 protein expression in colonic mucosae of (A) control and (B) AOM injected Zk-Ob, Zk-Ln, and SD animals, and (C) Bar graphs of mean densitometric values.

Colonic mucosal homogenates, 300 μg of protein per sample, were separated by SDS-PAGE, and transferred onto membranes. Following incubation with primary antibodies and corresponding AP-conjugated secondary antibodies, blots were developed with BCIP/NBT solution, and bands quantified by densitometric analyses. Values in (C) are pixels (arbitrary units) and are mean ± SE, n=6 per group. Each band represents a colon sample from one animal, and groups are as indicated. Bars without a common superscript[(x,y,z)] are significantly different, p<0.05, as determined by ANOVA analyses with LSD and Tukey post hoc tests. Zk-Ob: Zucker obese, Zk-Ln: Zucker lean, SD: Sprague dawley, subscript c indicates control animals.
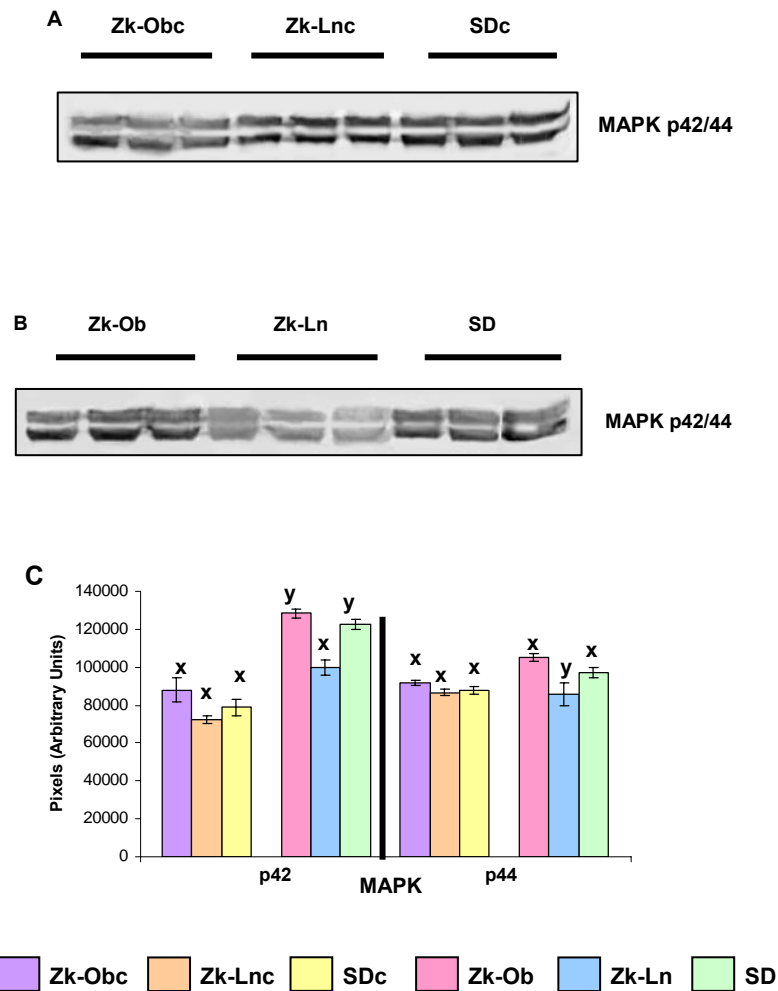
Overall, the differences between control and AOM injected colon mucosae were not significant. Early stages of carcinogenesis exhibit more vulnerability towards transformations in the mucosa. Moreover, physiological conditions of the animal do not have global effects on cancer progression as some stages are more sensitive than others. Thus, the modest changes that are observed between control and AOM animals are possibly due to the mature stage of cancer in these animals.

6.4.4 Comparison of protein expression between tumors and colonic mucosae

Protein levels were compared between tumors and corresponding normal appearing colonic mucosae, presented on an equal protein basis (Figure 6-15). Similar patterns within tumors and mucosal groups were retained as described previously. Analyses indicated significantly higher protein levels in tumors from all groups than mucosae. It is interesting to note that Zk-Ob tumors in particular had relatively higher levels of TNFR2, NF-κB, IGF-IRα, and MAPK. These proteins are implicated in mediation of cell survival, and their increased presence in tumors substantiate their roles in providing a growth advantage. Overall, the remarkable distinction between tumor and mucosal protein levels demonstrated that changes in protein expression may be more specific to neoplastic lesions.

Higher protein level of NF-κB is also substantiated by increased active NF-κB levels in tumors compared to colonic mucosae (Figure 6-16).

A

TNFR1

TNFR2

TNF-α

27 kDa 17 kDa

B

NF-κB

IκBα

IKKβ

Top Bottom

Zk-Ob(CM) Zk-Ln(CM) SD(CM) Zk-Ob(T) Zk-Ln(T) SD(T)
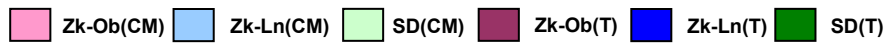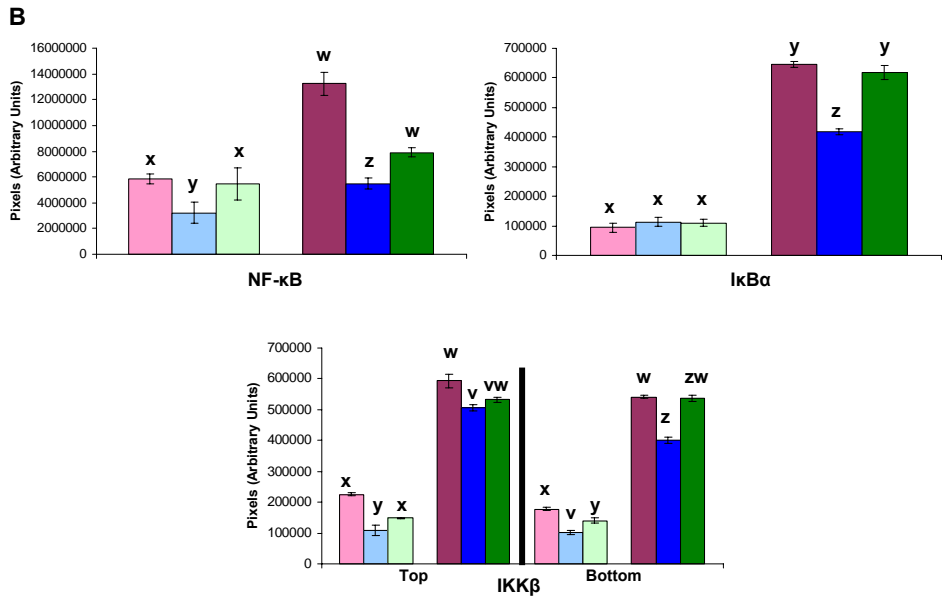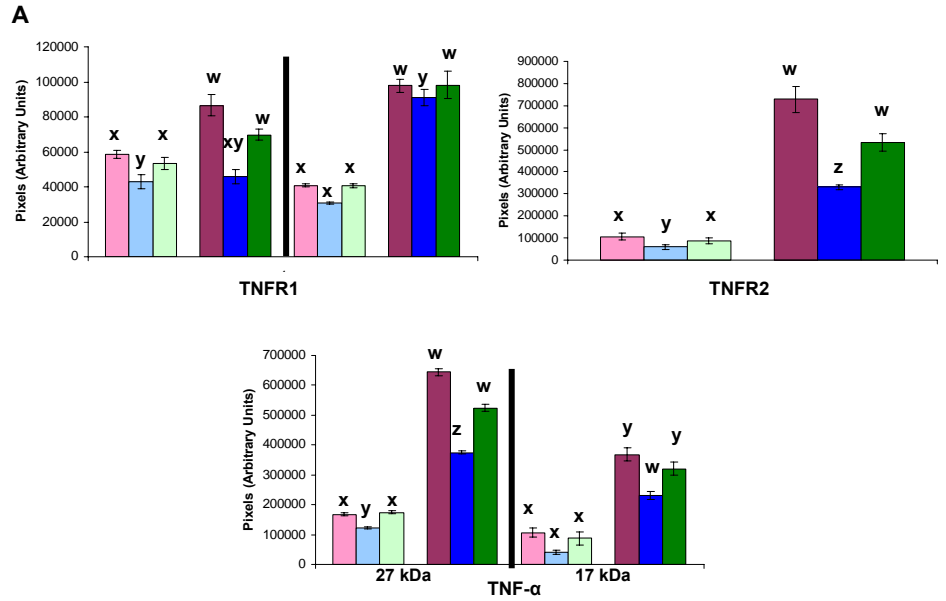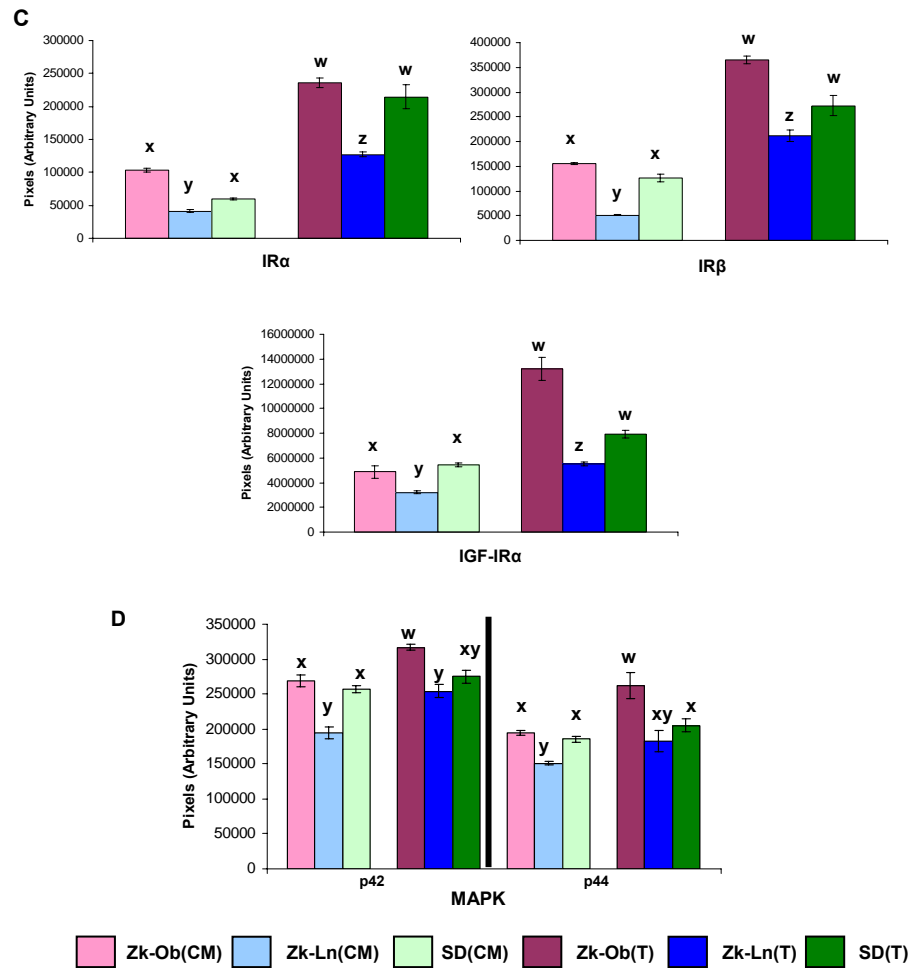
Figure 6-15: Bar graphs of mean densitometric values showing comparisons between tumors and colonic mucosae in Zk-Ob, Zk-Ln, and SD rats for protein expression of (A) TNF-α, TNFR1, and TNFR2, (B) NF-κB, IκBα, and IKKβ, (C) IGF-IRα, IRα, and IRβ, and (D) MAPK p42/44.

Densitometric values from tumor and colonic mucosae were compared to evaluate changes in protein expression. Three times protein was loaded for colon versus tumors samples. Thus, densitometry values from tumor data were adjusted to represent equal amounts of protein. Values are pixels (arbitrary units), and represent mean ± SE, n=6 per group. Bars without a common superscript[(w,x,y,z)] are significantly different, $p < 0.05$, as determined by ANOVA analyses with LSD and Tukey post hoc tests. CM: colonic mucosae, T: tumors, Zk-Ob: Zucker obese, Zk-Ln: Zucker lean, SD: Sprague dawley.
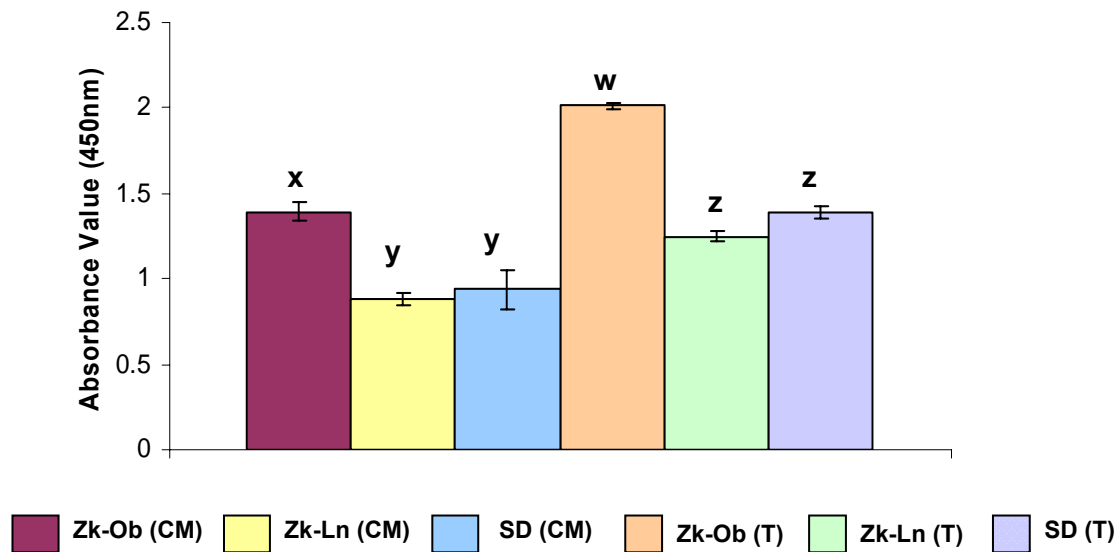
Figure 6-16: Comparison between colonic mucosae and tumors in Zk-Ob, Zk-Ln, and SD rats for active NF-κB levels.

Assay was carried out using the TransAM kit as per manufacture instructions. Briefly, colonic mucosal and tumor homogenates, 10 μg of protein per sample, were incubated with an oligonucleotide specific to NF-κB. Subsequent incubation with primary antibody specific to the p65 subunit was followed by exposure to HRP-conjugated secondary antibody and developing solution. Absorbance was read at 450nm. Values are mean ± SE, n=6 per group. Bars without a common superscript[(w,x,y,z)] are significantly different, $p < 0.05$, as determined by ANOVA analyses with LSD and Tukey post hoc tests. CM: colonic mucosae, T: tumors, Zk-Ob: Zucker obese, Zk-Ln: Zucker lean, SD: Sprague dawley.

6.4.5 IHC Analyses

IHC analyses was performed on Zk-Ob, Zk-Ln, and SD tumor sections for NF-κB, IκBα, TNF-α, TNFR1, and TNFR2 proteins. Unlike immunoblotting which provided quantitative data, IHC was used to determine possible differences in the spatial expression of key molecules of interest. This methodology was used qualitatively and changes in protein levels in tumors were further compared with surrounding, normal appearing colonic mucosa.

General Morphology

One section from each tumor was stained with a combination of H&E stain. Hematoxylin stains the nuclei a blue-black color, while cytoplasm is stained pink by red counterstain eosin. Figure (6-17A) shows H&E sections of tumors with clusters of dysplastic crypts, infiltrating lymphocytes and stromal cells. Overall, a greater proportion of Zk-Ln and SD tumors were characterized as fibroadenomas. Figure (6-17B) shows normal appearing colonic crypts adjacent to tumor tissue.

TNF-α

IHC analyses for TNF-α showed overall diffuse staining throughout the tumor mass with no particular trend between the groups (Figure 6-18). Intense staining in the apical membrane was observed. It was important to note that luminal compartments of the tumor epithelium contained secretory products that exhibited intense staining. Three possibilities exist for the staining of luminal contents: 1) secretion of TNF-α by tumor tissue, 2) shedding of TNF-α bound to a membrane receptor, and 3) tumor cells are exuded due to TNF-α mediated cytotoxicity.
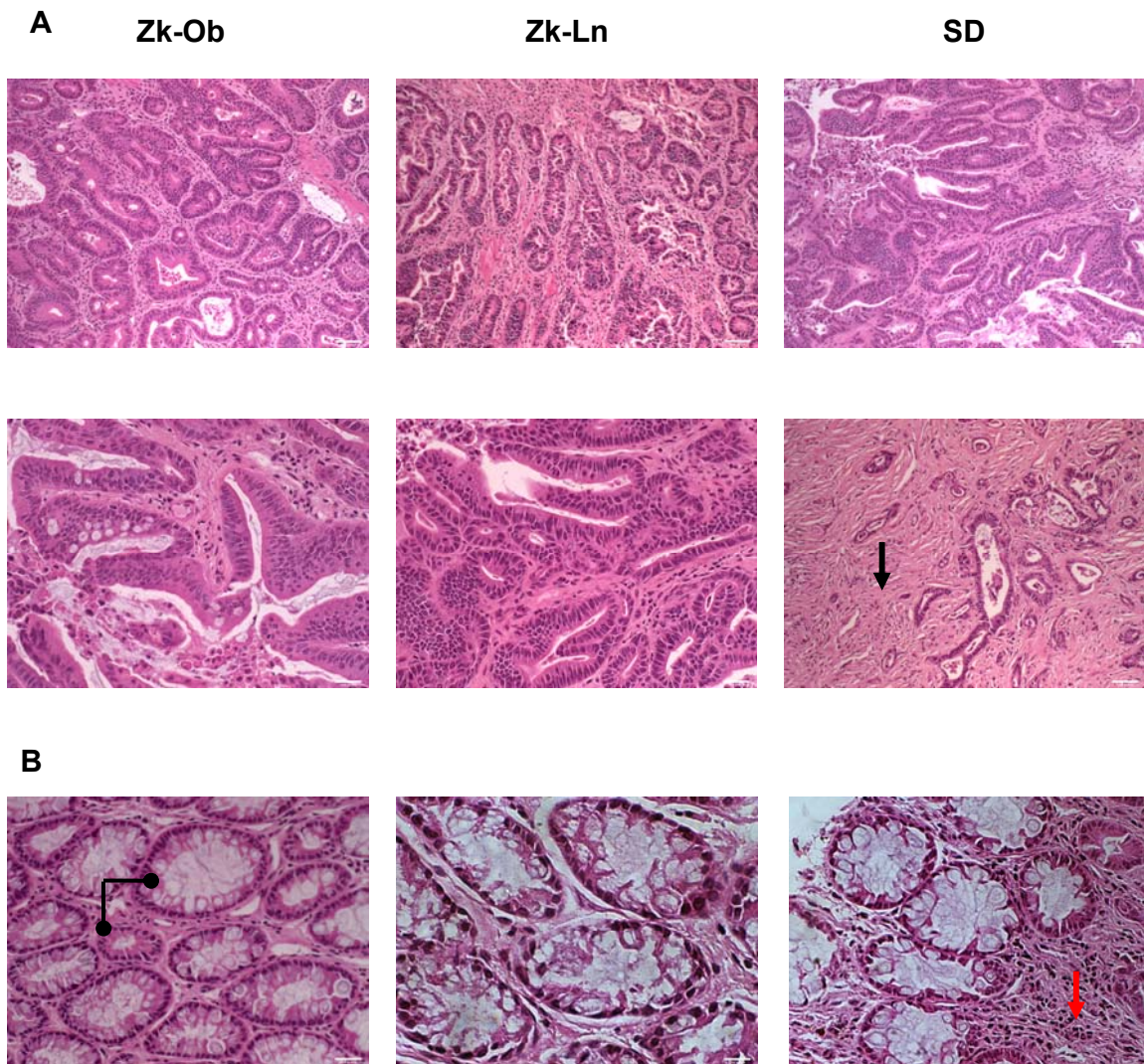
Figure 6-17: H&E staining of tumor sections from Zk-Ob, Zk-Ln, and SD animals showing (A) tumor (top panel 100x, bottom panel 200x), and (B) normal appearing tissue (400x).

Tumors were sectioned and stained with H&E for observation of general morphology. (A) Marked dysplasia was seen in all tumor types. Note fibrous characteristics of SD tumor (black arrow). (B) Normal appearing colonic crypts were observed in each tissue type. Note the variability of crypt sizes in Zk-Ob colonic section as depicted by the different sizes of the crypt lumen (round arrow). Infiltrating lymphocytes in SD section were observed (red arrow). Zk-Ob: Zucker obese, Zk-Ln: Zucker lean, SD: Sprague dawley.
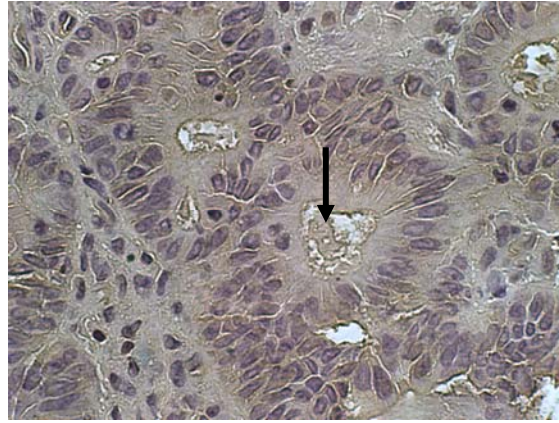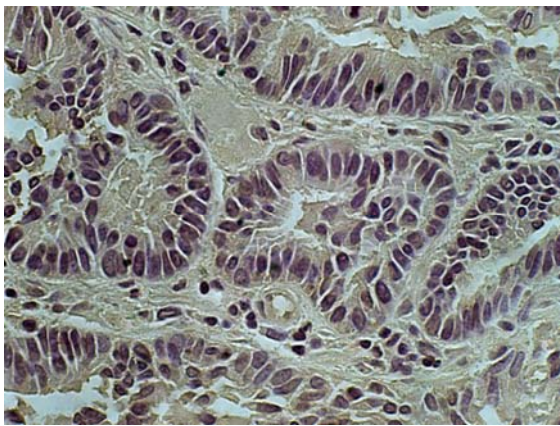
Zk-Ob

Zk-Ln

SD

Figure 6-18: IHC staining for TNF-α in Zk-Ob, Zk-Ln, and SD tumor sections (400x).

Sections were deparaffinized and dehydrated, incubated in blocking buffer, primary, and biotinylated secondary antibody respectively. Reaction was monitored following addition of enzyme conjugate and DAB chromagen, and sections were counterstained, rehydrated, and mounted with coverslips. Note marked staining in secretory materials exhibiting particular reactivity to antibody (black arrows), and intense staining of apical membrane (red arrow). Zk-Ob: Zucker obese, Zk-Ln: Zucker lean, SD: Sprague dawley.

TNFR1 and TNFR2

Localized intense staining for TNFR1 in epithelial cells and apical membrane was observed in all tumors (Figures 6-19). Secretory products with intense staining in the lumen of crypts were noted, possibly corresponding to soluble forms of receptors. Unexpectedly, diffuse nuclear staining was also seen throughout the tumor mass.

As in TNFR1, a similar staining pattern was observed for TNFR2 (Figure 6-20). Intense staining in the membrane and secretory products were observed, more notably than TNFR1. A similar pattern was seen with western blot analyses, where expression of TNFR2 was significantly higher that TNFR1 in tumors. Nuclear staining was more prominent in comparison to TNFR1. Zk-Ln tumors exhibited more diffuse staining in comparison to other groups.

NF-κB and IκBα

Both localized as well as diffuse staining was observed for p65 NF-κB, particularly in the apical membranes (Figure 6-21). Nuclear staining was more abundant in Zk-Ob tumors than Zk-Ln and SD, corresponding to high levels of active NF-κB determined previously. Zk-Ln and SD tumors had a higher proportion of stromal cell populations compared to Zk-Ob, which also exhibited marked reactivity to the antibody. No discernable pattern was observed between tumor groups for IκBα. Diffuse staining throughout the tumor mass with occasional nuclear staining was present (Figure 6-22)

In general, ICH analyses demonstrated localized intense staining in stromal elements of the tissue. It can therefore be speculated that there is communication present between the tumor and its microenvironment, which facilitates growth progression. For example, TNF-α present in the stroma can affect structure remodeling via inducing MMP, promote angiogenesis, and recruit macrophages and additional cytokine molecules (reviewed in Szlosarek et al. 2006).

Zk-Ob
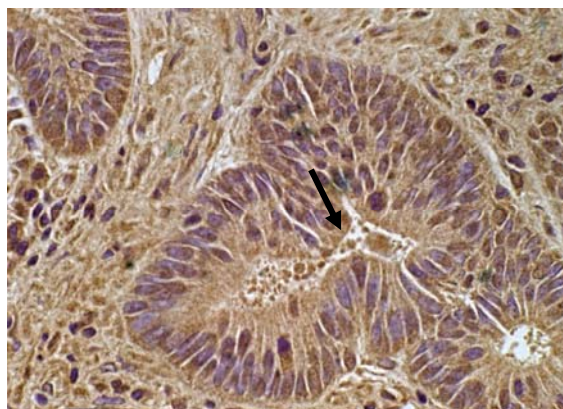
Zk-Ln
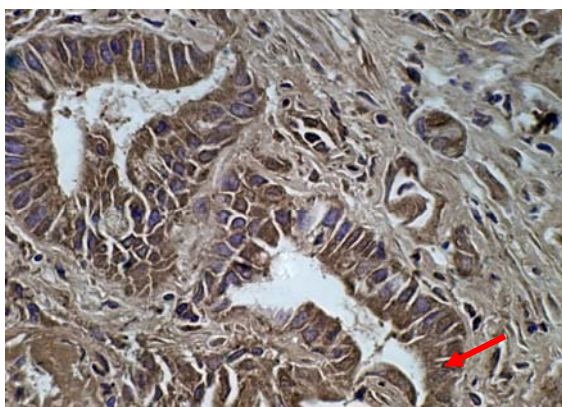
SD
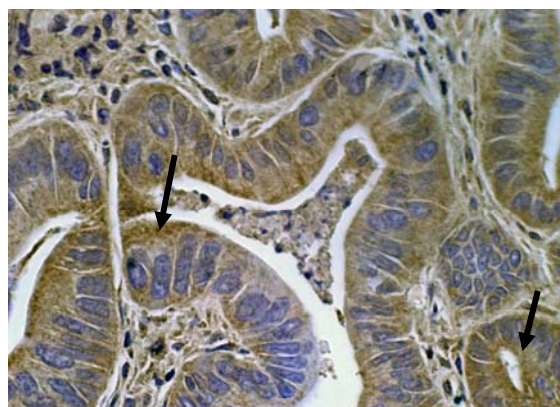
Figure 6-19: IHC staining for TNFR1 in Zk-Ob, Zk-Ln, and SD tumor sections (400x).

Sections were deparaffinized and dehydrated, incubated in blocking buffer, primary, and biotinylated secondary antibody respectively. Reaction was monitored following addition of enzyme conjugate and DAB chromagen, and sections were counterstained, rehydrated, and mounted with coverslips. Note marked staining in secretory materials exhibiting particular reactivity to antibody in Zk-Ob tumor (red arrow), and intense staining of apical membrane in Zk-Ln and SD tumors (black arrow). Zk-Ob: Zucker obese, Zk-Ln: Zucker lean, SD: Sprague dawley.
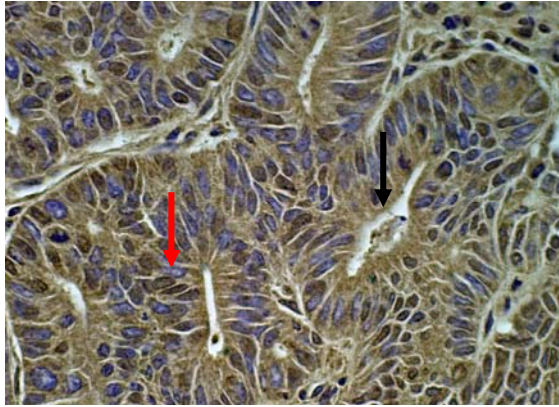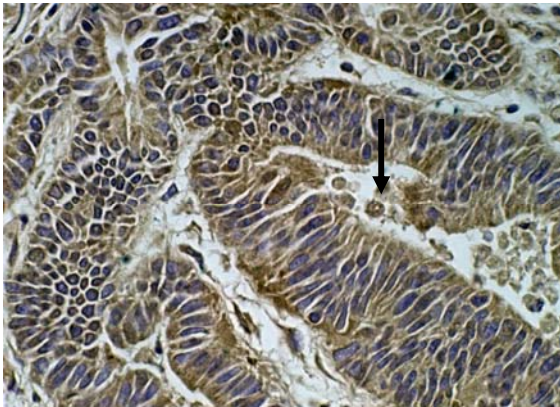
Zk-Ob

Zk-Ln

SD
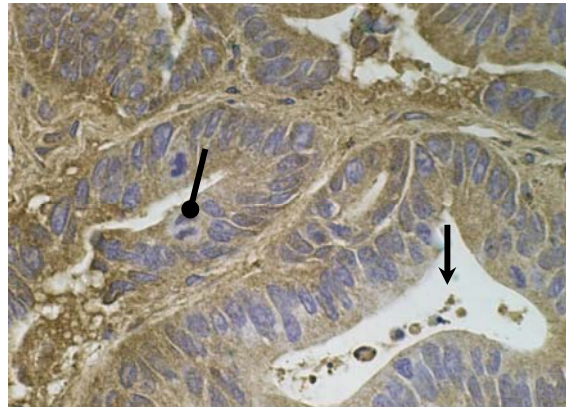
Figure 6-20: IHC staining for TNFR2 in Zk-Ob, Zk-Ln, and SD tumor sections (400x).

Sections were deparaffinized and dehydrated, incubated in blocking buffer, primary, and biotinylated secondary antibody respectively. Reaction was monitored following addition of enzyme conjugate and DAB chromagen, and sections were counterstained, rehydrated, and mounted with coverslips. Note marked staining in secretory materials exhibiting particular reactivity to antibody (black arrows), and an area of intense nuclear staining in Zk-Ob tumor (red arrow). Note: a dividing cell (round arrow). Zk-Ob: Zucker obese, Zk-Ln: Zucker lean, SD: Sprague dawley.
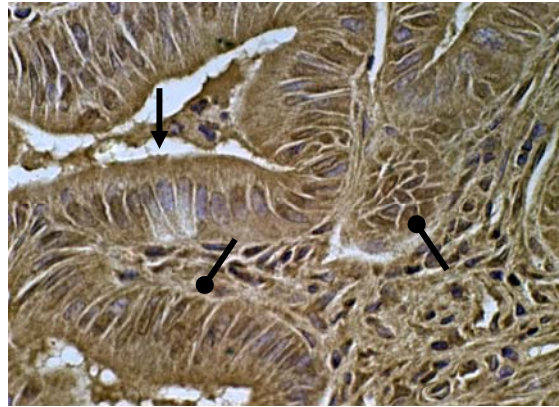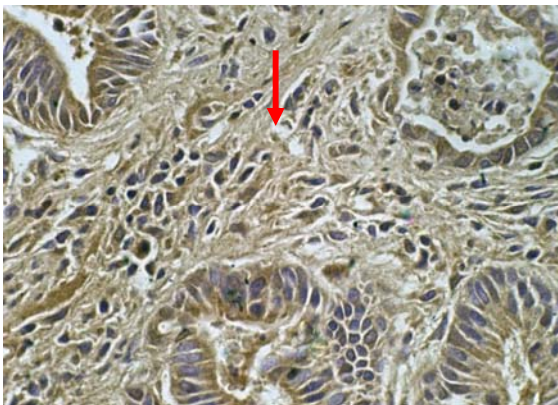
Zk-Ob

Zk-Ln

SD
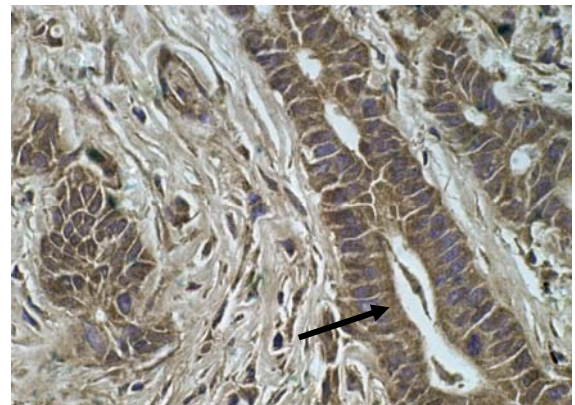
Figure 6-21: IHC staining for NF-κB in Zk-Ob, Zk-Ln, and SD tumor sections (400x).

Sections were deparaffinized and dehydrated, incubated in blocking buffer, primary, and biotinylated secondary antibody respectively. Reaction was monitored following addition of enzyme conjugate and DAB chromagen, and sections were counterstained, rehydrated, and mounted with coverslips. Note marked staining in apical membranes (black arrows), and nuclear staining in Zk-Ob tumors (round arrow). Fibroblasts in Zk-Ln tumors also exhibited particular reactivity to antibody (red arrow). Zk-Ob: Zucker obese, Zk-Ln: Zucker lean, SD: Sprague dawley.
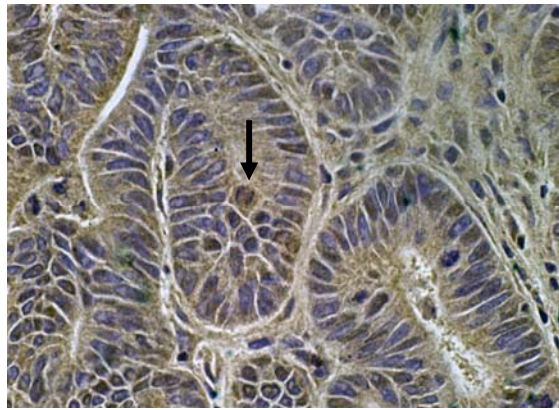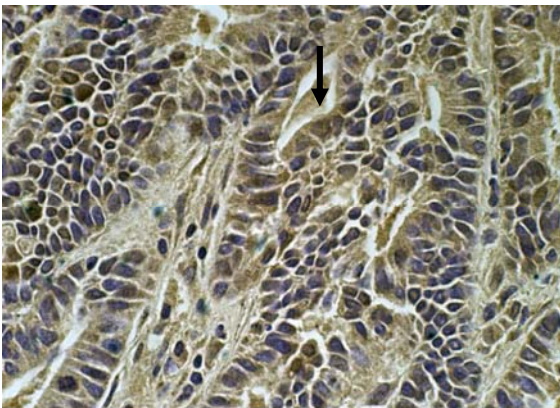
Zk-Ob

Zk-Ln   **SD**
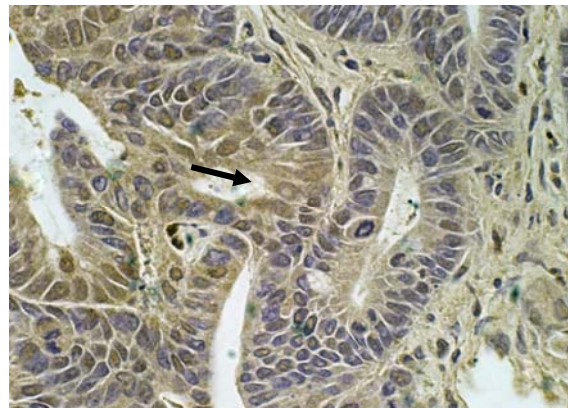
Figure 6-22: IHC staining for IκBα in Zk-Ob, Zk-Ln, and SD tumor sections (400x).

Sections were deparaffinized and dehydrated, incubated in blocking buffer, primary, and biotinylated secondary antibody respectively. Reaction was monitored following addition of enzyme conjugate and DAB chromagen, and sections were counterstained, rehydrated, and mounted with coverslips. Note nuclear staining present in all groups (black arrows). Zk-Ob: Zucker obese, Zk-Ln: Zucker lean, SD: Sprague dawley.

Chapter 7

Study 3: Differences in protein expression patterns in distal and proximal tumors of Zk-Ob rats.

7.1 Study Background and Objectives

In study 2B, it was observed that the tumor distribution pattern along the colonic axis was different in Zk-Ob versus Zk-Ln rats (Table 6-5). To be specific, it was noted that the majority of tumors in Zk-Ob rats were located in most distal region of the colon. This observation was in keeping with recent interests generated in the field of cancer biology that proximal and distal tumors represent biologically different disease states. An overall abundance of tumors in Zk-Ob rats allowed a more detailed comparison of tumor phenotype with regards to location along the colonic axis.

Evidence from the last decade has established that colon carcinogenesis originating from different colonic regions, distal and proximal, represent two individual disease states. Incidence rates of distal versus proximal tumors also differ, and are affected by geographical status, age, gender, shifting dietary patterns, and physical inactivity (Iacopetta 2002, Distler and Holt 1997).

Distal and proximal colons are distinct organs representing different developmental, anatomical, and functional properties (Gervaz et al. 2004). In the same respect, cancers appearing in these two sites have individual properties. Tumors along the colonic axis have different embryonic origins and unique biological and genetic properties (Lindbolm 2001). Previous studies in our lab have demonstrated inconsistencies along the colonic axis during experimental colon carcinogenesis as ACF appeared earlier and more rapidly in the distal versus proximal colon (Bird 1995).

Mechanisms by which these lesions develop, and their growth response to genetic and environmental variables also differ (Iacopetta 2002). Distal tumors follow the polyp-carcinoma sequence as proposed in the Vogelstein model, and are characterized by chromosomal instability. More steady proximal tumors develop via inherited nonpolyposis colon cancer, and share microsatellite instability (Bufill 1990). Evaluation of the differing phenotypes of distal and proximal tumors will give further

insight into directing future epidemiological studies, as well as diagnostic and treatment approaches for colon cancer.

Importantly, the association between obesity and colon cancer is more often seen with the distal rather than proximal colon (Gunter and Leitzmann 2006). However, the cellular and mechanistic changes involved are yet to be elucidated. Due to the high incidence of tumors in Zk-Ob animals in this study, it was possible to investigate differences in distal versus proximal lesions with regards to obesity associated colon cancer.

Specific objective of this study was:

To determine if tumors in Zk-Ob rats present in the distal colon exhibit different phenotypes from those present in the proximal colon. In particular, expression of key proteins of the TNF-α, NF-κB and insulin pathways were investigated as identified below:

- TNF-α, TNFR1, and TNFR2
- NF-κB, IκBα, and IKKβ
- IRα, IRβ, and IGF-IRα
- MAPK p42/p44

7.2 Methodological Approach

Details of experimental procedures are provided in Chapter 4 Materials and Methods. Briefly, Zk-Ob, rats were injected with AOM, and terminated after 30 weeks. Location and size of tumors along the colonic axis were recorded. Tumors were excised and stored at -80°C for further analyses. Zk-Ob tumors originating from distal colon (0-4cm from the rectal end) or proximal colon (8-16 cm from the rectal end) were selected, homogenized and proteins were separated by SDS-PAGE. Following transfer, membranes were incubated with primary, then AP conjugated secondary antibodies, and developed with BCIP/NBT solution. Specific proteins analyzed in tumors included TNF-α, TNFR1, TNFR2, NF-κB, IκBα, IKKβ, IRα, IRβ, IGF-IRα, and MAPK p42/p44.

7.3 Results and Discussion

Study 2B demonstrated a higher tumor distribution and size in the distal versus proximal colon, leading to further investigation into possible differences in tumor phenotype. Due to high tumor incidence in Zk-Ob animals, it was possible to analyze tumors from the distal and proximal regions (0-8cm and 8-16cm from the rectal end respectively) for possible differences in protein expression in TNF-α, NF-κB and insulin pathways.

While no difference was seen in the levels of both 17 and 27kDa TNF-α, levels of TNFR1 and TNFR2 were lower and higher respectively in distal tumors (Figure 7-1). NF-κB and IKKβ expression were significantly higher in distal tumors, while IκBα levels were higher in proximal tumors (Figure 7-2). Compared to the levels noted in the proximal tumors, all of IGF-IRα, IRα, and IRβ levels were significantly higher in distal tumors (Figure 7-3). With regards to MAPK, p42 subunit had similar expression among tumors regardless of their location, while p44 level was higher in distal tumors (Figure 7-4).

In general, higher expression was observed in distal rather than proximal tumors for all proteins that were evaluated. Upregulation of NF-κB pathway may correlate with increased cell survival and growth, promoting increased tumorigenesis in the distal colonic axis. Higher levels of TNFR2 versus TNFR1 once again suggest the tumor phenotype to be directed towards the survival outcome of TNF-α pathway. The increased sizes of distal tumors further correspond to upregulation of survival signaling, supporting the prominent association between obesity and colon cancer in the distal rather than proximal colon. Results from this study support the observation that distal and proximal tumorigeneses represent biologically different disease states.

Figure 7-1: Representative western blots of TNF-α, TNFR1, and TNFR2 protein expression in distal and proximal tumors of Zk-Ob rats (A), and (B) Bar graphs of mean densitometric values.

Tumors were selected from distal (0-8cm) and proximal (8-16cm) regions of the colon, measured from the rectal end. Tumor homogenates, 100 μg of protein per sample, were prepared for western blot analyses, separated by SDS-PAGE, and transferred onto membranes. Following incubation with primary antibodies and corresponding AP-conjugated secondary antibodies, blots were developed with BCIP/NBT solution, and bands quantified by densitometry analyses. Values in (B) are pixels (arbitrary units) representing mean ± SE, n=6 per group. Each band represents a tumor from one animal, and groups are as indicated. Bars without a common superscript[(x,y)] are significantly different, $p<0.05$, as determined by t-test. Zk-Ob: Zucker obese, Zk-Ln: Zucker lean, SD: Sprague dawley.

Figure 7-2: Representative western blots of NF-κB, IκBα, and IKKβ protein expression in distal and proximal tumors of Zk-Ob rats (A), with (B) Bar graphs of mean densitometric values.

Tumors were selected from distal (0-8cm) and proximal (8-16cm) regions of the colon, measured from the rectal end. Tumor homogenates, 100 μg of protein per sample, were separated by SDS-PAGE, and transferred onto membranes. Following incubation with primary antibodies and corresponding AP-conjugated secondary antibodies, blots were developed with BCIP/NBT solution, and bands quantified by densitometry analyses. Values in (B) are pixels (arbitrary units) representing mean ± SE, n=6 per group. Each band represents a tumor from one animal, and groups are as indicated. Bars without a common superscript[(x,y)] are significantly different, p<0.05, as determined by t-test. Zk-Ob: Zucker obese, Zk-Ln: Zucker lean, SD: Sprague dawley.

Figure 7-3: Representative western blots of IGF-IRα, IRα, and IRβ protein expression in distal and proximal tumors of Zk-Ob rats (A), with (B) Bar graphs of mean densitometric values.

Tumors were selected from distal (0-8cm) and proximal (8-16cm) regions of the colon, measured from the rectal end. Tumor homogenates, 100 μg of protein per sample, were prepared for western blot analyses, separated by SDS-PAGE, and transferred onto membranes. Following incubation with primary antibodies and corresponding AP-conjugated secondary antibodies, blots were developed with BCIP/NBT solution, and bands quantified by densitometry analyses. Values in (B) are pixels (arbitrary units) representing mean ± SE, n=6 per group. Each band represents a tumor from one animal, and groups are as indicated. Bars without a common superscript[(x,y)] are significantly different, p<0.05, as determined by t-test. Zk-Ob: Zucker obese, Zk-Ln: Zucker lean, SD: Sprague dawley.
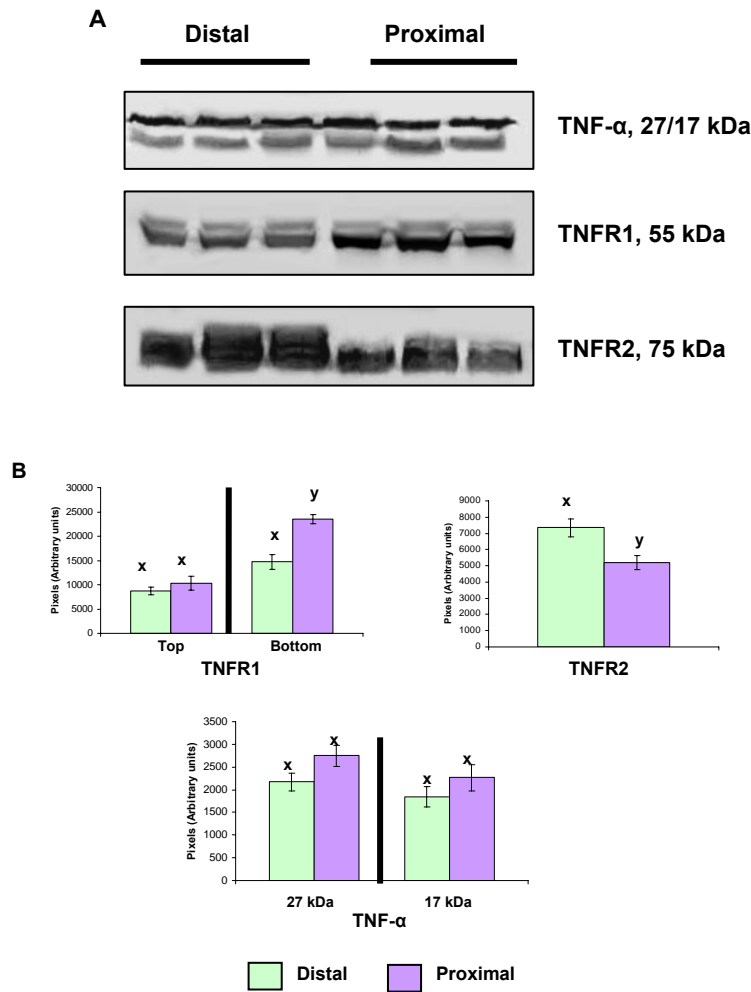
Figure 7-4: Representative western blot of MAPK p42/44 protein expression in distal and proximal tumors of Zk-Ob rats (A), with (B) Bar graphs of mean densitometric values.

Tumors were selected from distal (0-8cm) and proximal (8-16cm) regions of the colon, measured from the rectal end. Tumor homogenates, 100 μg of protein per sample, were separated by SDS-PAGE, and transferred onto membranes. Following incubation with primary antibodies and corresponding AP-conjugated secondary antibodies, blots were developed with BCIP/NBT solution, and bands quantified by densitometry analyses. Values in (B) are pixels (arbitrary units) representing mean ± SE, n=6 per group. Each band represents a tumor from one animal, and groups are as indicated. Bars without a common superscript[x,y] are significantly different, $p<0.05$, as determined by t-test. Zk-Ob: Zucker obese, Zk-Ln: Zucker lean, SD: Sprague dawley.
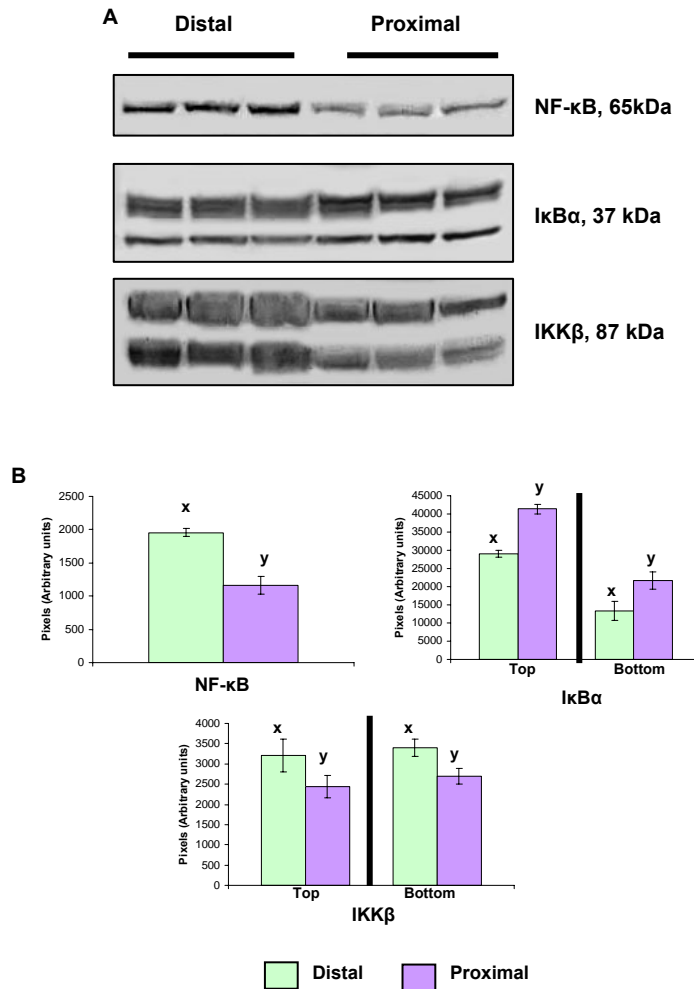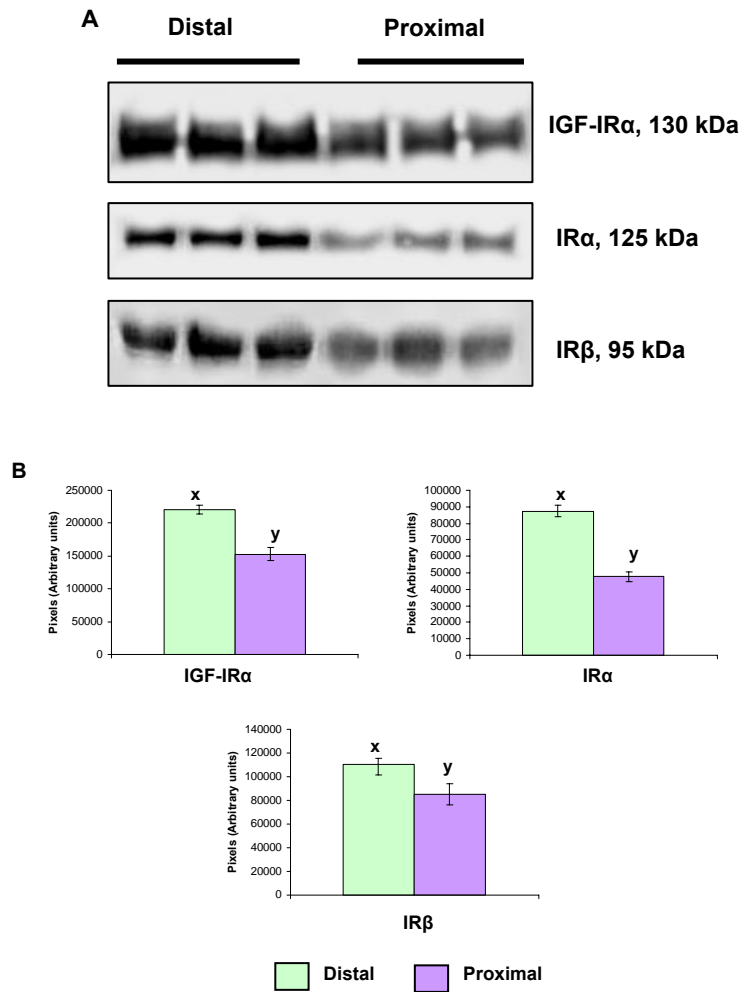
General Discussion and Conclusion

The primary objective of this thesis was to investigate changes in tumor phenotype as affected by an obese physiological state. In particular, it was postulated that physiologically elevated TNF-α in an obese state will induce increased expression of transcriptionally active NF-κB in tumors, which subsequently transcribes genes crucial to cell survival. Insulin resistance, oxidative stress, and a pro-inflammatory environment are few of the biological consequences of elevated TNF-α and NF-κB pathway activation, and further contribute to disease progression. It was thereby hypothesized that tumors in obesity associated colon cancer will have accelerated growth due to their resistance towards TNF-α mediated cytotoxicity, and their ability to use TNF-α mediated responses in favor for growth. Three major studies were conducted to investigate this hypothesis, and a brief discussion of major findings follows.

In Study 1, HT-29 colon adenocarcinoma cells were used as a preliminary model to investigate cellular and molecular changes associated with the TNF-α resistant phenotype. The main finding demonstrated the ability of HT-29 cells to resist TNF-α induced cytotoxicity is due to augmented expression of NF-κB. Elevated levels of NF-κB in response to exogenous TNF-α supported that hypothesis that the NF-κB pathway is critical for cell survival. Inhibition of NF-κB via SJW treatment demonstrated that HT-29 cells could be sensitized towards TNF-α mediated cytotoxicity, further substantiating the role of NF-κB in TNF-α resistance. Upregulation of TNFR2, and decreased expression of TNFR1 upon TNF-α treatment suggests another strategy by which cells are utilizing exogenous TNF-α for survival. This study provided important clues as to what may be expected for investigating the TNF-α resistant phenotype in tumors, and supported the working hypothesis that chronic exposure to elevated TNF-α will exert a tumor promoting effect.

In study 2, Zk-Ob rats were used as a model to investigate tumor phenotype in obesity associated colon cancer due to their inherent elevated TNF-α levels and metabolic dysregulation. Lean counterparts Zk-Ln rats, and SD rats functioned as control groups. It was hypothesized that elevated levels of TNF-α in Zk-Ob animals would exert a tumor promoting effect by inducing increased expression of transcriptionally active NF-κB.

The physiological differences among the three animal genotypes were remarkable. As expected, the body weights of Zk-Ob rats were significantly higher than Zk-Ln and SD groups. It was noted that AOM injected tumors bearing animals had lower body weights than non-injected animals. This could be due to compromised food intake related to physiological distress from tumorigenesis. Zk-Ln rats, while having significantly lower body weights than the SD rats, had a higher tumor incidence. This suggests that a lean body mass is not necessarily protective to carcinogenesis, and emphasizes genotype to be crucial in determining the tumor outcome. It was also noted that organ weights, particularly liver and kidney weights of the Zk-Ob rats, were heavier than Zk-Ln and SD groups. Previous studies have indicated Zk-Ob rats to be sensitive to liver steatosis and kidney disease (Raju and Bird 2006).

AOM injected Zk-Ob rats had a notably higher spleen weight than rest of the groups, suggesting that the immune system in Zk-Ob rats was highly sensitive to the presence of tumors. These animals exhibit a chronic inflammatory state and how immune cells may be participating in tumorigenesis remains to be evaluated.

Hematological assessment of tumor bearing rats showed a few key differences. In particular, monocyte and platelet counts were significantly elevated in Zk-Ob rats than Zk-Ln or SD groups. Both of these blood components affect carcinogenesis. Monocytosis occurs in response to chronic inflammation, physiological stress, and cancer. Upon entering tissues, monocytes become macrophages, which are known generators of TNF-α. Tumor associated macrophages particularly have critical roles in tumor growth promotion which are still under review (Hussein 2006). In addition, platelets are involved in metastasis of cancer cells, and serve as a source for cytokines, growth factors, and bioactive lipids (Mousa 2006). Whether these two blood components are playing any roles in obesity associated colon carcinogenesis remains to be determined.

Plasma values for insulin, leptin, and TNF-α corroborated previous observations that Zk-Ob rats have elevated levels of these hormones and cytokine than Zk-Ln and SD counterparts (Zucker and Zucker 1962). Similarly, blood lipid levels confirmed dyslipidemia in Zk-Ob rats.

Evaluation of oxidative markers demonstrated notably higher levels in Zk-Ob animals than Zk-Ln and SD rats. It was noted that o-tyrosine and n-tyrosine were abundant in Zk-Ob regardless of the presence of tumors. This clearly supports previously published research that Zk-Ob rats are in a constant state of inflammation and have increased levels of ROS (Vincent et al. 1999). It is important to note that the pro-inflammatory state in Zk-Ob rats due to high levels of ROS and TNF-α may be conducive to generation of pre-neoplastic lesions that have potential to develop into tumors, whereas Zk-Ln or SD rats do not exhibit this state to the same degree.

The role of inflammation in a number of chronic illnesses including cancer is an important area under active investigation (Macarthur et al. 2004). Whether chronic inflammation supports tumor growth or is co-carcinogenic in nature remains to be established. Previous studies suggest that the inflamed colon is highly sensitive to colon carcinogenesis, while sustained inflammation may not necessarily promote the growth of pre-existing preneoplastic lesions (Baijal et al. 1998). Inflammation is a complex process that may differ depending on the type of inflammatory agent, duration, and severity of the inflammation, as well as the physiological state of the host organism. Whereas there is agreement that inflammation plays a key role in cancer, specific effects during initiation and promotional stages of carcinogenesis remains to evaluated.

Tumor outcome and incidence data revealed important information. As expected, tumor incidence and multiplicity were higher in Zk-Ob rats than Zk-Ln. It was interesting to note however, that Zk-Ln rats had a higher tumor incidence and multiplicity than SD, suggesting that genotype and physiological status of the host is important to tumor development. Most studies on experimentally induced colon carcinogenesis have used male SD rats, while this study used female rats. The role of estrogens in cancer is not yet fully understood, and hormonal profiles of these animals may have had additional effects. Furthermore, it is convention to use a dosage of 15mg/kg body weight AOM carcinogen to induce carcinogenesis. Due to the known increased sensitivity of Zk-Ob rats to carcinogenesis, a 10mg/kg body weight dose was given in this study to avoid over-toxicity to the animals. This lower dosage of carcinogen may also explain the lower tumor incidence in SD rats, which are less sensitive to cancer than the Zucker strain.

While tumor incidence was higher in Zk-Ln than SD rats, SD tumors were larger in size. It can therefore be suggested that exogenous factors such as TNF-α may be more important in augmenting survival and progression of selected lesions. Moreover, an increased level of TNF-α before initiation

of carcinogenesis may be more crucial for enhanced tumor incidence and tumor multiplicity than afterwards.

In this study, tumors were markedly distinct from colonic mucosa by increased protein expression. It was noted that all tumors, regardless of their origin exhibited elevated levels of TNF-α, TNFR, NF-κB, IKKβ, IR, IGF-IR, and MAPK, supporting the concept that these proteins are important for their growth. Zk-Ob and SD tumors shared similar patterns of protein levels, although Zk-Ob animals had a higher number of tumors, while SD tumors were larger in size. These observations indicate that tumor populations among the groups exhibited heterogeneity that may have been influenced by the genotype and physiological conditions of the animals (Figure 8-1). In particular, physiological circumstances in the Zk-Ob animals may favor preneoplastic lesions to tumor development by upregulating survival pathways. In SD rats, fewer of these lesions progressed into tumors. Zk-Ln tumors on the other hand, were least responsive to growth. It was clear that tumors in Zk-Ob rats exhibited a more aggressive phenotype than those in the Zk-Ln and SD rats. This observation provides support to the contention that tumor microenvironment plays an important role in providing them with growth autonomy and possible resistance to death signaling.
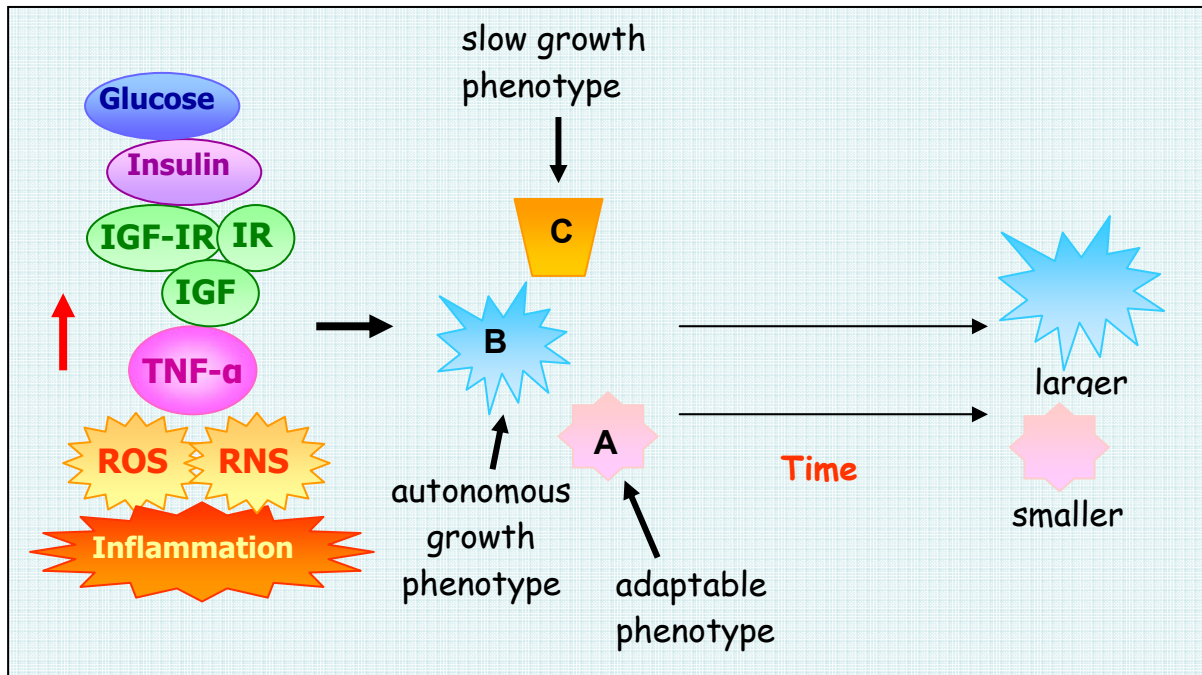
Figure 8-1: Hypothetical scheme to describe biological heterogeneity of tumorigenesis as affected by physiological conditions.

Growth potential of tumors is affected by genotype and physiological status of the host. Factors such as TNF-α, inflammation and insulin resistance may cooperatively contribute to tumorigenesis. Lesion A adapts rapidly to external growth factors, but is smaller in size than lesion B, which is well equipped for autonomous growth. Finally, lesion C has slow adaptation and growth. Zk-Ob tumors primarily resembled phenotype A, with some B and C lesions as well. SD rats had tumors predominantly with phenotype B, as demonstrated by their large size, and some C phenotypical tumors. Finally, Zk-Ln tumors mostly exhibited phenotype C.

Biochemical analyses of tumor tissues and colonic mucosae supported the concept that augmented expression of molecules associated with growth and survival is common to tumor tissue. NF-κB as well as specific receptors such as TNFR2, IR, and IGF-IR appear to be central to tumor phenotype. Role of these molecules in carcinogenesis has been extensively reviewed (Gunter and Leitzmann 2006, Lin and Karin 2003). It is well known that many of these molecules are involved in signaling pathways eventually influencing and co-operating with each other in rendering growth autonomy to the tumor tissue. Overall, Zk-Ob tumors exhibited highest levels of proteins that Zk-Ln and SD groups, supporting that physiological status of these animals had a notable impact on tumor phenotype with regards to protein expression. A schematic representation of pathway interactions and their effect on tumor promotion is given in Figure 8-2. It is important to note that this representation is not inclusive, and is an attempt to explain possible circumstances that promote tumorigenesis. Further study into these associations and pathway cross talk is warranted.

It is important to note that minor differences in physiological and biochemical parameters were found between respective AOM injected and control animals from the three genotypes. This observation suggests that most notable changes due to carcinogen injections occur in early stages of cancer. In addition, Zk-Ob and SD rats had very similar levels of plasma and protein parameters. This maybe due to the heavier body weight and higher plasma TNF-α in SD rats, contributing to a physiological similarity to Zk-Ob rats. Although, caution must be exercised in interpretation of results, as tumor multiplicity and incidence in SD animals was lowest among the groups.
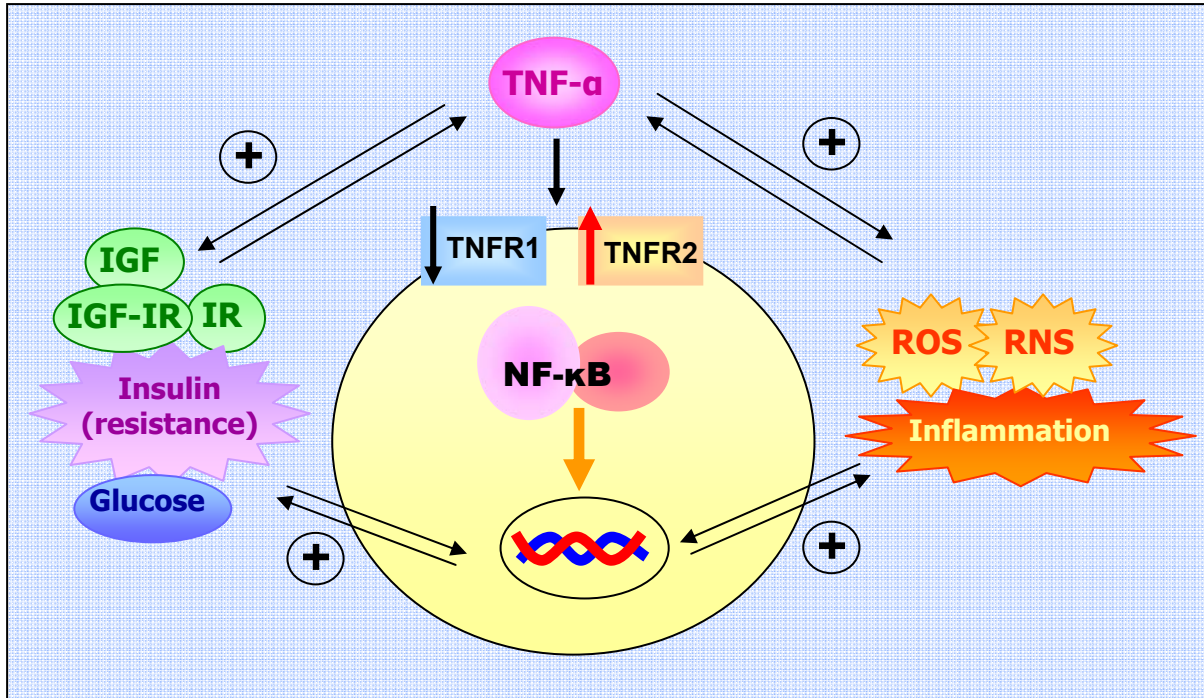
Figure 8-2: Multiple pathway interactions promoting tumorigenesis.

Elevated levels of TNF-α promote NF-κB activity, inflammation, and insulin resistance, while these factors can also upregulate TNF-α levels. Insulin resistance, inflammation and associated ROS and RNS may also initiate NF-κB, and vice versa. TNFR2 appears to be upregulated in the presence of exogenous TNF-α in comparison to TNFR1. The interplay of these mechanisms appears to provide a favorable environment for tumorigenesis.

The hypothesis of this research was that Zk-Ob tumors will exhibit a phenotype that would exhibit resistance to TNF-α. To elaborate, it was speculated that elevated levels of exogenous TNF-α may provide additional stimulus to developing preneoplastic lesions, which in turn would adjust their biological make up to upregulate signals leading to survival and growth. For example, in this study it was observed that pathway activity of NF-κB was elevated in Zk-Ob tumors. Also, TNFR2, which is implicated in mediation of survival outcomes, was upregulated in comparison to TNFR1.

Whereas this hypothesis is congruent to ongoing interest in TNF-α, it was recognized that Zk-Ob rats had elevated levels of a number of additional active components implicated in carcinogenesis. Physiological levels of insulin and IGF-IR are elevated along with TNF-α in Zk-Ob, whereas these are relatively lower Zk-Ln and SD rats. Previously it has been shown that insulin and IGF-IR are important growth factors for gastrointestinal tissue and provide protection to several cell types, including colon cancer cells, against pro-apoptotic signals (Remacle-Bonnet et al. 2000). The presence of elevated insulin, IGF-IR and TNF-α could act synergistically to provide superior survival and growth conditions to developing preneoplastic lesions and tumors. It has been demonstrated in cancer cell lines that activated NF-κB is also involved in IGF mediated cell survival. Moreover, inhibition of NF-κB and MAPK is crucial for reversing the survival signal mediated via IGF, as well as TNF-α (Remacle-Bonnet et al. 2000). Substantial evidence exists suggesting that TNF-α, IGF, and insulin signaling cross talk, and work synergistically to provide an ideal growth environment for tumors developing in the colon.

Therefore, while it is reasonable to suggest that while TNF-α and associated signaling is playing a major role, participation of other molecules cannot be ruled out. Moreover, biological heterogeneity among preneoplastic lesions and the fact they may respond differently to physiological modulators depending on their biological make up, developmental stage, and location of the colons must be considered.

Presence of elevated IGF-IR and IR in Zk-Ob tumors raises an interesting question, as the small intestine and colon do not require receptor mediation for glucose uptake. Thus, the role of insulin and more importantly, related receptors in colonic tumors becomes an important consideration. Other studies have demonstrated insulin associated tumor growth promotion (Giovannucci 2001). Possible

mechanisms involve activation of NF-κB and survival signaling, although further study in this area is required.

The location of tumors along the colonic axis in Zk-Ob versus Zk-Ln or SD rats was also different, supporting the emerging concept that genotype/physiological state of the host affects development and distribution of tumors. High number of tumors in Zk-Ob rats allowed investigation into whether distal colonic tumors are different from those from proximal regions in the same host in Study 3.

By examining expression levels of various proteins as favoring tumor growth, it may be concluded that distal tumors exhibit a superior phenotype than proximal tumors. To be specific, increased levels of TNFR2, NF-κB, IGR-IRα, and IR were observed in distal tumors. It is possible that developing tumors have variable access to systemic modulators depending on their location in the colon. Little information is known on the vascular supply of distal versus proximal lesions, and further study would give insight into growth characteristics of tumors in different regions of the colon. As stated previously, the colon consists of different compartments differing from each other anatomically, developmentally, and physiologically. It is thereby reasonable to assume that preneoplastic lesions occurring in different regions would also behave and respond differently.

The distal colon responds quite actively to inflammation, and an increase in inflammatory cells and their aggregates are more commonly observed in the distal rather than proximal colon (personal communication, RB). In addition, the distal colon responds differently to AOM, and the appearance and growth of preneoplastic ACF differ according to colonic regions. Most immune activity in the colon is attributed to gut associated lymphoid tissue (GALT). Previous studies have shown that in carcinogen injected mice, a significant correlation between tumors and GALT tissue was observed in the distal rather than proximal colon (Carter et al. 1994). Interestingly, there was no such relationship between ACF and GALT, indicating differing responses of preneoplastic and neoplastic lesions. It is also possible that as selected preneoplastic lesions develop into tumors, GALT may develop in response to presence of tumors.

Epidemiologically, proximal tumors appear more prominently in the elderly, possibly due to slower growth rates (Iacopetta 2002). In North American populations, the incidence of proximal tumors is at a rise, making it important to study biological differences among distal and proximal tumors, and the factors affecting their incidence. The preliminary findings in this study are noteworthy, and support

130

the conjecture that distal and proximal colons are two different organs, and tumorigenesis in these two sites also represent two different disease states.

Conclusions

Research documented in this thesis demonstrated that the physiological status of the host intricately affects tumor phenotype. In particular, the TNF-α resistant phenotype is involved with multiple signaling interplays as demonstrated by both *in vitro* and animal models.

HT-29 cells treated with exogenous TNF-α exhibited elevated levels of NF-κB, suggesting that this pathway is critical for cell survival signaling. A similar response was seen *in vivo* with the Zk-Ob animal model.

Zk-Ob rats exhibited a number of differences with regards to physiological parameters from their Zk-Ln or SD counterparts. Some of these differences were not expected, and included increased plasma level of oxidative stress markers, and increased number of platelets and monocytes in Zk-Ob than Zk-Ln or SD rats. Distribution pattern of colonic tumors in Zk-Ob rats showed a higher number in distal than in proximal regions compared to Zk-Ln and SD rats.

Protein expression levels differentiated neoplastic tissue from the normal appearing colonic mucosae. In particular, all tumors expressed reduced TNFR1 and increased levels of TNFR2, NF-κB, IKKβ, IR, IGF-IR, and MAPK compared to their surrounding normal appearing mucosae.

Tumors appearing in Zk-Ob rats exhibited significantly higher levels of the proteins involved in augmented activity of NF-κB, supporting the hypothesis elevated levels of TNF-α is tumor promoting. Moreover, insulin and IGF-IR may exert a synergistic effect with TNF-α to provide growth advantage to tumors.

The level of specific proteins such as TNFR1, TNFR2, NF-κB, IR, IGF-IR, and MAPK p44 were differently expressed in distal than proximal colonic tumors in Zk-Ob rats. This observation suggested that development of tumors in different regions of the colon differ under the same physiological conditions.

For future studies, it would be important to evaluate gene and protein products of NF-κB transcription related to cell survival to further elucidate its role in tumor promotion. Moreover, it would be important to look at microscopic preneoplastic lesions to determine whether these phenotypes are present at early stages of carcinogenesis. This would also give insight into the cross talk between NF-κB activation, inflammation and insulin resistance and how these mechanisms interplay to provide a favorable environment for tumorigenesis. Furthermore, it is necessary to assess the response of obesity-associated tumors to known chemotherapeutics. Effects of drugs may be different in altered physiological states, and further study into their mechanisms is warranted.

Appendix A

Abbreviations

ACF	aberrant crypt foci
ALT	alanine aminotransferase
ANOVA	analysis of variance
AP	alkaline phosphatase
APC	adenomatous polyposis coli
AO	acridine orange
AOM	azoxymethane
AST	aspartate aminotransferase
BCIP/NBT	5-Bromo-4-Chloro-Indolyl-Phosphatase/ Nitroblue tetrazolium
CB	conjugated bilirubin
CBC	complete blood count
CK	creatinine kinase
DAB	3,3-diaminobenzidine tetrahydrochloride
DAG	1,2-diacylglyercol
DD	death domain
DMH	1,2-dimethylhydrazine
EGCG	epigallocatechin gallate
ELISA	enzyme linked immunosorbent assay
EMSA	electrophoretic mobility shift assay
EtBr	ethidium bromide
FADD	Fas associated death domain
Fas_L	Fas ligand
$FLIP_L$	FLICE inhibitory protein
GALT	Gut -associated lymphoid tissue
HAQ	1-hydroxyanthraquinone
Hb	hemoglobin
HCT	hematocrit
HDL	high density lipoprotein
H&E	hematoxylin and eosin

HP	hyperforin
HPex	hyperforin extract
HPLC	high-performance liquid chromatography
HRP	horseradish peroxidase
HY	hypericin
HYex	hypericin extract
IAP	inhibitor of apoptosis proteins
IFN	interferon
IGF-1	insulin like growth factor-1
IGF-IRα	insulin like growth factor-I-receptor-α
IHC	immunohistochemistry
IκB	inhibitor of NF-κB
IKK	IκB kinase
IL	interleukin
iNOS	inducible nitric oxide synthase
IR	insulin receptor
JNK	c-Jun amino-terminal kinase
LDL	low density lipoprotein
LSD	least significant difference
MAM	methylazoxymethanol
MAPK	mitogen activated protein kinase
MCH	mean corpuscular hemoglobin
MCHC	mean corpuscular hemoglobin concentration
MCV	mean corpuscular volume
MTT	3-(4,5-dimethylthiazol-2-yl)-2,5-diphenyltetrazolium bromide
NEMO	NF-κB essential modulator
NIK	NF-κB-inducing kinase
NF-κB	nuclear transcription factor-κB
PARP	poly (ADP ribose) polymerase
PMA	phorbol ester phorbol 12-myristate 13-acetate
RAIDD	RIP associated Ich-1/CED with death domain
RBC	red blood cell count

RDW	red cell distribution width
RHD	Rel homology domain
RIP	receptor interacting protein
RNS	reactive nitrogen species
ROS	reactive oxygen species
SD	Sprague-Dawley rats
SDc	Sprague-Dawley rats control group
SDS-PAGE	Sodium Dodecyl Sulfate Polyacrylamide Gel Electrophoresis
SJW	St. John's Wort
SODD	silencer of death domain
TACE	TNF-α converting enzyme
TB	total bilirubin
TG	triglycerides
TIL	tumor infiltrating lymphocyte
TNBS	trinitrobenzene sulfonic acid
TNF-α	tumor necrosis factor-α
TNFR1	tumor necrosis factor receptor 1
TNFR2	tumor necrosis factor receptor 2
sTNFR1	soluble tumor necrosis factor receptor 1
sTNFR2	soluble tumor necrosis factor receptor 2
TRADD	TNF Receptor I associated death domain
TRAF	TNF Receptor Associated factor
TRAIL	TNF-related apoptosis-inducing ligand
TRAMP	TNF receptor apoptosis-mediating protein
WBC	white blood cell count
Zk-Ln	Zucker lean rats
Zk-Lnc	Zucker lean rats control group
Zk-Ob	Zucker obese rats
Zk-Obc	Zucker obese rats control group

Appendix B
CBC and Plasma Test Descriptions

CBC Analyses

RBC: Red Blood Cell Count , number of red blood cells in a blood sample

HCT: Percentage of red blood cells

Hb: Hemoglobin count, protein that picks up oxygen in the lungs and delivers it to the peripheral tissues

Platelets: involved in blood clotting

RDW: Measures the range of sizes of red blood cells in a blood sample

MCH: Hemoglobin amount per red blood cell

MCV: Average red blood cell size

MCHC: Hemoglobin concentration per red blood cell.

WBC: White Blood Cell Count (leukocyte count). The number of white blood cells blood including neutrophils, band cells (slightly immature neutrophils), T-type lymphocytes, B-type lymphocytes, monocytes, eosinophils, and basophils.

Segregated neutrophils: mature immune cells involved in phagocytosis

Lymphocytes: involved in humoral and cellular immune responses, antibody production, antigen presentation

Monocytes: involved in phagocytosis, antigen presentation

Eosinophils: involved in phagocytosis, high levels indicate allergic reactions, infection

Plasma Analyses

TG: storage form of fat consisting of three fatty acids and glycerol

HDL: a lipoprotein that transports cholesterol in the blood. High levels of HDL, as opposed to LDL are considered beneficial.

Cholesterol: fatty steroid produced by the liver, involved in membrane fluidity and hormone formation

Glucose: monosaccharide sugar, source of energy for the body

CK: Creatinine kinase assay, high levels indicating stress to muscle, heart or brain

ALT: measures amount of alanine aminotransferase enzyme in the blood, high levels indicate liver disease

AST: measures amount of aspartate aminotransferase enzyme in the blood, high levels indicate liver disease

CB, TB: bilirubin is a breakdown of hemoglobin, high levels indicate liver dysfunction

Appendix C

Figures and Tables
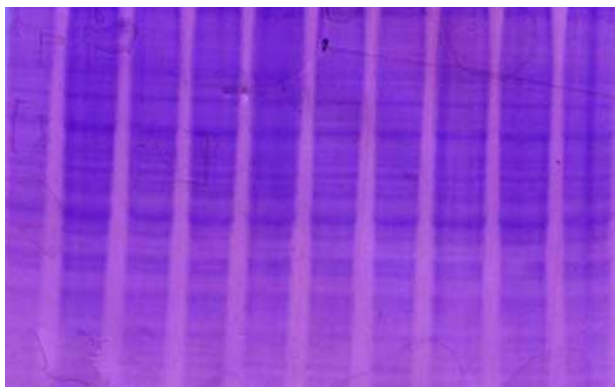
Figure C1: Coomassie stain of gel showing equal loading and adequate separation of protein.
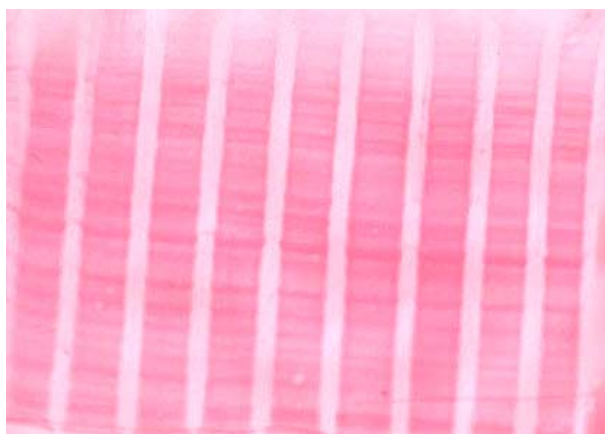
Figure C2: Ponceau-S staining of membranes showing equal loading and adequate protein transfer.
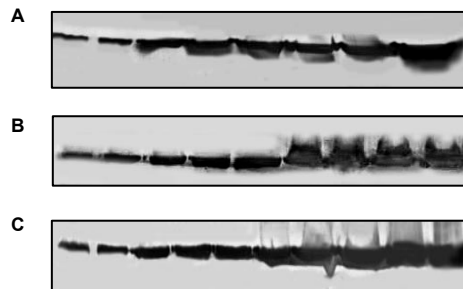
Figure C3: Linear range western blots for β-actin for (A) cells, (B) colonic mucosa, and (C) tumors.

Increasing amounts of protein from cell, mucosal, or tumor homogenates were loaded, separated by SDS-PAGE, and transferred on membranes. Following incubation with primary and secondary antibodies, membranes were exposed, and protein saturation points determined for subsequent analyses.
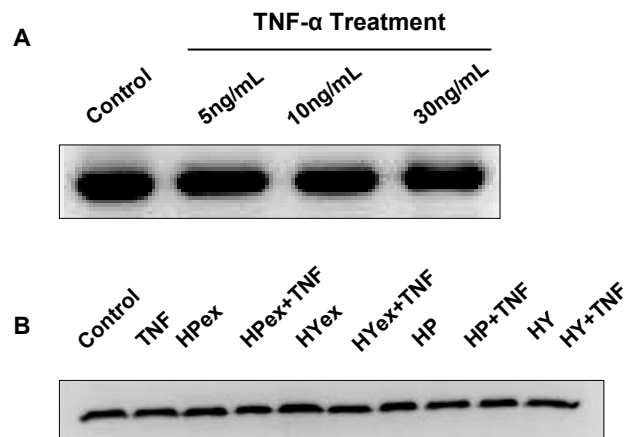
Figure C4: Western blots of β-actin protein expression in HT-29 cells treated with (A) TNF-α, and (B) TNF-α and SJW extracts and standards.

HT-29 cells were treated with TNF-α and/or SJW, and processed for western blot analyses. Proteins were separated by SDS-PAGE and transferred onto membranes. Blots were then incubated with primary antibody for β-actin, followed by HRP conjugated secondary antibody, and exposed in FluorChem™ imager. Equal loading and constant protein expression of β-actin was observed.
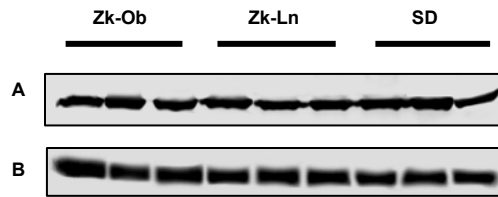
Figure C5: Western blots of β-actin protein expression in colon mucosae of (A) control and (B) AOM injected Zk-Ob, Zk-Ln, and SD rats.

Colonic mucosal proteins were separated by SDS-PAGE and transferred onto membranes. Blots were then incubated with primary antibody for β-actin, followed by AP conjugated secondary antibody, and exposed with BCIP/NBT solution. Equal loading and constant protein expression of β-actin was observed.
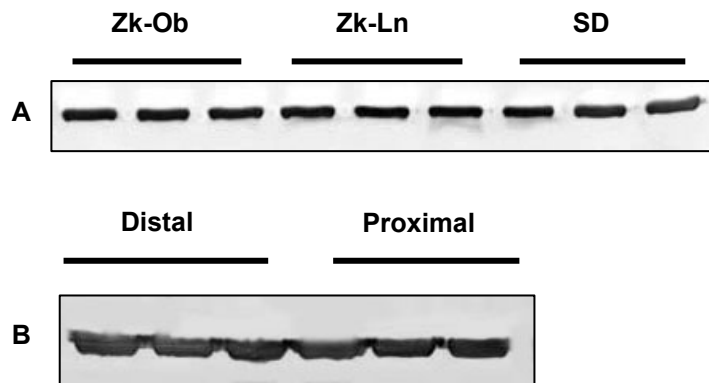
Figure C6: Western blots of β-actin protein expression in (A) Zk-Ob, Zk-Ln, and SD tumors, and (B) distal and proximal tumors from Zk-Ob rats.

Tumor proteins were separated by SDS-PAGE and transferred onto membranes. Blots were then incubated with primary antibody for β-actin, followed by AP conjugated secondary antibody, and exposed with BCIP/NBT solution. Equal loading and constant protein expression of β-actin was observed.
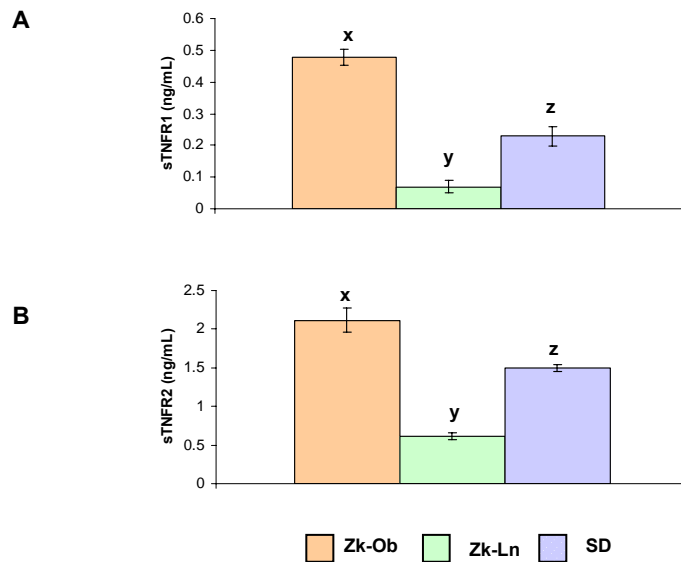
Figure C7: Levels of (A) sTNFRI and (B) sTNFRII in tumors of Zk-Ob, Zk-Ln and SD rats.

Samples were incubated in a 96 well plate pre-coated with antibody. Wells were then aspirated, washed, and further incubated with conjugated antibody. Reaction was monitored upon addition of substrate solution, and absorbance read at 450nm. Values are mean ± SE, n=6 tumors per group. Bars without a common superscript[(x,y,z)] are significantly different, $p<0.05$, as determined by ANOVA analyses with LSD and Tukey post hoc tests. Zk-Ob: Zucker obese, Zk-Ln: Zucker lean, SD: Sprague dawley.
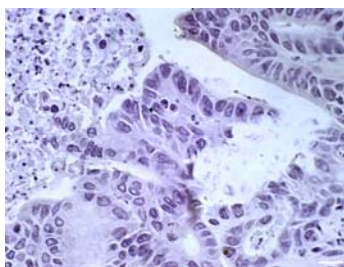
Figure C8: Negative control for IHC analyses. Sections were analyzed as per described IHC protocol, with the exception of incubation with primary antibody. As seen, no reaction (brown colouring) is observed, ensuring specificity of the procedure.

Table C1: Comparison of relative hypericin and hyperforin amounts in LD50 values of SJW extracts and standards[a].

Compound	LD_{50} Value	Amount HP (μg) in LD_{50}	Amount HY (μg) in LD_{50}
HPex	10 μL/mL	1.36	0.018
HYex	10 μL/mL	0.76	0.06
HP	10 μM	1.068	---
HY	7.5 μM	---	0.76

[a]HY: hypericin, HYex: hypericin extract, HP: hyperforin, HPex: hyperforin extract.

 HPLC analyses of extracts confirmed total amount of active constituent of HY and HP present (data provided by University of Guelph). Relative amount of HY and HP constituents in both extracts were compared to amount of HY and HP in commercially available standards, using LD_{50} values from the MTT assay as a reference point. Unlike hyperforin, which was similar between extract and standard, the amount of hypericin in the LD_{50} dose of extract was relatively low in comparison to its standard.

143

Table C2: Biochemical analyses of plasma samples collected from control and AOM injected Zk-Ob, Zk-Ln and SD animals[a].

CK (U/L)	138.7 ± 12.7^x	302.3 ± 78.6^y	108.2 ± 9.7^x	228.3 ± 25.4^y	269.6 ± 67.2^y	123.4 ± 16.9^x
ALT (U/L)	61.7 ± 6.4^{xy}	67.0 ± 18.4^{xy}	63.6 ± 4.0^{xy}	59.8 ± 5.5^x	53.5 ± 4.1^x	87.4 ± 12.2^y
AST (U/L)	115.7 ± 31.2^x	196.3 ± 19.1^x	97.0 ± 5.2^x	133.7 ± 14.9^x	109.6 ± 12.2^x	142.7 ± 31.7^x
CB (μmol/L)	0 ± 0^x	3.3 ± 1.25^y	0 ± 0^x	0 ± 0^x	0.63 ± 0.2^z	0.13 ± 0.1^z
TB (μmol/L)	1.7 ± 0.3^x	4.8 ± 1.0^y	3 ± 0.5^{xy}	2.9 ± 0.5^x	3.1 ± 0.6^{xy}	4.4 ± 0.3^y

[a]Plasma was isolated from heparinized blood samples collected at termination of 30 week old control and AOM injected Zk-Ob, Zk-Ln, and SD animals. Biochemical parameters were tested as indicated where CK: creatinine kinase, ALT: alanine aminotransferase, AST: aspartate aminotransferase, CB: conjugated bilirubin, TB: total bilirubin. Values expressed as mean ± SE, with at least n=8 per group. Values in a row without a common superscript [w,x,y,z] are significantly different, $p < 0.05$, as determined by ANOVA analyses with LSD and Tukey post hoc tests. Overall Zk-Ob animals had higher levels of each parameter than Zk-Ln and SD rats. AOM: azoxymethane, Zk-Ob: Zucker obese, Zk-Ln: Zucker lean, SD: Sprague dawley, subscript c indicates control animals.

References

Adam J.M., Raju J., Khalil N., Bird R.P. 2000. Evidence for the involvement of dietary lipids on the modulation of transforming growth factor-beta 1 in the platelets of male rats. *Mol Cell Biochem.* 211(1-2):145-52.

Aderka D., Engelman H., Maor Y., Brakebusch C., Wallach D. Stabilization of the bioactivity of tumor necrosis factor by its soluble receptors. *J Exp Med.* 175(2):323-9.

Agostinis P., Vantieghema A., Merlevede W., de Witte P.A.M. 2002. Hypericin in cancer treatment: more light on the way. *Int J Biochem Cell Biol.* 34: 221-241.

Anderson M.G., Nakada M.T., DeWitte M. 2004. Tumor necrosis factor-α in the pathogenesis and treatment of cancer. *Curr Opin Pharmacol.* 4:314–20.

Aparicio T., Guilmeau S., Goiot H., Tsocas A., Laigneau J.P., Bado A., Sobhani I., Lehy T. 2004. Leptin reduces the development of the initial precancerous lesions induced by azoxymethane in the rat colonic mucosa. *Gastroenterology.* 126(2):499-510.

Ashkenazi A., Dixit V.M. 1998. Death Receptors: signalling and modulation. *Science.* 287:1305–18.

Baeuerle P.A., Baltimore D. 1988. Ikappa B: a specific inhibitor of the NF-kappa B transcription factor. *Science.* 242(4878):540-6.

Baier P.K., Wolff-Vorbeck G., Eggstein S., Baumgartner U., Hopt U.T. 2005. Cytokine expression in colon carcinoma. *Anticancer Res.* 25(3B):2135-9.

Baijal P.K., Fitzpatrick D.W., Bird R.P. 1998. Comparative effects of secondary bile acids, deoxycholic and lithocholic acids, on aberrant crypt foci growth in the postinitiation phases of colon carcinogenesis. *Nutr Cancer.* 31(2):81-9.

Balkwill F. 2002. Tumor necrosis factor or tumor promoting factor? *Cytokine & Growth Factor Rev.* 13:135–41.

Barth R.J. Jr, Camp B.J., Martuscello T.A., Dain B.J., Memoli V.A. 1996. The cytokine microenvironment of human colon carcinoma. Lymphocyte expression of tumor necrosis factor-alpha and interleukin-4 predicts improved survival. *Cancer.* 78(6):1168-78.

Beg A.A., Baltimore D. 1996. An essential role for NF-kappaB in preventing TNF-alpha-induced cell death. *Science.* 274(5288):782-4.

Beyaert R., Fiers W. 1994. Molecular mechanisms of tumor necrosis factor-induced cytotoxicity. What we do understand and what we do not. *FEBS Lett.* 340(1-2):9-16.

Bird R.P. 1987. Observation and quantification of aberrant crypts in the murine colon treated with a colon carcinogen: preliminary findings. *Cancer Lett.* 37(2):147-51.

Bird R.P. 1995. Role of aberrant crypt foci in understanding the pathogenesis of colon cancer. *Cancer Lett.* 93(1):55-71.

Bird R.P. 1997. *In vitro* and *in vivo* models of gastrointestinal toxicology. In: Sipes I.G., McQueen C.A., Gohdolfi A.J. (Eds.). Comprehensive Toxicology. Elsevier Science Ltd., Pergamon, NY, USA, 657-669.

Bird R.P. 1998. Abberant crypt foci system to study cancer preventative agents in colon. In: Hanausek M. and Walaszek Z. (Eds). Tumor Marker Protocols. Humana Press Inc. Totowa, NJ, USA, 465-74.

Bonizzi G., Karin M. 2004. The two NF-kappaB activation pathways and their role in innate and adaptive immunity. *Trends Immunol.* 25(6):280-8.

Bork P.M., Bacher S., Schmitz M.L., Kaspers U., Heinrich M. 1999. Hypericin as a non-antioxidant inhibitor of NF-kappa B. *Planta Med.* 65(4):297-00.

Braun J., Sieper J. 2003. Overview of the use of the anti-TNF agent infliximab in chronic inflammatory diseases. *Expert Opin Biol Ther.* 3(1):141-68.

Bray G. A. 1977. Experimental models for the study of obesity: introductory remarks. *Fed.Proc.*, *36:* 148–153.

Bremner P., Heinrich M. 2002. Natural products as targeted modulators of the nuclear factor-kappaB pathway. *J Pharm Pharmacol.* 54(4):453-72.

Bruno M.E., Kaetzel C.S. 2005. Long-term exposure of the HT-29 human intestinal epithelial cell line to TNF causes sustained up-regulation of the polymeric Ig receptor and proinflammatory genes through transcriptional and posttranscriptional mechanisms.
J Immunol. 174(11):7278-84.

Bufill J.A. 1990. Colorectal cancer: evidence for distinct genetic categories based on proximal or distal tumor location. *Ann Intern Med.* 113(10):779-88.

Carter JW, Lancaster HK, Hardman WE, Cameron IL. 1994. Distribution of intestine-associated lymphoid tissue, aberrant crypt foci, and tumors in the large bowel of 1,2-dimethylhydrazine-treated mice. *Cancer Res.* 54(16):4304-7.

Charles P., Elliott M.J., Davis D., Potter A., Kalden J.R., Antoni C., Breedveld F.C., Smolen J.S., Eberl G., deWoody K., Feldmann M., Maini R.N. Charles P., Elliott M.J. 1999. Regulation of cytokines, cytokine inhibitors, and acute-phase proteins following anti-TNF-alpha therapy in rheumatoid arthritis. *J Immunol.* 163(3):1521-8.

Chen X., Kandasamy K., Srivastava R.K. 2003. Differential roles of RelA (p65) and c-Rel subunits of nuclear factor kappa B in tumor necrosis factor-related apoptosis-inducing ligand signaling. *Cancer Res.* 63(5):1059-66.

Cheng L., Lai M.D. 2003. Aberrant crypt foci as microscopic precursors of colorectal cancer. *World J. Gastroenterol.* 9(12): 2642-9.

Coley W.B. 1906. Late results of the treatment of inoperable sarcoma by the mixed toxins of erysipelas and bacillus prodigiosus. *Am J Med Sci.* 131:375–430.

Corpet D.E., Pierre F. 2003. Point: From Animal Models to Prevention of Colon Cancer. Systematic Review of Chemoprevention in Min Mice and Choice of the Model System. *Cancer Epidemiol Biomarkers Prev*.12:391–400.

Cotran R.S., Kumar V., Collins T. 1999. Robbins pathologic basis of disease. 6th Ed. W.B. Sounders Company, Philadelphia, USA.

Curtis C.H. 1991. Chemical and Physical Carcinogenesis: Advances and perspectives for the 1990s. *Cancer Res.* Suppl 51:5023-44S.

Cusack J.C. Jr, Liu R., Houston M., Abendroth K., Elliott P.J., Adams J., Baldwin A.S. Jr. 2001. Enhanced chemosensitivity to CPT-11 with proteasome inhibitor PS-341: implications for systemic nuclear factor-kappaB inhibition. *Cancer Res*. 61(9):3535-40.

Davies E., Tsang C.W., Ghazali A.R., Harris R.M., Waring R.H. 2004. Effects of culture with TNF-alpha, TGF-beta and insulin on sulphotransferase (SULT 1A1 and 1A3) activity in human colon and neuronal cell lines. *Toxicol In Vitro.* 18(6):749-54.

Ding Q., Ko T.C., Evers B.M. 1998. Caco-2 intestinal cell differentiation is associated with G1 arrest and suppression of CDK2 and CDK. *Am J Physiol Cell Physiol*. 275: C1193-C1200.

Distler P., Holt P.R. 1997. Are right- and left-sided colon neoplasms distinct tumors? *Dig Dis.* 15(4-5):302-11.

Doerre S., Corley R.B. 1999. Constitutive nuclear translocation of NF-kappa B in B cells in the absence of I kappa B degradation. *J Immunol.* 163(1):269-77.

Dranoff, G. 2004. Cytokines in cancer pathogenesis and cancer therapy. *Nat Rev Cancer.* 4(1):11-22.

Duan H, Dixit VM. 1997. RAIDD is a new 'death' adaptor molecule. *Nature*. 385(6611):86-9.

Fearon E.R., Vogelstein B. 1990. A genetic model for colorectal tumorigenesis. *Cell*. 61(5):759–767.

Fogh, J. and Trempe, G. 1975. *Human Tumor Cells in vitro*. Plenum Press. NewYork. pp:115-41.

Fontaine V., Mohand-Said S., Hanoteau N., Fuchs C., Pfizenmaier K., Eisel U. 2002 Neurodegenerative and neuroprotective effects of tumor Necrosis factor (TNF) in retinal ischemia: opposite roles of TNF receptor 1 and TNF receptor 2. *J. Neurosci.* 22(7):RC216.

Foo S.Y., Nolan G.P. 1999. NF-kappaB to the rescue: RELs, apoptosis and cellular transformation. *Trends Genet.* 15(6):229-35.

Formiguera X, Canton A. 2004. Obesity: epidemiology and clinical aspects. *Best Pract Res Clin Gastroenterol*. 18(6):1125-46.

Freeman HJ. 2004. Risk of gastrointestinal malignancies and mechanisms of cancer development with obesity and its treatment. *Best Pract Res Clin Gastroenterol*. 8(6):1167-75.

Frezza E.E., Wachtel M.S., Chiriva-Internati M. 2005. The influence of obesity on the risk of developing colon cancer. *Gut.* 55(2):285-91.

Furukawa S., Fujita T., Shimabukuro M., Iwaki M., Yamada Y., Nakajima Y., Nakayama O., Makishima M., Matsuda M., Shimomura I. 2004. Increased oxidative stress in obesity and its impact on metabolic syndrome. *J Clin Invest*. 114(12):1752-61.

Gadducci A., Ferdeghini M., Castellani C., Annicchiarico C., Gagetti O., Prontera C., Bianchi R., Facchini V. 1995. Serum levels of tumor necrosis factor (TNF), soluble receptors for TNF (55- and 75-kDa sTNFr), and soluble CD14 (sCD14) in epithelial ovarian cancer. *Gynecol Oncol*. 58(2):184-8.

Galisteo M., Sanchez M., Vera R., Gonzalez M., Anguera A., Duarte J., Zarzuelo A. 2005. A Diet Supplemented with Husks of Plantago ovata Reduces the Development of Endothelial Dysfunction, Hypertension, and Obesity by Affecting Adiponectin and TNF-{alpha} in Obese Zucker Rats. *J Nutr*. 135(10):2399-404.

Gerber M., Corpet D. 1999. Energy balance and cancers. *Eur. J. Cancer Prev.*, 8: 77–89.

Gervaz P., Bucher P., Morel P. 2004. Two colons-two cancers: paradigm shift and clinical implications. *J Surg Oncol.* 88(4):261-6.

Gilmore TD, Cormier C, Jean-Jacques J, Gapuzan ME. 2001. Malignant transformation of primary chicken spleen cells by human transcription factor c-Rel. *Oncogene.* 20(48):7098-103.

Giovannucci E. 2001. Insulin, insulin-like growth factors and colon cancer: a review of the evidence. *J Nutr.* 131(11 Suppl):3109S-20S.

Goldsby R.A., Kindt T.J., Osborne B.A., Kuby J. 2003. Immunology Fifth Edition. W.H. Freeman and Company New York.

Green J.E., Hudson T. 2005. The Promise of Genetically Engineered Mice for Cancer Prevention Studies. *Nat Rev Cancer.* 5(3):184-98.

Greene F.L., Lamb L.S., Barwick M. 1987. Colorectal cancer in animal models--a review. *J Surg Res.* 43(5):476-87.

Greten F.R., Eckmann L., Greten T.F., Park J.M., Li Z.W., Egan L.J., Kagnoff M.F., Karin M. 2004. IKKbeta links inflammation and tumorigenesis in a mouse model of colitis-associated cancer. *Cell.* 118(3):285-96.

Gunter M.J., Leitzmann M.F. 2006. Obesity and colorectal cancer: epidemiology, mechanisms and candidate genes. *J Nutr Biochem.* 17(3):145-56.

Hague A., Hicks D.J., Hasan F., Smartt H., Cohen G.M., Paraskeva C., MacFarlane M. 2005. Increased sensitivity to TRAIL-induced apoptosis occurs during the adenoma to carcinoma transition of colorectal carcinogenesis. *Br J Cancer.* 92(4):736-42.

Hakansson L., Adell G., Boeryd B., Sjogren F., Sjodahl R. 1997. Infiltration of mononuclear inflammatory cells into primary colorectal carcinomas: an immunohistological analysis. *Br J Cancer.* 75(3):374-80.

Han S.Y., Choung S.Y., Paik I.S., Kang H.J., Choi Y.H., Kim S.J., Lee M.O. 2000. Activation of NF-kappaB determines the sensitivity of human colon cancer cells to TNFalpha-induced apoptosis. *Biol Pharm Bull.* 23(4):420-6.

Hardwick J.C., van den Brink G.R., Offerhaus G.J., van Deventer S.J., Peppelenbosch MP. 2001. NF-kappaB, p38 MAPK and JNK are highly expressed and active in the stroma of human colonic adenomatous polyps. *Oncogene.* 20(7):819-27.

Hayden M.S., Ghosh S. 2006. Good cop, bad cop: the different faces of NF-kappaB. *Cell Death Differ.* 13(5):759-72.

Higuchi M., Aggarwal B.B. 1994a. TNF induces internalization of the p60 receptor and shedding of the p80 receptor. *J Immunol.* 152(7):3550-8.

Higuchi M., Aggarwal B.B. 1994b. Differential roles of two types of the TNF receptor in TNF-induced cytotoxicity, DNA fragmentation, and differentiation. *J Immunol.* 152(8):4017-25.

Hohmann H.P., Remy R., Brockhause M., Van-Loon A. P. G. M. 1989. Two different cell types have different major receptors for human tumor necrosis factor (TNF-a). *J. Biol. Chem.* 264:14927.

Hoffmann A., A. Levchenko, M.L. Scott, Baltimore D. 2002. The IκB-NF- κB signaling module: temporal control and selective gene activation. *Science.* 298:1241-1245.

Hofmann C., Lorenz K., Braithwaite S.S., Colca J.R., Palazuk B.J., Hotamisligil G.S., Spiegelman B.M. 1994. Altered gene expression for tumor necrosis factor-alpha and its receptors during drug and dietary modulation of insulin resistance. *Endocrinology.* 134(1):264-70.

Hostanska K., Reichling J., Bommer S., Weber M., Saller R. 2003. Hyperforin a constituent of St John's wort (Hypericum perforatum L.) extract induces apoptosis by triggering activation of caspases and with hypericin synergistically exerts cytotoxicity towards human malignant cell lines. *Eur J Pharm Biopharm.* 56:121-132.

Hotamisligil G.S., Shargill N.S., Spiegelman B.M. 1993. Adipose expression of tumor necrosis factor-alpha: direct role in obesity-linked insulin resistance. *Science.* 259(5091):87-91.

Hussein M.R. 2006. Tumour-associated macrophages and melanoma tumourigenesis: integrating the complexity. *Int J Exp Pathol.* 87(3):163-76.

Iacopetta B. 2002. Are there two sides to colorectal cancer? *Int J Cancer.* 101(5):403-8.

Inoue H., Shiraki K., Yamanaka T., Ohmori S., Sakai T., Deguchi M., Okano H., Murata K., Sugimoto K., Nakano T. 2002. Functional expression of tumor necrosis factor-related apoptosis-inducing ligand in human colonic adenocarcinoma cells. *Lab Invest.* 82(9):1111-9.

Itzkowitz, S.H. and Yio, X. 2004. Inflammation and Cancer IV. Colorectal cancer in inflammatory bowel disease: the role of inflammation. *Am J Physiol Gastrointest Liver Physiol* 287:G7–G17.

Jemal A., Murray T., Ward E., Samuels A., Tiwari R.C., Ghafoor A., Feuer E.J., Thun M.J. 2005. Cancer Statistics, 2005. *CA Cancer J Clin* 55(1):10-30.

Jung HC, Eckmann L, Yang SK, Panja A, Fierer J, Morzycka-Wroblewska E, Kagnoff MF. 1995. A distinct array of proinflammatory cytokines is expressed in human colon epithelial cells in response to bacterial invasion. *J Clin Invest.* 95(1):55-65.

Keith M., Norwich K.H., Wong W., Jeejeebhoy K.N. 2000. The tissue distribution of tumor necrosis factor-alpha in rats: a compartmental model. *Metabolism.* 49(10):1309-17.

Kim H.J., Hawke N., Baldwin A.S. 2006. NF-kappaB and IKK as therapeutic targets in cancer. *Cell Death Differ.* 13(5):738-47.

Kimura M., Haisa M., Uetsuka H., Takaoka M., Ohkawa T., Kawashima R., Yamatsuji T., Gunduz M., Kaneda Y., Tanaka N., Naomoto Y. 2003. TNF combined with IFN-alpha accelerates NF-kappaB-mediated apoptosis through enhancement of Fas expression in colon cancer cells. *Cell Death Differ.* 10(6):718-28.

Kiunga GA, Raju J, Sabljic N, Bajaj G, Good CK, Bird RP. 2004. Elevated insulin receptor protein expression in experimentally induced colonic tumors. *Cancer Lett.* 211(2):145-53.

Kojima M., Morisaki T., Sasaki N., Nakano K., Mibu R., Tanaka M., Katano M. 2004. Increased nuclear factor-kB activation in human colorectal carcinoma and its correlation with tumor progression. *Anticancer Res*. 24(2B):675-81.

Komninou D., Ayonote A., Richie J.P. Jr., Rigas B. 2003. Insulin resistance and its contribution to colon carcinogenesis. *Exp Biol Med.* 228(4):396-405.

Kumarathasan P., Vincent R. 2003. New approach to the simultaneous analysis of catecholamines and tyrosines in biological fluids. *J Chromatogr A*. 987(1-2):349-58.

Langkopf F., Atzpodien J. 1994. Soluble tumour necrosis factor receptors as prognostic factors in cancer patients. *Lancet*. 344(8914):57-8.

Laqueur G.L., Spatz M. 1968. Toxicology of cycasin. *Cancer Res.* (11):2262-7.

Lee WM, Lu S, Medline A, Archer MC. 2001. Susceptibility of lean and obese Zucker rats to tumorigenesis induced by N-methyl-N-nitrosourea. *Cancer Lett.* 162(2):155-60.

Lejeune F.J., Ruegg C., Lienard D. 1998. Clinical applications of TNF-alpha in cancer. *Curr Opin Immunol.* 10:573-80.

Li J.H., Yu J.P., Yu H.G., Xu X.M., Yu L.L., Liu S.Q. 2005. Expression and significance of nuclear factor kappaB p65 in colon tissues of rats with TNBS-induced colitis. *World J Gastroenterol.* 11(12):1759-63.

Lin A., Karin M. 2003. NF-kappaB in cancer: a marked target. *Semin Cancer Biol.* 13(2):107-14.

Lindblom A. 2001. Different mechanisms in the tumorigenesis of proximal and distal colon cancers. *Curr Opin Oncol*. 13(1):63-9.

Liu Z, Uesaka T, Watanabe H, Kato N. 2001. High fat diet enhances colonic cell proliferation and carcinogenesis in rats by elevating serum leptin. *Int J Oncol*. 19(5):1009-14.

Lotz M., Setareh M., von Kempis J., Schwarz H. 1996. The nerve growth factor/tumor necrosis factor receptor family. *J Leukoc Biol*. 60(1):1-7.

Luhrs H., Kudlich T., Neumann M., Schauber J., Melcher R., Gostner A., Scheppach W., Menzel T.P. 2002. Butyrate-enhanced TNFalpha-induced apoptosis is associated with inhibition of NF-kappaB. *Anticancer Res*.22(3):1561-8.

Ma J., Pollak M.N., Giovannucci E., Chan J.M., Tao Y., Hennekens C.H., Stampfer M.J. 1999. Prospective study of colorectal cancer risk in men and plasma levels of insulin-like growth factor (IGF)-I and IGF-binding protein-3. *J Natl Cancer Inst*. 91:620–5.

Macarthur M., Hold G.L., El-Omar E.M. 2004. Inflammation and Cancer II. Role of chronic inflammation and cytokine gene polymorphisms in the pathogenesis of gastrointestinal malignancy. *Am J Physiol Gastrointest Liver Physiol* 286:G515–G520.

Madhusudan S., Foster M., Muthuramalingam S.R., Braybrooke J.P., Wilner S., Kaur K., Han C., Hoare S., Balkwill F., Talbot D.C., Ganesan T.S., Harris A.L. 2004. A phase II study of etanercept (Enbrel), a tumor necrosis factor alpha inhibitor in patients with metastatic breast cancer. *Clin Cancer Res*. 10(19):6528-34.

Mao Y., Pan S., Wen S.W., Johnson K.C. 2003. Canadian Cancer Registries Epidemiology Research Group. Physical inactivity, energy intake, obesity and the risk of rectal cancer in Canada. *Int J Cancer*. 105(6): 831-7.

Martinez M.E. 2005. Primary prevention of colorectal cancer: lifestyle, nutrition, exercise. *Recent Results Cancer Res*.166:177-211.

Matsuzawa Y. 2006. Therapy Insight: adipocytokines in metabolic syndrome and related cardiovascular disease. *Nat Clin Pract Cardiovasc Med*. 3(1):35-42.

McCaleb M. L., Sredy, J. 1992. Metabolic abnormalities of the hyperglycemic obese Zucker rat. *Metabolism*. 41: 522–525.

McLellan E.A., Medline A., Bird R.P. 1991. Dose response and proliferative characteristics of aberrant crypt foci: putative preneoplastic lesions in rat colon. *Carcinogenesis* 12(11): 2093-8.

Micheau O. and Tschopp J. 2003. Induction of TNF Receptor I-Mediated Apoptosis via Two Sequential Signaling Complexes. *Cell*. 114:181-90.

Molitor J.A., Walker W.H., Doerre S., Ballard D.W., Greene W.C. 1990. NF-kappa B: a family of inducible and differentially expressed enhancer-binding proteins in human T cells. *Proc Natl Acad Sci U S A*. 87(24):10028-32.

Moore K.L. and Dalley A.F. 1999. Clinically Oriented Anatomy 4th Edition. Lippincott, Williams and Wilkins. pp:249-251.

Mousa S.A. 2006. Role of current and emerging antithrombotics in thrombosis and cancer. *Drugs Today (Barc)*. 42(5):331-50.

Mueller H, Kassack MU, Wiese M. 2004. Comparison of the usefulness of the MTT, ATP, and calcein assays to predict the potency of cytotoxic agents in various human cancer cell lines. *J Biomol Screen.* 9(6):506-15.

Nakanishi C., Toi M. 2005. Nuclear factor-kappaB inhibitors as sensitizers to anticancer drugs. *Nat Rev Cancer.* 5(4):297-9.

Nelson-Dooley C., Della-Fera M.A., Hamrick M., Baile C.A. 2005. Novel treatments for obesity and osteoporosis: targeting apoptotic pathways in adipocytes. *Curr Med Chem.* 12(19):2215-25.

Nunez N.P., Oh W.J., Rozenberg J., Perella C., Anver M., Barrett J.C., Perkins S.N., Berrigan D., Moitra J., Varticovski L., Hursting S.D., Vinson C. 2006. Accelerated tumor formation in a fatless mouse with type 2 diabetes and inflammation. *Cancer Res.* 66(10):5469-76.

Pajonk F., Scholber J., Fiebich B. 2005. Hypericin-an inhibitor of proteasome function. *Cancer Chemother Pharmacol.* 55(5):439-46.

Park E.J., Pezzuto J.M. 2002. Botanicals in cancer chemoprevention. *Cancer and Metastasis Reviews* 21: 231–255.

Pearson G., English J.M., White M.A., Cobb M.H. 2001. ERK5 and ERK2 cooperate to regulate NF-kappaB and cell transformation. *J Biol Chem.* 276(11):7927-31.

Pennica D, Hayflick JS, Bringman TS, Palladino MA, Goeddel DV. 1985. Cloning and expression in Escherichia coli of the cDNA for murine tumor necrosis factor. *Proc Natl Acad Sci USA.* 82(18):6060-4.

Perkins N.D., Gilmore T.D. 2006. Good cop, bad cop: the different faces of NF-kappaB. *Cell Death Differ.* 13(5):759-72.

Philip M., Rowley D.A., Schreiber H. 2004. Inflammation as a tumor promoter in cancer induction. *Semin Cancer Biol.* 14:433–439.

Pikarsky E., Ben-Neriah Y. 2006. NF-kappaB inhibition: a double-edged sword in cancer? *Eur J Cancer.* 42(6):779-84.

Pitot H.C., Hikita H., Dragan Y., Sargent L., Haas M. 2000. Review article: the stages of gastrointestinal carcinogenesis--application of rodent models to human disease. *Aliment Pharmacol Ther.* Suppl 1:153-60.

Pocard M., Tsukui H., Salmon E., Dutrillaux B., Poupon M. 1996. Efficiency of Orthotopic Xenograft Models for Human Colon Cancers. *In Vivo.* 10:463-470.

Radtke F., Clevers H. 2005. Self-Renewal and Cancer of the Gut:Two Sides of a Coin. *Science.* 307:1904-1909.

Raju J. Bird R.P. 2006. Alleviation of hepatic steatosis accompanied by modulation of plasma and liver TNF-alpha levels by Trigonella foenum graecum (fenugreek) seeds in Zucker obese (fa/fa) rats. *Int J Obes.* 30(8):1298-307.

Raju J., Bird R.P. 2003. Energy restriction reduces the number of advanced aberrant crypt foci and attenuates the expression of colonic transforming growth factor beta and cyclooxygenase isoforms in Zucker obese (fa/fa) rats. *Cancer Res*. 63(20): 6595-601.

Rapp K., Schroeder J., Klenk J., Stoehr S., Ulmer H., Concin H., Diem G., Oberaigner W., Weiland S.K. 2005. Obesity and incidence of cancer: a large cohort study of over 145,000 adults in Austria. *Br J Cancer.* 93(9):1062-7.

Reaven G.M. 1988. Role of insulin resistance in human disease. *Diabetes.* 37:1595–1600.

Reddy S.A., Chaturvedi M.M., Darnay B.G., Chan H., Higuchi M., Aggarwal B.B.1994. Reconstitution of nuclear factor kappa B activation induced by tumor necrosis factor requires membrane-associated components. Comparison with pathway activated by ceramide. *J Biol Chem.* 269(41):25369-72.

Reddy B.S. 2004. Studies with the azoxymethane-rat preclinical model for assessing colon tumor development and chemoprevention. *Environ Mol Mutagen*. 44:26-35.

Remacle-Bonnet M.M., Garrouste F.L., Heller S., Andre F., Marvaldi J.L., Pommier G.J. 2000. Insulin-like growth factor-I protects colon cancer cells from death factor-induced apoptosis by potentiating tumor necrosis factor alpha-induced mitogen-activated protein kinase and nuclear factor kappaB signaling pathways. *Cancer Res*. 60(7):2007-17.

Roncucci L., Stamp D., Medline A., Cullen J.B., Bruce W.R. 1991. Identification and qualification of aberrant crypt foci and adenoma in the human colon. *Hum Pathol.* 22: 287-294.

Roscetti G., Franzese O., Comandini A., Bonmassar E. 2004. Cytotoxic Activity of Hypericum perforatum L. on K562 Erythroleukemic Cells: Differential Effects between Methanolic Extract and Hypericin. *Phytother Res.* 18:66-72.

Russo M.P., Bennett B.L., Manning A.M., Brenner D.A., Jobin C. 2002. Differential requirement for NF-kappaB-inducing kinase in the induction of NF-kappaB by IL-1beta, TNF-alpha, and Fas. *Am J Physiol Cell Physiol.* 283(1):C347-57.

Ryan K.M., Ernst M.K., Rice N.R., Vousden K.H. 2000. Role of NF-kappaB in p53-mediated programmed cell death. *Nature.* 404(6780):892-7.

Samad F., Uysal K.T., Wiesbrock S.M., Pandey M., Hotamisligil G.S., Loskutoff D.J. 1999. Tumor necrosis factor a is a key component in the obesity-linked elevation of plasminogen activator inhibitor 1. *Proc. Natl. Acad. Sci. USA.* 96:6902–7.

Sasaki N., Morisaki T., Hashizume K., Yao T., Tsuneyoshi M., Noshiro H., Nakamura K., Yamanaka T., Uchiyama A., Tanaka M., Katano M. 2001. Nuclear factor-kappaB p65 (RelA) transcription factor is constitutively activated in human gastric carcinoma tissue. *Clin Cancer Res.* 7(12):4136-42.

Schmitz H., Fromm M., Bentzel C.J., Scholz P., Detjen K., Mankertz J., Bode H., Epple H.J., Riecken E.O., Schulzke J.D. 1999. Tumor necrosis factor-alpha (TNFalpha) regulates the epithelial barrier in the human intestinal cell line HT-29/B6. *J. Cell Sci.* 112(Pt 1):137-46.

Schreck R., Rieber P., Baeuerle P.A. 1991. Reactive oxygen intermediates as apparently widely used messengers in the activation of the NF-kappa B transcription factor and HIV-1. *EMBO J.* 10(8):2247-58.

Schutze S., Wiegmann K., Machleidt T., Kronke M. 1995. TNF-induced activation of NF-kappa B. *Immunobiology.* 193(2-4):193-203.

Seidelin J.B., Nielsen O.H. 2005. Continuous cytokine exposure of colonic epithelial cells induces DNA damage. *Eur J Gastroenterol Hepatol.* 17(3):363-9.

Sen R., Baltimore D. 1986. Multiple nuclear factors interact with the immunoglobulin enhancer sequences. *Cell.* 46(5):705-16.

Senftleben U., Cao Y., Xiao G., Greten F.R., Krahn G., Bonizzi G., Chen Y., Hu Y., Fong A., Sun S.C., Karin M. 2001. Activation by IKKa of a second, evolutionary conserved, NF-kB signaling pathway. *Science.* 293: 1495–99.

Shaw DI, Hall WL, Williams CM. 2005. Metabolic syndrome: what is it and what are the implications? *Proc Nutr Soc.* 64(3):349-57.

Shishodia S., Aggarwal B.B. 2002. Nuclear factor-kappaB activation: a question of life or death. *J Biochem Mol Biol.* 35(1):28-40.

Shishodia S., Aggarwal B.B. 2004. Nuclear factor-kappaB: a friend or a foe in cancer? *Biochem Pharmacol.* 68(6):1071-80.

Siebenlist U., Franzoso G., Brown K. 1994. Structure, regulation and function of NF-kappa B. *Annu Rev Cell Biol.* 10:405-55.

Sonnenberg G.E., Krakower G.R., Kissebah A.H. 2004. A novel pathway to the manifestations of metabolic syndrome. *Obes Res.* 12(2):180-6.

Sorrentino M.J. 2005. Implications of the metabolic syndrome: the new epidemic. *Am J Cardiol.* 96(4A):3E-7E.

Stattin P., Lukanova A., Biessy C., Soderberg S., Palmqvist R., Kaaks R., Olsson T., Jellum E. 2004. Obesity and colon cancer: does leptin provide a link? *Int J Cancer.* 109(1):149-52.

Stone N.J., Saxon D. 2005. Approach to treatment of the patient with metabolic syndrome: lifestyle therapy. *Am J Cardiol.* 96(4A):15E-21E.

Straczkowski M., Kowalska I., Nikolajuk A., Adamska A., Karolczuk-Zarachowicz M., Karczewska-Kupczewska M., Kozlowska A., Gorska M. 2006. Plasma levels of soluble tumor necrosis factor-alpha receptors are related to total and LDL-cholesterol in lean, but not in obese subjects. *Cardiovasc Diabetol.* 5(1):14.

Suganuma M., Okabe S., Marino M.W., Sakai A., Sueoka E., Fujiki H. 1999. Essential role of tumor necrosis factor alpha (TNF-alpha) in tumor promotion as revealed by TNF-alpha-deficient mice. *Cancer Res.* 59:4516–8.

Szlosarek P., Charles K.A., Balkwill F.R. 2006. Tumour necrosis factor-alpha as a tumour promoter. *Eur J Cancer.* 42(6):745-50.

Reddy B.S. 2004. Studies with the Azoxymethane–Rat Preclinical Model for Assessing Colon Tumor Development and Chemoprevention. *Environmental and Molecular Mutagenesis.* 44:26–35.

Rojas-Cartagena C., Flores I., Appleyard C.B. 2005. Role of tumor necrosis factor receptors in an animal model of acute colitis. *Cytokine.* 32(2):85-93.

Russo M.P., Bennett B.L., Manning A.M., Brenner D.A., Jobin C. 2002. Differential requirement for NF-kappaB-inducing kinase in the induction of NF-kappaB by IL-1beta, TNF-alpha, and Fas. *Am J Physiol Cell Physiol.* 283(1):C347-57.

Ryan KM, Ernst MK, Rice NR, Vousden KH. 2000. Role of NF-kappaB in p53-mediated programmed cell death. *Nature.* 404(6780):892-7.

Thommesen L., Laegreid A. 2005. Distinct differences between TNF receptor 1- and TNF receptor 2-mediated activation of NFkappaB. *J Biochem Mol Biol.* 2005. 38(3):281-9.

Tong X., Yin L., Washington R., Rosenberg D.W., Giardina C. 2004. The p50-p50 NF-kappaB complex as a stimulus-specific repressor of gene activation. *Mol Cell Biochem.* 265(1-2):171-83.

Vaculova A., Hofmanova J., Soucek K., Kovarikova M., Kozubik A. 2002. Tumor necrosis factor-alpha induces apoptosis associated with poly(ADP-ribose) polymerase cleavage in HT-29 colon cancer cells. *Anticancer Res.* 22(3):1635-9.

Vandenabeele P., Declercq W., Beyaert R., Fiers W. 1995. Two tumour necrosis factor receptors: structure and function. *Trends Cell Biol.* 5(10):392-9.

Van Antwerp D.J., Martin S.J., Kafri T., Green D.R., Verma I.M. 1996. Suppression of TNF-alpha-induced apoptosis by NF-kappaB. *Science.* 274(5288):787-9.

Van Antwerp D.J., Martin S.J., Verma I.M., Green D.R. 1998. Inhibition of TNF-induced apoptosis by NF-kappa B. *Trends Cell Biol.* 8(3):107-11.

van Weerden W.M., Romijn J.C. 2000. Use of Nude Mouse Xenograft Models in Prostate Cancer Research.*The Prostate.* 43:263–271.

Varfolomeev E.E. and Ashkenazi A. 2004. Tumor Necrosis Factor: An Apoptosis JuNKie? *Cell.* 116: 491–497.

Viac J., Vincent C., Palacio S., Schmitt D., Claudy A. 1996. Tumour necrosis factor (TNF) soluble receptors in malignant melanoma: correlation with soluble ICAM-1 levels. *Eur J Cancer.* 32A(3):447-9.

Viatour P., Merville M.P., Bours V., Chariot A. 2005. Phosphorylation of NF-kappaB and IkappaB proteins: implications in cancer and inflammation. *Trends Biochem Sci.* 30(1):43-52.

Vincent H. K., Powers S. K., Stewart D. J., Shanely R. A., Demirel H., Naito H. 1999. Obesity is associated with increased myocardial oxidative stress. *Int. J. Obes.* 23:67-74.

Wajant H., Pfizenmaier K., Scheurich P. 2003. Tumor necrosis factor signaling. *Cell Death Differ.* 10(1):45-65.

Wang C.Y., Mayo M.W., Baldwin A.S. Jr. 1996. TNF- and cancer therapy-induced apoptosis: potentiation by inhibition of NF-kappaB. *Science.* 274(5288):784-7.

Warzocha K., Ribeiro P., Bienvenu J., Roy P., Charlot C., Rigal D., Coiffier B., Salles G. 1998. Genetic polymorphisms in the tumor necrosis factor locus influence non-Hodgkin's lymphoma outcome. *Blood* 91:3574–81.

Weber R.V., Stein D.E., Scholes J., Kral J.G. 2000. Obesity potentiates AOM-induced colon cancer. *Dig Dis Sci.* 45(5):890-5.

Yang Z., Costanzo M., Golde D.W., Kolesnick R.N. 1993. Tumor necrosis factor activation of the sphingomyelin pathway signals nuclear factor kappa B translocation in intact HL-60 cells. *J Biol Chem.* 268(27):20520-3.

Yin L., Laevsky G., Giardina C. 2001. Butyrate suppression of colonocyte NF-kappa B activation and cellular proteasome activity. *J Biol Chem.* 276(48):44641-6.

Yoshimi N., Sato S., Makita H., Wang A., Hirose Y., Tanaka T., Mori H. 1994. Expression of cytokines, TNF-alpha and IL-1 alpha, in MAM acetate and 1-hydroxyanthraquinone-induced colon carcinogenesis of rats. *Carcinogenesis.*15(4):783-5.

Yu L.L., Yu H.G., Yu J.P., Luo H.S., Xu X.M., Li J.H. 2004. Nuclear factor-kappaB p65 (RelA) transcription factor is constitutively activated in human colorectal carcinoma tissue. *World J Gastroenterol.* 10(22):3255-60.

Zucker L.M., Zucker T.F. 1961. Fatty, a new mutation in the rat. *J Hered*. 51-52:275-278.

Zucker T.F., Zucker L.M. 1962. Hereditary obesity in the rat associated with high serum fat and cholesterol. *Proc Soc Exp Biol Med.* 110:165-171.

Zwacka R.M., Stark L., Dunlop M.G. 2000. NF-kappaB kinetics predetermine TNF-alpha sensitivity of colorectal cancer cells. *J Gene Med.* 2(5):334-43.